

POST-CRACK BEHAVIOR OF MACRO-FIBER REINFORCED CONCRETE

A Thesis  
SUBMITTED TO THE FACULTY OF  
UNIVERSITY OF MINNESOTA  
BY

Bryce Robert Hansen

IN PARTIAL FULFILLMENT OF THE REQUIREMENTS  
FOR THE DEGREE OF  
MASTER OF SCIENCE

Dr. Manik Barman

January 2018

© Bryce R Hansen 2018

## ACKNOWLEDGMENTS

### **Major Funding**

- Minnesota Department of Transportation
- University of Minnesota Duluth

### **Aggregate Donations**

- Duluth Ready Mix

### **Admixture Donations**

- BASF Corporation

### **Concrete Fiber Donations**

- ABC Polymer Industries
- General Resource Technology
- W.R. Grace
- Propex Operation Co., LLC
- The Euclid Chemical Company
- BASF Corporation
- Elasto Plastic Concrete
- Bekaert Dramix
- Sika Corporation U.S.
- Forta Corporation

### **Undergraduate Laboratory Assistance**

- Noah Tapper
- Sam Butler
- Jake Pilz
- Lucas Kaari
- Josh Benolken

## **DEDICATION**

*I would like to dedicate this thesis and my work to my parents and Miranda for their continued support and care.*

## ABSTRACT

Structural fibers are used in thin concrete overlays, pavements, and many other civil engineering structures for improving concretes long-term performance. These fibers improve the structural integrity of concrete by enhancing the post-crack performance and load transfer efficiency of concrete in un-dowelled thin concrete overlays. However, the pavement industry often encounters problem in selecting the appropriate type of fibers and their corresponding dosages. The primary objective of this study was to conduct a laboratory study to quantify the benefit of structural fibers in terms of pre-and post-crack behaviors in flexural specimens and to, as a goal, provide methods that characterize the behavior of fibers in fiber reinforced concrete (FRC).

In this study, two new properties (post-crack toughness and post-crack performance (PCP) index) were proposed. Eleven different types of fibers were tested at three different dosages each for regular strength mixes (total 33 mixes). Also, four other low strength FRC mixes were considered. Hardened concrete properties of all these FRC mixes were compared with the control plain concrete mix. The following hardened concrete properties were considered: compressive strength, modulus of elasticity, modulus of rupture, residual strength, residual strength ratio, post-crack toughness, and PCP index. The study found good correlations between properties of fibers and FRC performance. It was found that fibers having a crimped, embossed, twisted or hooked-end geometry greatly outperform straight fibers. Post crack toughness was seen to produce stronger and more accurate correlations to cracked FRC, while the PCP index provided a tool for evaluating a fiber's ability to add post crack performance with an increase in a fiber's volume fraction. The mechanistic estimation method was developed to complete two

tasks; estimate the fibers effective working stress (EWS) and to provide a tool for approximating a FRC's flexural performance.

As an auxiliary component to the core of this study, joint performance (as it pertains to concrete slabs -on -ground) was also evaluated. This separate study drew correlations between joint performance and fiber dosage and then compared joint performance to flexural performance.

## TABLE OF CONTENTS

ACKNOWLEDGMENTS .....	i
DEDICATION .....	ii
ABSTRACT .....	iii
TABLE OF CONTENTS.....	v
LIST OF TABLES.....	viii
LIST OF FIGURES .....	ix
1 INTRODUCTION .....	1
1.1 Background .....	1
1.2 Objectives and Significance .....	2
1.3 Thesis Organization.....	2
2 REVIEW OF LITERATURE.....	5
2.1 Introduction.....	5
2.2 Fibers.....	5
2.2.1 Steel Fibers.....	6
2.2.2 Synthetic Fibers .....	9
2.2.3 Glass Fibers.....	14
2.2.4 Natural Fibers.....	14
2.3 Fiber Reinforced Concrete (FRC) .....	16
2.3.1 ASTM C1609 Four-Point Flexural Test for FRC .....	16
2.3.2 Steel Fiber Reinforced Concrete (SFRC) .....	18
2.3.3 Glass Fiber Reinforced Concrete (GFRC).....	24
2.3.4 Synthetic Fiber Reinforced Concrete (SNFRC) .....	25
2.3.5 Natural Fiber Reinforced Concrete (NFRC).....	27
2.3.6 Hybrid Fiber Reinforced Concrete.....	28
2.4 Conclusion.....	29
3 RESEARCH METHODOLOGY .....	30
3.1 Introduction .....	30
3.2 Development of Laboratory Analysis Methods .....	30
3.2.1 Post-Crack Toughness .....	31
3.2.2 Post Crack Performance (PCP) Index.....	32
3.3 Presentation of a Mechanistic Estimation Method.....	34
3.4 Experimental Laboratory Testing Plan .....	35

3.5 Conclusion.....	36
<b>4 MATERIALS, TESTING, AND PROCEDURES .....</b>	<b>37</b>
4.1 Introduction .....	37
4.2 Material .....	37
4.2.1 Fibers.....	37
4.2.2 Aggregate.....	39
4.2.3 Mixture Design .....	41
4.2.4 Mixture Designations.....	42
4.3 Concrete Mixing Procedure .....	43
4.4 Plastic (Fresh) Concrete Testing .....	45
4.4.1 Slump Test .....	45
4.4.2 Air Content by Pressure Method.....	46
4.5 Hardened Concrete Testing.....	47
4.5.1 Compressive Strength Testing .....	47
4.5.2 Modulus of Elasticity .....	48
4.5.3 Flexural Testing per ASTM C1609 .....	49
4.6 Conclusion.....	52
<b>5 ANALYSIS AND DISCUSSION OF LABORATORY RESULTS .....</b>	<b>53</b>
5.1 Introduction .....	53
5.2 Plastic (Fresh) Concrete Properties .....	53
5.2.1 Air Content by Pressure Method.....	54
5.2.2 Slump and Workability .....	55
5.3 Hardened Concrete Results .....	56
5.3.1 Uncracked Concrete Properties.....	56
5.3.2 Cracked Concrete Properties.....	62
5.4 Conclusion.....	81
<b>6 PRESENTATION OF A MECHANISTIC ESTIMATION METHOD FOR EFFECTIVE FIBER TENSILE STRENGTH .....</b>	<b>83</b>
6.1 Introduction .....	83
6.2 Approximate Calculations of Residual Strength.....	83
6.2.1 Assumptions Considered in this Method .....	84
6.2.2 Calculation of Effective Working Stress .....	88
6.3 Effective Working Stress (EWS) of Fibers .....	89
6.3.1 Effect of Fiber Type and Dosage on EWS.....	90
6.3.2 General Estimates for EWS .....	90
6.3.3 Direct Tension (DT) Test.....	91

6.3.4	Comparison of DT and EWS .....	93
6.4	Conclusion.....	93
7	CONCLUSION .....	94
8	BIBLIOGRAPHY .....	97
A	APPENDIX: LITERATURE REVIEW .....	100
B	APPENDIX: FIBER IMAGES.....	102
C	APPENDIX: MIXTURE RESULTS.....	108
D	APPENDIX LOAD VERSUS DISPLACEMENT PLOTS .....	111
E	APPENDIX: JOINT PERFORMANCE OF FRC .....	130
1)	Introduction .....	130
2)	Joint Performance Testing.....	130
3)	Joint Performance Properties: Load Transfer Efficiency (LTE) .....	132
4)	Joint Performance Properties: Differential Joint Energy Dissipation (DJD) ....	133
5)	Testing Matrix and Plan .....	133
6)	Plastic and Hardened Concrete Properties .....	134
7)	Joint Performance Results: Fiber Geometry .....	134
8)	Joint Performance Results: Fiber Dosage .....	136
9)	Joint Performance and Flexural Performance Correlation Charts .....	140
10)	Conclusion.....	141

## LIST OF TABLES

Table 2-1. Range of ACI recommended aggregate gradation for SFRC .....	21
Table 3-1. Testing matrix for the work conducted. ....	36
Table 4-1. Description of fibers investigated in this research .....	39
Table 4-2. Percent passing table for fine and coarse aggregate in this study. ....	41
Table 4-3. Base mixture design for concrete mixes for this study.....	42
Table 4-4. Nomenclature for the mixture designation .....	43
Table 5-1. Dosage and average 28 day RSR values are presented for synthetic fibers and steel fibers respectively.....	67
Table 5-2. Single factor ANOVA statistical comparisons of the synthetic fibers for each dosage investigated in this study.....	76
Table 5-3. Factor statistical comparisons of synthetic fiber geometries at 0.75% volume fraction. ....	76
Table 5-4. Post-crack behavior in terms of the PCP index. ....	77
Table 6-1. Comparison of fiber geometries at various fiber dosages in terms of EWS. ...	91
Table 6-2. A comparison of fiber tensile forces in terms of fiber cross-sectional area not concrete cross-sectional area.....	93
Table A-1. General properties of selected fiber types (after PCA, 2015).....	100
Table A-2. Typical properties of natural fibers (after ACI 544.1R, 2009). ....	101
Table A-3. Range of proportions for normal weight steel fiber reinforced concrete (after ACI 544.1R, 2009).....	101
Table C-1. Properties collected from ASTM 1609 testing. ....	108
Table C-2. Compressive Properties of FRC tested in this work. ....	109
Table C-3. Fresh concrete properties for the mixtures evaluated in this work. ....	110
Table E-1. Plastic and hardened concrete properties for the mixtures in this work. ....	134

## LIST OF FIGURES

Figure 2-1. Various steel fiber geometries (after ACI 544.1R, 2009) .....	7
Figure 2-2. Steel fibers having hooked-end geometry.....	8
Figure 2-3. Steel fibers with crimped geometry in whole length. ....	8
Figure 2-4. Steel fibers with flattened end.....	8
Figure 2-5. Monofilament synthetic fibers (Barman, 2014). ....	10
Figure 2-6. Fibrillated synthetic fibers (Barman, 2014). ....	10
Figure 2-7. Macro synthetic fibers (Barman, 2014). ....	10
Figure 2-8. Polyolefin fibers, next to ruler length in centimeters (Barman, 2014).....	13
Figure 2-9. Picture of the polypropylene fibers (a) straight geometry, (b) crimped geometry (after Barman, 2014).....	14
Figure 2-10. Fibers bridging a crack and providing post-crack performance (Gaddam, 2016). .....	16
Figure 2-11. Range of load versus deflection curves for plain and reinforced concrete ..	18
Figure 2-12. Effect of fiber reinforcement index and fiber geometry on the measured slump (after ACI 544.1R, 2009). .....	19
Figure 2-13. Compressive strength vs. percentage of fibers by volume.....	22
Figure 2-14. Peak flexural strength vs. percentage of fibers by volume .....	23
Figure 3-1. Example of a load versus mid span displacement plot. ( $V_f$ = volume fraction of fibers with respect to the total weight of concrete) .....	32
Figure 3-2. Residual strength versus Reinforcement Index Plot is plotted for a typical fiber. ....	33
Figure 3-3. RSR is displayed as a function of volume fraction of fibers in the mixture..	34
Figure 3-4. Flow chart of work conducted.....	35
Figure 4-1. Coarse aggregate and fine aggregate used in this project. ....	40
Figure 4-2. Gradations for the coarse and fine aggregates used in this project. ....	40
Figure 4-3. Concrete mixer used in this study. ....	44
Figure 4-4. Fiber balling in a concrete mixture. ....	44
Figure 4-5. Slump test on FRC mixture.....	46
Figure 4-6. The air content by pressure method test is in progress. ....	47
Figure 4-7. An example of a concrete compression test per ASTM C39. ....	48
Figure 4-8. An example of a Modulus of Elasticity test per ASTM C469. ....	49
Figure 4-9. An example of a flexural performance test for fiber-reinforced concrete per ASTM C1609. ....	50
Figure 4-10. An example of a crack developed after peak load was achieved in a flexural performance test.....	51
Figure 4-11. Typical displacement versus load plots: (a) synthetic (b) steel fiber, (c) no fibers. ....	51
Figure 5-1. Air content as a function of reinforcement index.....	54
Figure 5-2. Slump as a function of reinforcement index. ....	56

Figure 5-3. Compressive strength as a function of reinforcement index .....	58
Figure 5-4. The modulus of elasticity as a function of reinforcement index.....	58
Figure 5-5. Modulus of rupture as a function of volume fraction for FRC mixtures together. ....	61
Figure 5-6. The volume fraction versus the modulus of rupture for each fiber considered in this work. ....	61
Figure 5-7. The residual strength as a function of volume fraction.....	63
Figure 5-8. Post-crack toughness as a function of volume fraction.....	64
Figure 5-9. The residual strength ratio as a function of volume fraction. ....	64
Figure 5-10. Residual strength as a function of volume fraction for all synthetic and steel fibers separately. ....	66
Figure 5-11. Post-crack toughness ad a function of volume fraction. ....	66
Figure 5-12. The residual strength as a function of dosage and geometry of fibers.....	68
Figure 5-13. The post-crack toughness as a function of dosage and geometry of fibers..	68
Figure 5-14. Residual strength as a function of fiber length for synthetic fibers at different dosages implored. ....	70
Figure 5-15. Post-crack toughness as a function of fiber length for synthetic fibers at different dosages implored.....	70
Figure 5-16. Residual strength as a function of aspect ratio for synthetic fibers at different dosages implored. ....	71
Figure 5-17. Post-crack toughness as a function of aspect ratio for synthetic fibers at different dosages implored.....	72
Figure 5-18. Residual strength as a function of concrete compressive strength for selected synthetic fibers at 0.5% volume fraction. ....	73
Figure 5-19. Post-crack toughness as a function of concrete compressive strength for selected synthetic fibers at 0.5% volume fraction. ....	73
Figure 5-20. Modulus of rupture and residual strength as a function of concrete compressive strength for synthetic fibers at 0.5% volume fraction.....	74
Figure 5-21. Post-crack toughness as a function of concrete compressive strength for synthetic fibers at 0.5% volume fraction. ....	74
Figure 5-22. Post-crack performance in terms of normalized RS and volume fraction. ..	77
Figure 5-23. PCP index as a function of fiber length. ....	78
Figure 5-24. RS as a function of RI. ....	79
Figure 5-25. Post-crack toughness as a function of RI. ....	80
Figure 5-26. RS and PCP Index ratio as a function of volume fraction. ....	80
Figure 5-27. Post-crack toughness and PCP Index ratio as a function of volume fraction. ....	81
Figure 6-1. Idealized fiber layout in a flexural specimen. ....	86
Figure 6-2. Diagram showing the location of forces about a beam cross section. ....	87
Figure 6-3. EWS as a function of volume fraction. ....	89

Figure 6-4. EWS as a function of volume fraction .....	90
Figure 6-5. Direct tension test conducted as an extra step to this work.....	92
Figure 6-6. DT test specimen results. ....	92
Figure B-1. Image of Fiber 1.....	102
Figure B-2. Image of Fiber 2.....	102
Figure B-3. Image of Fiber 3.....	103
Figure B-4. Image of Fiber 4.....	103
Figure B-5. Image of Fiber 5.....	104
Figure B-6. Image of Fiber 6.....	104
Figure B-7. Image of Fiber 7.....	105
Figure B-8. Image of Fiber 8.....	105
Figure B-9. Image of Fiber 9.....	106
Figure B-10. Image of Fiber 10. ....	106
Figure B-11. Image of Fiber 11. ....	107
Figure D-1. Load versus displacement curves for H.S.S.1.25.....	111
Figure D-2. Load versus displacement curves for H.S.S.1.5.....	111
Figure D-3. Load versus displacement curves for H.S.S.1.75.....	112
Figure D-4. Load versus displacement curves for H.S.S.2.25.....	112
Figure D-5. Load versus displacement curves for H.S.S.2.5.....	113
Figure D-6. Load versus displacement curves for H.S.S.2.75.....	113
Figure D-7. Load versus displacement curve for H.S.S.3.25. ....	114
Figure D-8. Load versus displacement curves for H.S.S.3.5.....	114
Figure D-9. Load versus displacement curves for H.S.S.3.75.....	115
Figure D-10. Load versus displacement curves for H.S.S.4.25.....	115
Figure D-11. Load versus displacement curves for H.S.S.4.5.....	116
Figure D-12. Load versus displacement curves for H.S.S.4.75.....	116
Figure D-13. Load versus displacement curves for H.S.T.5.25.....	117
Figure D-14. Load versus displacement curves for H.S.T.5.5.....	117
Figure D-15. Load versus displacement curves for H.S.T.5.75.....	118
Figure D-16. Load versus displacement curves for H.S.C.6.25. ....	118
Figure D-17. Load versus displacement curves for H.S.C.6.5. ....	119
Figure D-18. Load versus displacement curves for H.S.C.6.75. ....	119
Figure D-19. Load versus displacement curves for H.S.E.7.25.....	120
Figure D-20. Load versus displacement curves for H.S.E.7.5.....	120
Figure D-21. Load versus displacement curves for H.S.E.7.75.....	121
Figure D-22. Load versus displacement curves for H.S.E.8.25.....	121
Figure D-23. Load versus displacement curves for H.S.E.8.5.....	122
Figure D-24. Load versus displacement curves for H.S.E.8.75.....	122
Figure D-25. Load versus displacement curves for H.S.E.9.25.....	123
Figure D-26. Load versus displacement curves for H.S.E.9.5.....	123

Figure D-27. Load versus displacement curves for H.S.E.9.75.....	124
Figure D-28. Load versus displacement curves for H.L.EC.10.25.....	124
Figure D-29. Load versus displacement curves for H.L.EC.10.5.....	125
Figure D-30. Load versus displacement curves for H.L.EC.10.75.....	125
Figure D-31. Load versus displacement curves for H.S.T.11.25.....	126
Figure D-32. Load versus displacement curves for H.S.T.11.5.....	126
Figure D-33. Load versus displacement curves for H.S.T.11.75.....	127
Figure D-34. Load versus displacement curves for a plain concrete mixture. ....	127
Figure D-35. Load versus displacement curves for L.S.S.4.5. ....	128
Figure D-36. Load versus displacement curves for L.S.T.5.5. ....	128
Figure D-37. Load versus displacement curves for L.S.C.6.5. ....	129
Figure D-38. Load versus displacement curves for L.S.E.9.5. ....	129
Figure E-1. Image of the joint performance test. ....	131
Figure E-2. General cyclical plot with description of variables. ....	132
Figure E-3. Differential joint displacement as a function of load applied to the loaded slab. ....	133
Figure E-4. LTE as a function of crack width for the fibers tested in this study for 0.5% V <sub>f</sub> .....	135
Figure E-5. DJD as a function of crack width for the fibers tested in this study at 0.5% V <sub>f</sub> . ....	136
Figure E-6. Average loaded slab displacement as a function of crack width. ....	136
Figure E-7. LTE as a function of crack width to compare the effect of fiber dosage on joint performance. ....	137
Figure E-8. Differential joint energy as a function of crack width to compare the effect of fiber dosage on joint performance. ....	138
Figure E-9. Average loaded slab displacement as a function of crack width to compare the effect of fiber dosage on joint performance. ....	138
Figure E-10. LTE as a function of fiber dosage for a range of crack widths.....	139
Figure E-11. DJD as a function of fiber dosage for a range of crack widths.....	139
Figure E-12. Correlations between LTE, RS and suggesting an approximate RI. ....	140
Figure E-13. Correlations between DJD, RS and suggesting an approximate RI. ....	141

# **1 INTRODUCTION**

## **1.1 Background**

Structural fibers are used in a wide range of applications and include slabs at grade, elevated slabs, concrete overlays, and in any number of other locations. These fibers improve the structural integrity of concrete (i) by keeping cracks/joints tight and most importantly (ii) by transferring load across the concrete slabs when little or no reinforcing steel is used in slabs -on -ground. Structural fibers are presently available in different material compositions, stiffness, shapes, and aspect ratios (AR). Among the various types of structural fibers, structural synthetic fibers have become predominant in the last few decades due to their ease of handling, better dispersion characteristics, and strong durability characteristics. A large number of combinations of fiber types, lengths, and dosages have been utilized in concrete prior to this research. No significant research studies were conducted to characterize the general behavior of fibers for concrete mixtures.

While this work is seeking to characterize the behavior of fibers in the use of FRC in general, it stems from the immediate need to quantify the benefit of structural fibers in thin and ultra-thin concrete overlays, also known as whitetoppings. In that application, fibers are used to mitigate distresses related to concrete pavement, such as joint faulting, longitudinal and transverse panel cracks, and spalling. The characterization in this work will seek to quantify the benefit of various fiber properties (fiber length, AR, geometry, type, and dosage) with the goal of providing the ground work for future fiber selection methods and criteria.

## **1.2 Objectives and Significance**

FRC has been used in numerous laboratory-based research works and in pavement structures dating back to the 1990's in the United States. While many research projects and performance studies have been conducted (Rasmussen, 2004), no significant research has been conducted to characterize the behavior of specific fibers or establish a fiber selection method for FRC-based concrete overlays or any other specific application; however, flexural toughness or residual strength ratio (RSR) has often been specified as a composite quality control measure.

The primary objective of this project is to conduct a laboratory study to quantify the benefit of structural fibers in terms of pre-and post-crack behavior in flexural specimens and to, as a goal, provide methods that characterize the behavior of fibers in FRC. In the laboratory study, 11 fibers were studied, all with varying manufacturers, aspect ratios (AR), length, geometry and fiber type (material composition).

## **1.3 Thesis Organization**

This thesis consists of seven chapters, with each chapter seeking to meet a specific objective. The first chapter is the introductory chapter and consists of the background, research objectives and significance and this section itself 'thesis organization'.

The second chapter consists of the literature review. The literature review is broken into two sections: description of different fibers and effects of fibers on concrete. This chapter summarizes previous research work, as well as give pertinent information related to the present research work.

The third chapter presents the research methodology, where new analysis methods will be presented and described. Those analysis methods include post crack toughness, post-crack performance (PCP) index, and effective working stress (EWS). This chapter ends with the experimental laboratory testing plan.

The fourth chapter presents methods used in laboratory testing including a description of the materials used in this research and procedures for testing conducted in this work. A description of the concrete related materials (cement, fine and coarse aggregate, fibers, etc.) are provided in the materials section, while the methods presented in this section included information related to fresh and hardened concrete tests conducted.

The fifth chapter presents the pertinent results and discussions of the mixtures reported in this work. Those results include the plastic (fresh) and hardened concrete properties. The plastic properties consist of slump, and air content by pressure method, while the hardened concrete properties include compressive strength, chord modulus of elasticity and flexural performance testing per ASTM 1609. Discussion includes the analysis of results presented in this chapter. Relationships will be explored between fiber properties and hardened concrete properties. The fiber properties explored will include fiber length, effective diameter, geometry, and fiber type. The concrete properties considered will include chord modulus of elasticity, compressive strength, modulus of rupture (MOR) in flexure, toughness (flexure), and variations of residual strength.

The sixth chapter discusses the effective working stress (EWS) of fibers embedded into concrete. This method can be used as an additional analysis method in characterization or to calculate approximate fiber dosages for design mixtures.

In the seventh chapter, the conclusions and recommendations for future work will be presented.

The Appendix to this thesis contains five sections and is organized as follows:

- Appendix A: Tables and figures related to the literature review.
- Appendix B: Images of the fibers studied in this work.
- Appendix C: Mixture results not reported or discussed in the body of this thesis.
- Appendix D: Load versus displacement plots from the beams tested in this work.
- Appendix E: A draft report for a study conducted jointly with the work contained in the body of this report. This draft pertains to joint performance of FRC in concrete overlays and provides tools for estimating required fiber dosages. This section also proposes correlations between flexural and joint performances.

## **2 REVIEW OF LITERATURE**

### **2.1 Introduction**

The following literature review first discusses various mechanical and durability characteristics of fibers. Then, properties of fiber reinforced concrete are discussed in terms of the type of material used in the FRC mixture. Since this work focuses on characterization, little emphasis is given to applications of FRC.

### **2.2 Fibers**

Fibers are used for numerous applications in civil infrastructure. A large variety of fibers with varying mechanical properties, such as, tensile stress, modulus of elasticity, degradation characteristics, and strain at failure are available. Fibers vary in longitudinal geometry, effective diameter, cross-section shape, and aspect ratio. Aspect ratio is defined as the ratio of the length of the fiber to the effective diameter of the respective fiber. The properties of fibers can influence the behavior of the resulting FRC mixture in both the cracked and uncracked concrete states.

Fibers, as a whole, can be classified in to two categories: (i) structural or macro fibers and (ii) nonstructural or micro fibers. Misconceptions still exist with many engineers about the difference between structural and non-structural fibers; however, recent improvements in testing standards have given engineers better tools to differentiate between the two. As per Barborak (2011), structural fibers carry load and can be used to replace traditional reinforcement in certain non-structural applications, as well as minimize both early and late age cracking. Typical lengths for macro-fibers are greater than or equal to 1.5 inches. Non-structural fibers, which are less stiff than structural fibers, are generally utilized to minimize early age cracking. According to ACI 544.3R

Guide for Specifying, Proportioning, and Production of Fiber-Reinforced Concrete,” micro-synthetic fibers are defined as fibers with a diameter or equivalent diameters less than 0.012 in (0.3 mm), and macro-synthetic fibers have a diameters or equivalent diameters greater than 0.012 in (0.3 mm)” (ACI 544.3R, 2008).

As per ASTM C1116, Standard Specification for Fiber-Reinforced Concrete (ASTM C116, 2015), fibers are grouped into four categories that describe the parent material of the fiber.

- Type I: Steel
- Type II: Glass
- Type III: Synthetic
- Type IV: Natural

### **2.2.1 Steel Fibers**

Steel fibers are typically produced from carbon steel. Because carbon steels are subject to corrosion, fibers may be produced from stainless steel if deemed necessary (ACI 544.1R, 2009). The ASTM Standard A820, Standard Specification for Steel Fibers for Fiber-Reinforced Concrete, has identified five manufacturing methods of steel fibers and categorized them based on the parent source and production process, and designated them as Type I through Type V (ASTM A820, 2016):

- Type I: Cold-drawn wire
- Type II: Cut sheet
- Type III: Melt-extracted
- Type IV: Mill-cut
- Type V: Modified cold-drawn wire

Figure 2-1 shows different categories of steel fibers. Straight fibers with a round cross-section are typically produced by cutting cold-drawn wire. Fibers of this type can vary greatly in diameter ranging from 0.010 to 0.039 inch (ACI 544.1R, 2009). Straight fibers with a rectangular cross-section can be produced through either a shearing sheet or flattening wire. Steel fibers can also be cut or crimped to enhance the mechanical bond of the fibers to the concrete. Fibers can also be produced by a milling process that creates elongated chips with an irregular cross section. In a similar fashion, fibers can be melt-extracted. This method extracts fibers from a rotating block of near molten steel that allows for chips to be rapidly removed from the block and cooled, creating irregular-shaped fibers. Figure 2-2 through Figure 2-4 show photographs of some commonly available commercial steel fibers.

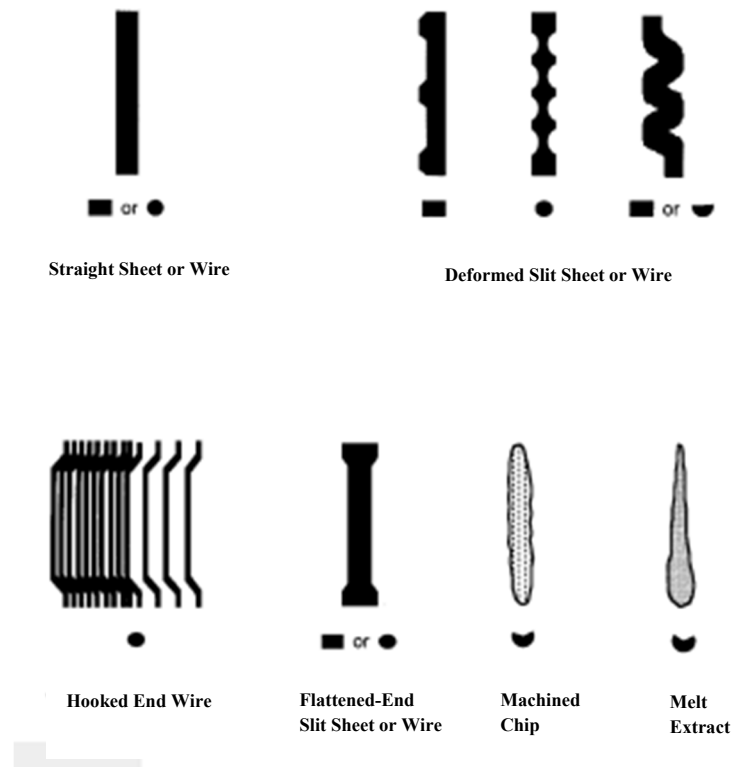


Figure 2-1. Various steel fiber geometries (after ACI 544.1R, 2009)

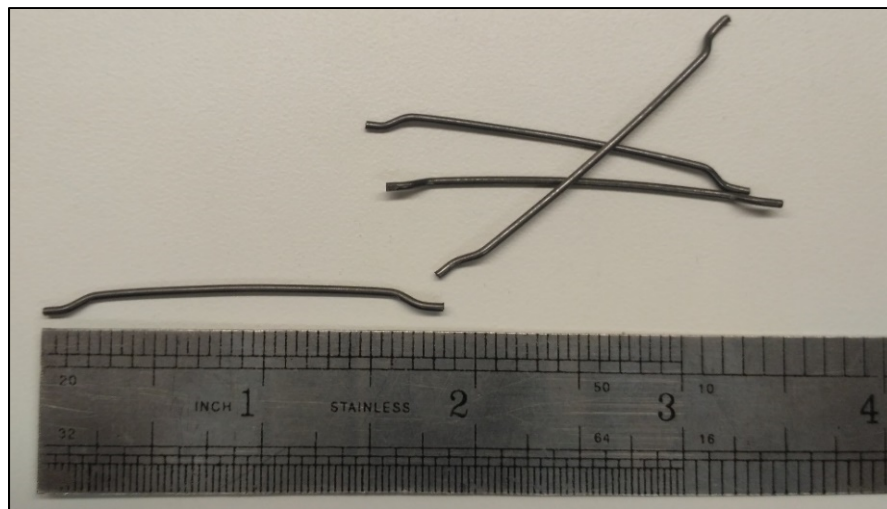


Figure 2-2. Steel fibers having hooked-end geometry.



Figure 2-3. Steel fibers with crimped geometry in whole length.

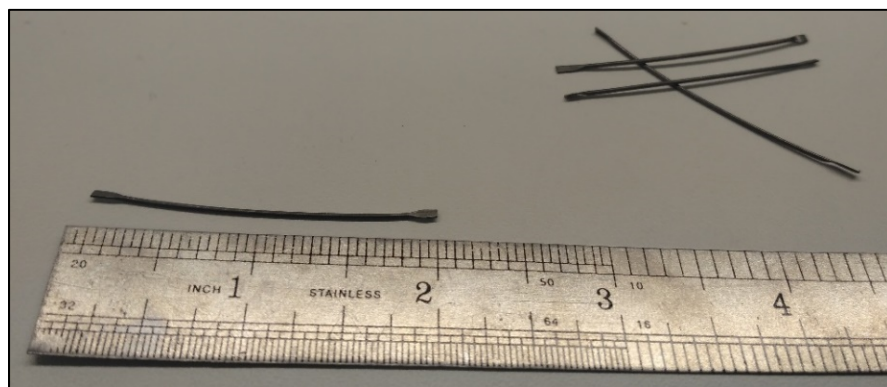


Figure 2-4. Steel fibers with flattened end.

ASTM A820 also specifies the mechanical properties of steel fibers. This specification requires that all steel fibers shall have a minimum average yielding tensile stress of 50 ksi and shall be capable of being bent around a 0.125-inch diameter pin to an angle of 90 degrees at a temperature not greater than 60° F without breaking (ASTM A820, 2016). The bending test provision in ASTM A820 is an indication of ductility to ensure that the fibers will not break during handling. The Portland Cement Association (PCA) suggests a range of mechanical properties of available steel fibers; see Table A-1 in Appendix A.

### **2.2.2 Synthetic Fibers**

Synthetic fibers are produced from a wide range of materials, such as, acrylic, aramid, carbon, nylon, polyester, basalt, polyolefin, polyethylene and the most popular polypropylene (PCA, 2015). Synthetic fibers can be monofilament, micro fibrillated, or macro monofilament. Micro monofilaments are typically small, thin single fibers, as shown in Figure 2-5. Fibrillated fibers are long interconnected bundles that unfurl when mixed into the concrete, see Figure 2-6 for an example. Macro fibers, also known as structural fibers, are similar to monofilaments, but are typically much stiffer and larger than monofilaments as shown in Figure 2-7. Synthetic fibers may also have embossed or textured surfaces to enhance the mechanical bond.

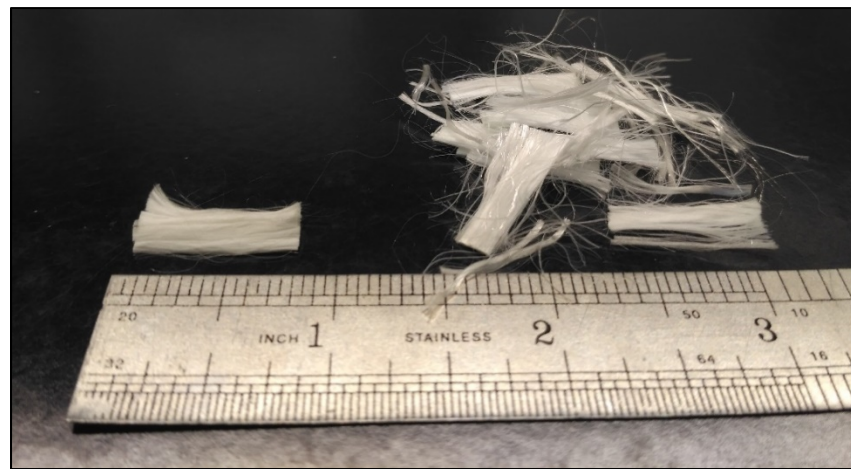


Figure 2-5. Monofilament synthetic fibers (Barman, 2014).

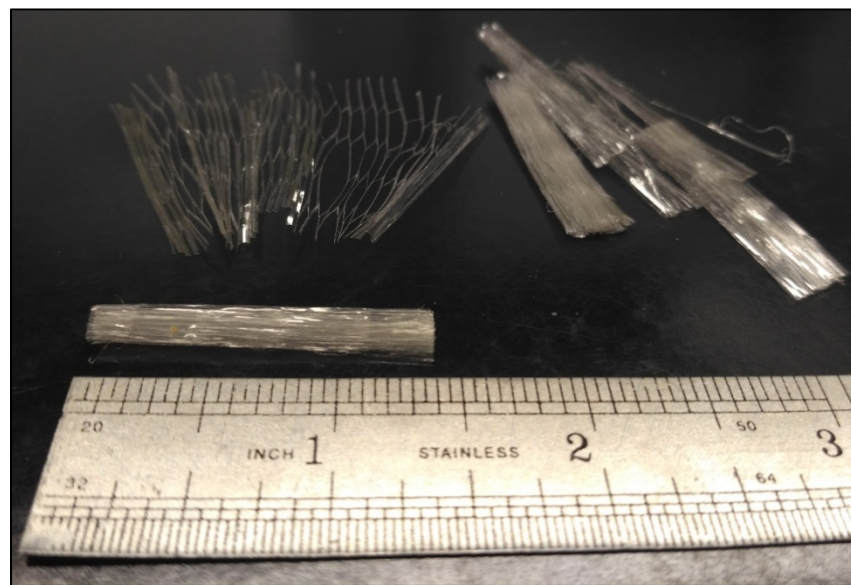


Figure 2-6. Fibrillated synthetic fibers (Barman, 2014).

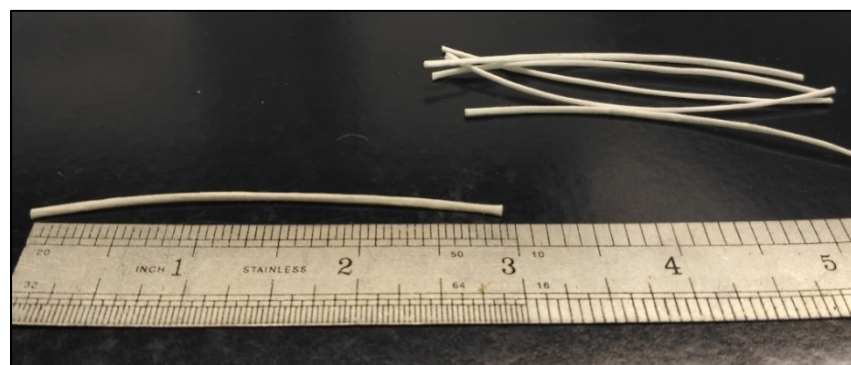


Figure 2-7. Macro synthetic fibers (Barman, 2014).

Acrylic fibers are a product of the textile industry and typically have a tensile strength between 30 and 50 ksi. Researchers have also developed higher tenacity acrylic fibers with tensile strengths up to 145 ksi. One disadvantage of these fibers is its absorption characteristics. They are capable of absorbing 1 to 2.5% of water by weight, which could create problems in fresh concrete properties (ACI 544.1R, 2009).

Aramid fibers possess relatively high strength to weight ratio (nearly 5.5 times lighter than steel) and has similar tensile properties of steel. According to the PCA, aramid fibers are fatigue and creep resistant with the ability to retain dimensional stability at 392<sup>0</sup> F (PCA, 2015). Aramid is hydrophilic and can absorb up to 4.3 % water by weight which could create a disadvantage in fresh concrete properties (ACI 544.1R, 2009).

Carbon fibers are typically produced in strands (tows) that may contain up to 12,000 individual filaments that are dispersed prior to introduction into the concrete matrix (ACI 544.1R, 2009). Carbon fibers are inert to most chemicals and are manufactured with a wide range of mechanical properties, but are typically selected for their high modulus and tensile capacity that may reach 600 ksi (PCA, 2015). Carbon fibers have typically been produced from carbonized polyacrylonitrile (PAN) yarn in a process called “hot-stretching”. Fibers created from PAN are either produced as HM (high modulus) fibers or HT (high tensile strength) fibers. It has been shown that carbon fibers can be made from coal pitch and petroleum, which are much less expensive than carbonized polyacrylonitrile yarn. Coal pitch based fibers are also manufactured into two types: GP (general purpose) and HP (high performance). GP fibers are low in tensile strength and elastic modulus due to their isotropic (non-oriented) fiber structure, whereas

HP (high performance) fibers are high in tensile strength and modulus of elasticity due to their highly oriented strand structure, which comes from a mesophase pitch material (ACI 544.1R, 2009).

Nylon fiber is a generic name for a family of polymers, typically used in a number of industries (ACI 544.1R, 2009). According to the PCA, nylon fibers are produced from a nylon polymer and transformed through stretching, extrusion and heating to form an oriented, crystalline fiber structure (PCA, 2015). Nylon is hydrophilic (water absorbing) and is typically capable of absorbing up to 4.5% water by weight. Typical mechanical properties of these fibers are provided in the Appendix, Table A-1.

Polyester fibers are typically only available in a monofilament form. One method for producing polyester fibers is a melt-extraction method where highly crystalline pellets are converted into filaments that are stretched and cut to the desired lengths. These fibers are nearly hydrophobic in nature and have been proven to not affect the hydration of portland cement. Little research is available to comment on polyesters ability to resist long-term fatigue or durability (ACI 544.1R, 2009).

Basalt fibers are not currently recognized by the PCA or the ACI. Basalt fibers are manufactured from ground basalt in a similar fashion to glass fibers. The fibers are drawn from the basalt at approximately 2700° F and shaped into the desired form. Basalt fibers may have a tensile strength of approximately 400 ksi and a modulus of elasticity of approximately 12,500 ksi (Prince, 2016).

Polyolefin fibers are either dry, wet, or melt spun into filaments. Dry and wet spinning utilizes solvents to allow the fiber to be extruded through a spinneret. The difference between dry and wet spinning lies in when the solvent is evaporated from the

fiber. Melt-extraction involves heating a powder to the point of being a liquid and again extruding it through a spinneret. Polyolefin fibers are typically durable but have been found to require UV protection (Vasile, 2000). Figure 2-9 shows a picture of some structural polyolefin fibers.

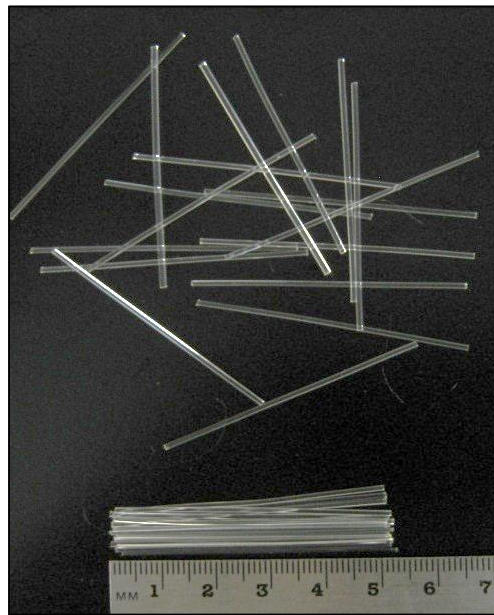


Figure 2-8. Polyolefin fibers, next to ruler length in centimeters (Barman, 2014).

Polyethylene fibers are typically produced with surface deformations or embossments that enhance mechanical bondage in the concrete matrix. These fibers are typically produced as a monofilament (ACI 544.1R, 2009).

The most popular synthetic fiber material, polypropylene, is chemically inert, hydrophobic, and lightweight. The polypropylene fibers can be produced as slender fibers with a rectangular cross section or as continuous cylindrical monofilaments and cut to a specified length. They can be of straight or crimped geometry along the length of the fibers. The mechanical properties of polypropylene are similar to that of polyethylene; however, Table A-1 in Appendix A shows that polypropylene has a much lower strain at

failure and a higher tensile strength (PCA, 2015). Figure 2-9 shows pictures of two macro-structural polypropylene fibers.

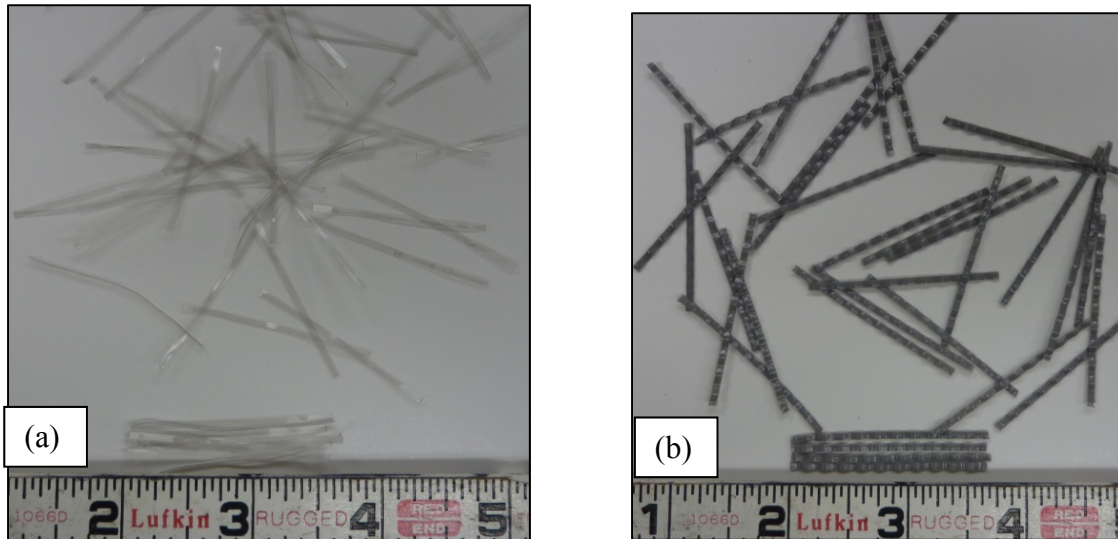


Figure 2-9. Picture of the polypropylene fibers (a) straight geometry, (b) crimped geometry (after Barman, 2014).

### 2.2.3 Glass Fibers

Glass fibers were originally produced from borosilicate (E-glass) and soda-lime (A-glass), their susceptibility to alkali attack was realized shortly after. When these glasses were subject to alkali attack, their mechanical properties would quickly deteriorate and cause the concrete to lose flexural and compressive strength (ACI 544.1R, 2009). As research continued, an alkali resistant glass (AR glass) was developed that resulted in improved long-term concrete properties. ASTM C1666 provides specifications of the physical shape of AR glass fibers and recommendation about the chemical composition of the fibers (ASTM C1666, 2015).

### 2.2.4 Natural Fibers

Natural fiber is a term used to describe fibers whose parent material is naturally occurring. This type includes or has included wood cellulose, sisal, coconut, bamboo,

jute, elephant grass and mammal hairs. Natural fibers are typically labeled as unprocessed natural fibers (UNF) or processed natural fibers (PNF). UNFs preceded the use of reinforced concrete and initially included the use of horse hair and straw in sun baked bricks and mortar. PNFs, traditionally wood pulp fibers, were initially developed to replace asbestos during World War I, but commercial use did not become popular until the 1980's (ACI 544.1R, 2009).

The mechanical properties of UNF's vary greatly based on parent material and moisture content. Many countries, mostly lesser developed regions, have experimented with the addition of UNF's to concrete and have found promising results. However, the durability of these fibers remains to be the point of concern because of reactions between the fibers and cement along with the swelling of fibers in the presence of water. See Table A-1 in the Appendix A for typical mechanical properties (ACI 544.1R, 2009).

## **2.3 Fiber Reinforced Concrete (FRC)**

FRC is known for its enhanced durability, better post-crack performance (Figure 2-10), reduced plastic shrinkage, reduced spalling, and high impact strength in comparison to plain concrete. In general, research has shown that fibers do not significantly increase the compressive strength or modulus of elasticity and tends to decrease the workability (Barman, 2014). Structural fibers improve the toughness, residual strength ratio (RSR), and load transfer efficiency (LTE) of plain concrete (Roesler et. al., 2008; Barman, 2014; ACI 544.1R, 2009)



Figure 2-10. Fibers bridging a crack and providing post-crack performance (Gaddam, 2016).

### **2.3.1 ASTM C1609 Four-Point Flexural Test for FRC**

ASTM C1609 (Standard Test Method for Flexural Performance of Fiber-Reinforced Concrete) is one of the most common test procedures for measuring flexural performance of FRC and will be utilized extensively in this work (ASTM C1609, 2012). While other FRC flexural tests are available, namely ASTM C1550 using a round panel, ASTM C1609 is the most common and relatively easy to conduct.

Figure 2-11 shows a representational schematic of load versus mid-span deflection curves for ASTM C1609 specimens of plain concrete and FRC, which shows the cracking flexural load and the post-crack contribution of the fibers. From ASTM C1609, a number of properties can be calculated, such as, modulus of rupture (MOR), toughness, equivalent flexural toughness ratio, residual strength (RS), and equivalent flexural stress ratio, which is referred as residual strength ratio (RSR) in a 2008 study by Roesler et al.

Toughness is defined as the area under the load versus mid-span deflection curve between 0 mils and 120 mills of mid-span deflection. MOR and RS represents the maximum tensile stress in the flexural specimen. MOR refers to the maximum flexural strength when the concrete cracking occurs. RS on the other hand represents the maximum flexural strength of the fibers at a given mid-span deflection. This work will refer to RS at 120 mils of mid-span deflection. MOR and RS can be defined by Equation 1. RSR is defined by the ratio of strengths at the peak load and 120 mils of mid-span deflection. Other relevant parameters will be discussed in Chapter 4, as required.

The following sections provide a discussion on the properties of different fiber reinforced concretes, often referring to these properties. The testing procedure as it relates to the setup used in this work will be discussed in Section 4.5.

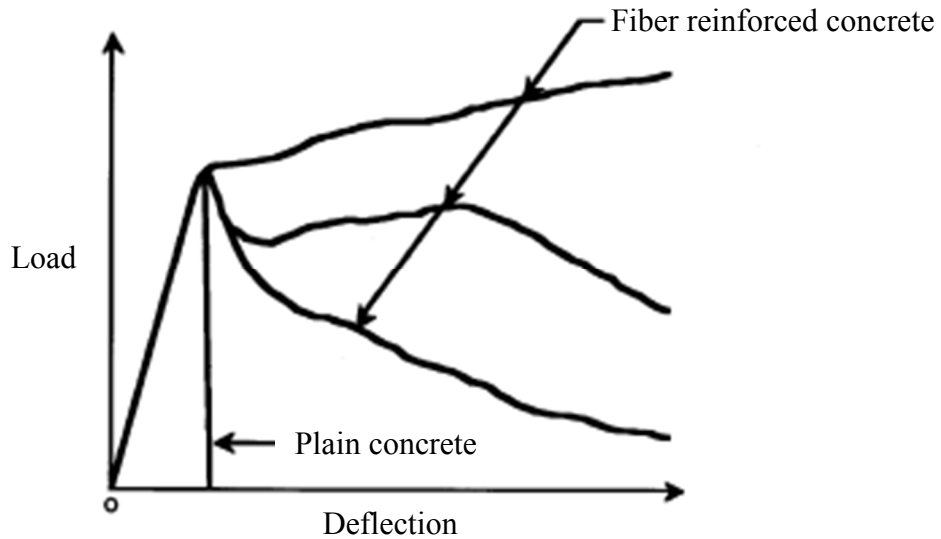


Figure 2-11. Range of load versus deflection curves for plain and reinforced concrete (after ACI Committee 544, 2009).

$$f = \frac{P*L}{b*d^2} \quad \text{Equation 1}$$

Where:

f is the stress in the extreme tension flange (psi).

P is the load at cracking

L is the total span length

b is the average width of the specimen

d is the average depth of the specimen

### 2.3.2 Steel Fiber Reinforced Concrete (SFRC)

Steel fiber reinforced concrete (SFRC) can be used for a number of applications that include slabs -on -ground, elevated slabs, bridges decks and numerous structural elements. Steel fibers are typically added to concrete in volume fractions of 0.25% to 1.5%, but can significantly increase the concrete density (ACI 544.1R, 2009). This section provides a discussion on the different properties of FRC prepared with SFRC.

### 2.3.2.1 Plastic (Fresh) Concrete Properties

With typical fiber dosages (0.25% to 1.5% volume fraction), the measured slump can be reduced by 1 to 4 inches compared to plain concrete (ACI 544.1R, 2009). Like other FRCs, the workability of SFRC is also affected by the fiber's aspect ratio, geometry, matrix proportions and fiber-matrix interfacial bond characteristics (Ramakrishnan, 1987). Figure 2-12 shows the decrease in slump as the reinforcement index increases. The reinforcement index is defined as the volume fraction multiplied by the aspect ratio of the fibers in use.

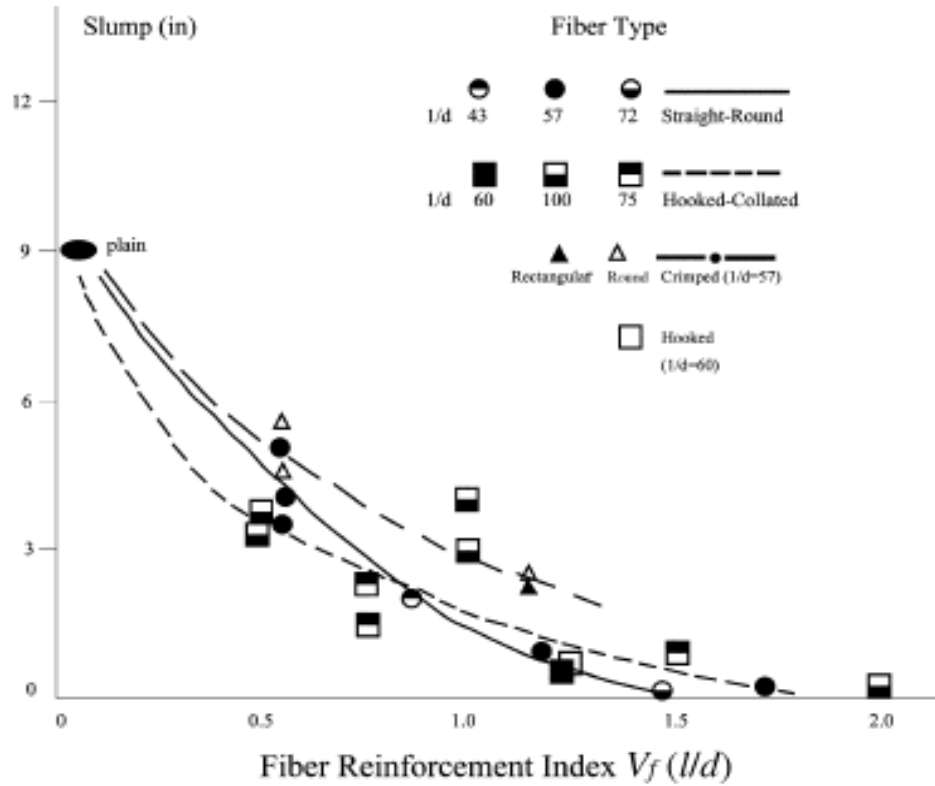


Figure 2-12. Effect of fiber reinforcement index and fiber geometry on the measured slump (after ACI 544.1R, 2009).

In addition to workability considerations, fiber balling is also an issue in SFRC. Steel fibers with an aspect ratio greater than 100 tend to interlock and either ball or form mats of fibers in the mixture (Hannant, 1978). For rigid macro fibers in general, fibers with an aspect ratio greater than 60 may require a blower or to be collated (glued) in order to inhibit balling and matting of fibers (ACI 544.1R, 2009). However, steel fibers with an aspect ratio of less than 50 are unlikely to become interlocked, ball or form mats within the matrix (Hannant, 1978). Balling and the formation of mats of fibers result in poor dispersion and large coefficients of variation in the hardened concrete properties. High aspect ratio fibers are able to positively affect the hardened concrete properties at lower dosages than low aspect ratio fibers, so other considerations must be made to reduce the likelihood of poor fiber dispersion. The American Concrete Institute (ACI Committee 544) states that the tendency of SFRC to have poor fiber dispersion is a function of the maximum size and overall aggregate gradation in the matrix (ACI 544.1R, 2009). The ACI 544 State-of-the-Art Report on Fiber Reinforced Concrete reapproved in 2002 makes a recommendation on the specification for the overall aggregate gradation when using a maximum aggregate size (Table 2-1). See Table A-3 for recommend SFRC mixture proportions.

Table 2-1. Range of ACI recommended aggregate gradation for SFRC  
(after ACI 544.1R, 2002).

Percent Passing for Maximum Size of Aggregate					
U.S. standard sieve size	3/8 inch (10mm)	1/2 inch (13 mm)	3/4 inch (19 mm)	1 inch (25 mm)	1.5 inch (38 mm)
2 (51 mm)	100	100	100	100	100
1 1/2 (38 mm)	100	100	100	100	85-100
1 (25 mm)	100	100	100	94-100	65-85
3/4 (19 mm)	100	100	94-100	76-82	58-77
1/2 (13 mm)	100	93-100	70-88	65-76	50-68
3/8 (10 mm)	96-100	85-96	61-73	56-66	46-58
#4 (5 mm)	72-84	58-78	48-56	45-53	38-50
#8 (2.4mm)	46-57	41-53	40-47	36-44	29-43
#16 (1.1 mm)	34-44	32-42	32-40	29-38	21-34
#30 (600 $\mu\text{m}$ )	22-33	19-30	20-32	19-28	13-27
#50 (300 $\mu\text{m}$ )	10-18	8-15	10-20	8-20	7-19
#100 (150 $\mu\text{m}$ )	2-7	1-5	3-9	2-8	2-8
#200 (75 $\mu\text{m}$ )	0-2	0-2	0-2	0-2	0-2

Research has shown that fibers do not affect free shrinkage, but delay the fracture of restrained concrete during shrinkage and they improve concrete creep characteristics (Altoubat & Lange, 2001). The addition of steel fibers may also increase the number of cracks that form during shrinkage, due to increased internal stresses, but these crack widths are much smaller than in plain concrete (ACI 544.1R, 2009).

### 2.3.2.2 Hardened Concrete Properties: Mechanical Properties

It has been reported that the addition of steel fibers at 1.5% volume fraction can increase the flexural strength by 150% and the direct tensile strength by up to 40% (PCA, 2015). In compression, it has been reported that the addition of steel fibers increases the

ultimate strength between 0% and 15% (ACI 544.1R, 2009). Research has also shown that the increase in fiber content does not linearly increase the mechanical properties of the concrete. Very high-volume fractions of steel fibers decrease the compressive strength and maximum ultimate flexural strength from the peak performance achieved, as shown in Figure 2-13 and Figure 2-14 (Mahadik & Kamane, 2014). According to ACI 544.1R (2009), Poisson's ratio and the modulus of elasticity of the FRC can be approximated to be equal to non-fibrous concrete until the fiber volume fraction exceeds 2% (ACI 544.1R, 2009).

SFRC has tensile capacity after the first crack, so it performs superior in toughness and impact strength as compared to plain concrete. Additions of steel fibers of up to 100 lb/yd<sup>3</sup> drastically increase these properties by enhancing the ductility (Balaguru et. al., 1992). SFRC typically fails when the fibers lose mechanical bondage and pulls from the concrete; fibers with hooked ends give the best toughness results (Balaguru et. al., 1992).

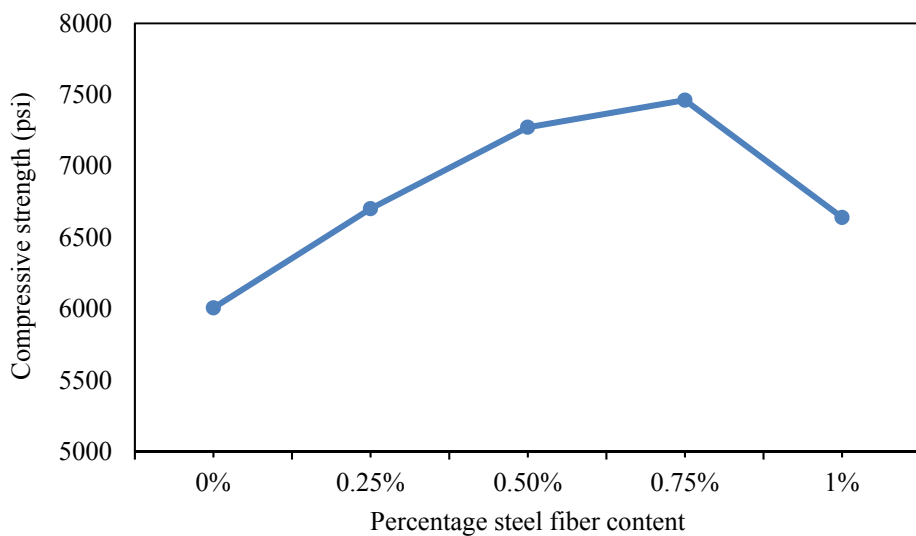


Figure 2-13. Compressive strength vs. percentage of fibers by volume  
(after Mahadik & Kamane, 2014)

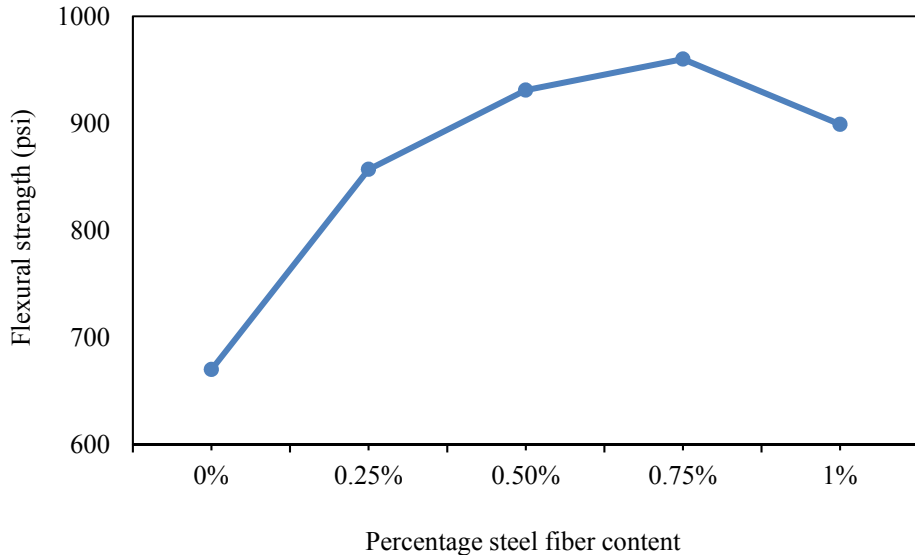


Figure 2-14. Peak flexural strength vs. percentage of fibers by volume (after Mahadik & Kamane, 2014).

### **2.3.2.3 Hardened Concrete Properties: Durability Characteristics**

Research that is available for freeze thaw durability of fiber reinforced concrete shows that the addition of steel fibers does not dramatically affect the end results when compared to plain concrete (Balaguru and Ramakrishnan, 1985). Most of the research that is available on freeze thaw durability and resistance of fiber reinforced concrete focuses on the corrosion resistance of the fibers (ACI 544R.5R, 2010).

Currently there are no standards available to evaluate corrosion in SFRC. Similar to traditional reinforcing bars, steel fiber corrosion is primarily caused by high chloride levels. ACI 544 recommends limiting chloride content to less than 0.6 percent by mass, however research has shown that low carbon content fibers are capable of resisting corrosion when exposed to 2% by mass chloride content in the concrete matrix (Mangat

and Gerusamy, 1987). The behavior of corroded steel fibers is highly dependent on the value of mass loss in the fibers cross section (Kosa and Naaman, 1990).

### **2.3.3 Glass Fiber Reinforced Concrete (GFRC)**

Glass fiber reinforced concrete (GFRC) can be mixed in standard mixers and cast using vibration or slip-forming. GFRC is most commonly used to make small complex shaped components and specialty cladding. AR-glass fibers can be added to concrete mixtures at weight proportions of up to 5% before balling becomes a concern (Pilkington, 1979). Generally, premixed GFRC's will only contain 2% to 3% by weight fibers (ACI 544.1R, 2009). Mixing must be closely controlled in order to minimize fiber damage in the abrasive environment of the mixing.

While the addition of AR glass to concrete mixtures initially increases the mechanical properties over plain concrete, exposure to an outdoor environment (moisture, ultra violet light, etc.) can lead to a reduction of up to 40% from the peak performance (prior to aging) in compressive, flexural and tensile strengths. GFRC also suffers from embrittlement (reduced strain capacity), which may lead to 20% reduction in toughness over the course of approximately 10 years (ACI 544.1R, 2009). The two main causes of long-term degradation of GFRC are alkali attack on the glass fibers and ongoing cement hydration. Ongoing cement hydration causes calcium hydroxide penetration of the fiber bundles which ultimately lowers the fibers tensile strength and increases embrittlement. ACI recommends GFRC for non-structural and architectural applications in their state-of the-art report. GFRC is not currently used in concrete overlays and will not be included in this study.

### **2.3.4 Synthetic Fiber Reinforced Concrete (SNFRC)**

Structural synthetic fibers are the most commonly used fibers in the last few decades. Comprehensive design methods for synthetic fiber reinforced concrete (SNFRC) for specific applications have not yet been developed, but many manufacturers often provide recommendations (ACI 544.1R, 2009). This section provides a discussion on the different properties of SNFRC.

#### ***2.3.4.1 Plastic (Fresh) Concrete Properties***

Research that has been conducted on the effects of synthetic fibers on workability has seen mixed results due to the large number of variables associated with the topic. However, it can be expected that the addition of fibers will decrease the workability (slump) depending on fiber dosage, aspect ratio, geometry, and a number of other considerations. This reduction in slump, due to the fiber addition, may increase the cohesiveness of the concrete and ultimately improve the slip-form characteristics associated with the mixture (Ludirdja and Yougn, 1992). Synthetic fibers placed in concrete at dosages greater than 1.0% by volume tend to form balls, but typically synthetic fibers perform better than steel or glass in those regards (Ludirdja and Yougn, 1992).

Plastic and drying shrinkage has been reported to be reduced by 12% to 25% for polypropylene fibers with volume ranges between 0.1% and 0.3%. It has also been noted that the addition of fibers may reduce bleeding, which is believed to be a result of reduced aggregate settlement and ultimately fewer capillary bleed channels. This effect reduces inter-granular pressures and shrinkage cracking (ACI 544.1R, 2009).

#### **2.3.4.2 Hardened Concrete Properties: Mechanical Properties**

Hardened concrete shows very little improvement to mechanical properties (compressive, tensile, and flexural strength) with low fiber additions (0.1% to 0.2% by volume) in the concretes uncracked states (Zollo, 1984). At higher volumes (e.g., 1.5% volume fraction), the compressive strength was not significantly altered whereas the ultimate tensile strength may increase by 80 percent (Tavakoli, 1994). Little research has been able to prove that synthetic fibers increase the modulus of rupture of the concrete; however, SNFRC has displayed excellent post crack strength and toughness (ACI 544.1R, 2009). It should be noted that synthetic fibers have a wide range of mechanical properties; therefore, it has been difficult in the past to draw conclusions regarding this topic.

The addition of certain synthetic fibers also has a significant effect on the failure mode of specimens in compressive test procedures. Compressive specimens where SNFRC is used tend to fail in a ductile manner and rarely exhibit explosive failure. These specimens can continue to sustain loads well after failure and endure large deformations (ACI 544.1R, 2009).

Research has provided contradictory results for impact strength, where some results show an increase in strength while others show no increase. On the other hand, improvement in the post-crack performance of SNFRC is one of the largest arguments for using synthetic fibers in concrete overlays. The fiber length and ability to bond in the concrete greatly affects its post-crack behavior. It has been found that twisted collated fibrillated polypropylene fibers or fibers with enlargements at its ends had the best mechanical bond strength (ACI 544.1R, 2009).

#### **2.3.4.3 Hardened Concrete Properties: Durability Characteristics**

Limited research is available on the freeze-thaw resistance of SNFRC. Research has shown however that the addition of synthetic fibers does not eliminate concrete degradation due to freeze-thaw damage, deeming it still necessary to air-entrain the concrete in question (Vondran, 1987).

#### **2.3.5 Natural Fiber Reinforced Concrete (NFRC)**

Unprocessed natural fibers (UNF) can have a wide range of effects on natural fiber reinforced concrete (NFRC) due to the wide range of fiber properties. The addition of UNFs to concrete leads to reduced workability due to the absorption properties of UNFs. UNFs are naturally occurring; therefore, the properties will vary with each fiber material type (see Table A-2 in Appendix A for typical values) and within each fiber type. Balling of fibers is also a concern, and like SFRC, balling can be controlled by reducing the aspect ratio, reducing the fiber content and minimizing the maximum aggregate size, etc. (see 2.2.2) (ACI 544.1R, 2009).

Research related to the use of UNF's on hardened concrete properties in FRC is limited (ACI 544.1R, 2009). These properties are also highly variable and unpredictable. The use of processed natural fibers (PNF) in NFRC are similar to the use of UNF's, but because the fibers are processed the concrete quality can be more tightly controlled. PNF's are susceptible to alkaline attack; therefore, long-term durability of the NFRC is a concern (ACI 544.1R, 2009). The increase in water demand due to PNF's absorption properties may also lead to a loss in concrete strength and durability. NFRC is currently not used in concrete overlays and will not be included in this study due to their variability.

### **2.3.6 Hybrid Fiber Reinforced Concrete**

Hybrid fiber reinforced concrete is described as the use of two or more different fibers in order to utilize the properties that can be obtained from the fibers individually. Hybrid fiber systems are used for two purposes: to reduce costs and to take advantage of various fibers properties in the concrete's matrix (ACI 544.1R, 2009). Mixing steel with polypropylene fibers has shown improvements in deflection response, ultimately enhancing both strength and toughness characteristics (Kobayashi and Cho, 1982). Fibers in combination often retain both fibers qualities making it possible to "tailor-make" hybrid fibers for specific applications (ACI 544.1R, 2009). This approach has become desirable due in part to the ability to enhance the elastic and post-elastic strength of the concrete (PCA, 2015).

Hybrid fiber reinforcement has shown that a well-designed mixture exceeds the benefits of the individual fibers performance. Fibers in hybrid FRC can be based on constitutive relationships, dimensions, or functions. Hybrids based on fiber constitutive response occurs when one fiber is stronger and more capable of bridging micro-cracks, delaying crack propagation. The second fiber in this system is much more flexible and leads to improved toughness and strain capacity in the post-elastic zone. Hybrids based on fiber dimension use smaller fibers to bridge micro cracks, leading to better elastic responses, whereas the second fiber is larger in length (and potentially diameter) in order to resist macro-crack propagation and development. Hybrid combinations are also selected based on fiber function. The first fiber will control fresh properties and control plastic shrinkage while the second fiber enhances the hardened concrete properties, either in the elastic and/or the post elastic region (Banthia and Sappakittipakorn, 2007).

## **2.4 Conclusion**

This chapter provided an introduction to fibers for FRC, along with typical plastic and hardened concrete properties of FRC. The literature review discussed the various material types (steel, synthetic, glass, and natural) that fibers are classified as and the physical characteristics of each material. Of the physical characteristics, durability, tensile strength, modulus of elasticity and geometry were all discussed. When discussing FRC, it was found that the addition of fibers reduces slump and generally creates poorer plastic concrete properties. On the other hand, the addition of fibers to concrete dramatically increases the performance of hardened concrete in the cracked state. To improve the uncracked concrete properties, the fibers must have a relatively high modulus of elasticity as compared to the concrete.

### **3 RESEARCH METHODOLOGY**

#### **3.1 Introduction**

The objective of the project was met by conducting an extensive laboratory study, which includes conducting compressive strength (ASTM C39), chord modulus of elasticity (ASTM C469), and flexural strength (ASTM C 1609) tests. In the first phase of this study, tests were conducted on concretes consisting of 11 different fibers at 3 dosages for each. In the second phase of this study, investigation has been extended to characterizing the contributions of fibers in weaker concretes (low compressive strength). Four types of fibers were considered for the second phase study.

This thesis work proposes two new analysis methods for comparing the behavior of FRCs prepared with different types of fibers. This work may serve as the foundation for accounting the benefits of structural fibers in the future mechanistic design procedure for thin concrete overlays. A detailed description of the research approach is described in this chapter.

#### **3.2 Development of Laboratory Analysis Methods**

In current practice, FRCs are commonly characterized by using MOR, RSR and flexural toughness. Since concrete typically exists either in a cracked or uncracked state, it is not necessary or appropriate to use properties that describe both of the states together. For example, MOR describes the hardened, uncracked flexural strength of concrete, but on the other hand the toughness and RSR describe concrete's behavior in both the cracked and uncracked conditions. This can lead to designs that use parameters that do not necessarily describe the actual field conditions. Also, as will be seen later

(Section 5.3.2.6) an increase in concrete strength reduces RSR because concrete strength effects the MOR much more significantly than it does to the RS.

The new parameters proposed in this study are likely to describe the post-crack behavior of FRCs in a more logical manner. It is anticipated that FRCs can be discriminated between the fiber types and dosages more easily and accurately than it can be done with the RSR. This thesis also proposes a new method for approximating the effective allowable tensile stress of fibers embedded into concrete.

### 3.2.1 Post-Crack Toughness

Figure 3-1 shows example load vs deflection curves for three concretes that consists of 0.25%, 0.5% and 0.75% V<sub>f</sub> fibers. As shown in this figure, a load vs displacement curve obtained in the ASTM C1609 test can be broken into 3 sections: (i) pre-crack zone, (ii) Zone A, and (iii) Zone B . The area under the curve in the pre-crack zone is typically similar between different fibers and may not significantly influence the overall toughness of the concrete in post-crack behavior perspective; however, the area under the curve in Zone A (area between the displacement at peak load and 30 mils of mid-span deflection) has been seen to increase for weaker, poorer performing fibers, as those fibers take a longer period of time to stabilize and form resistance to continued mid-span deflection after cracking.

The area of the load-deflection curve between 30 mils and 120 mils of mid-span deflection is referred as Zone B. Since FRC beams tested in the current and many other relevant studies show similar load-deflection behaviors in the pre-crack Zone and Zone A, Zone B purely represents the fibers' benefit to the composite (plain concrete plus fibers). Based on the results from several trial beams tested in this study, the area of the

load vs deflection between 30 mils and 120 mils was used for calculating the toughness under the Zone B. It was observed that Zone A ends approximately near the 30 mils mid-span deflection. This toughness is referred to as the post-crack toughness in this thesis, and the ASTM C 1609 test results were used to investigate the application of this parameter.

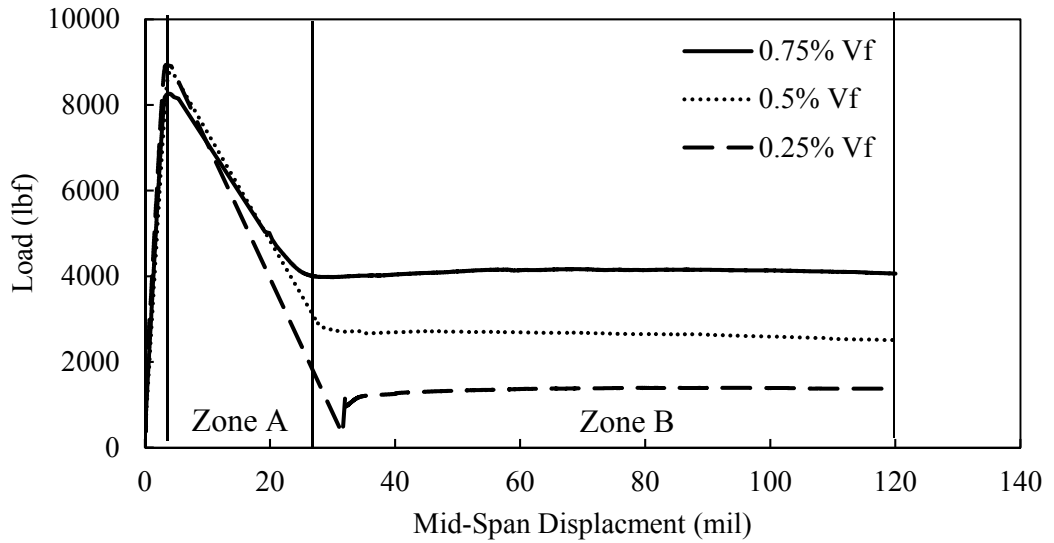


Figure 3-1. Example of a load versus mid span displacement plot. ( $V_f$  = volume fraction of fibers with respect to the total weight of concrete)

### 3.2.2 Post Crack Performance (PCP) Index

The second property is referred to as the post-crack performance (PCP) index, which is proposed to recognize a fibers' efficiency across multiple fiber dosages. Figure 3-2 shows a relationship between fibers  $V_f$  and residual strength normalized with the standard atmospheric pressure (14.7 psi). The residual strength is normalized to make this property a true index, unitless. This PCP index is calculated by summing the area under the volume fraction vs normalized RS (Figure 3-2). This index will allow for the simultaneous direct numerical comparison of the benefit of a specific fiber, geometry, or other variable. The PCP index characterizes a fibers ability to resist crack propagation.

This index will prove to be invaluable because graphical comparison of fiber behavior, for example, the use of RSR versus volume fraction plots as shown in Figure 3-3, can be difficult and subjective when considering several fibers and variables. As shown in this figure, fibers do not always contribute uniformly across the various fiber dosages. The PCP index can be used to qualify fibers for use in application, create stronger correlations to fiber volume fraction, and serve as a quality control measure for fiber selection.

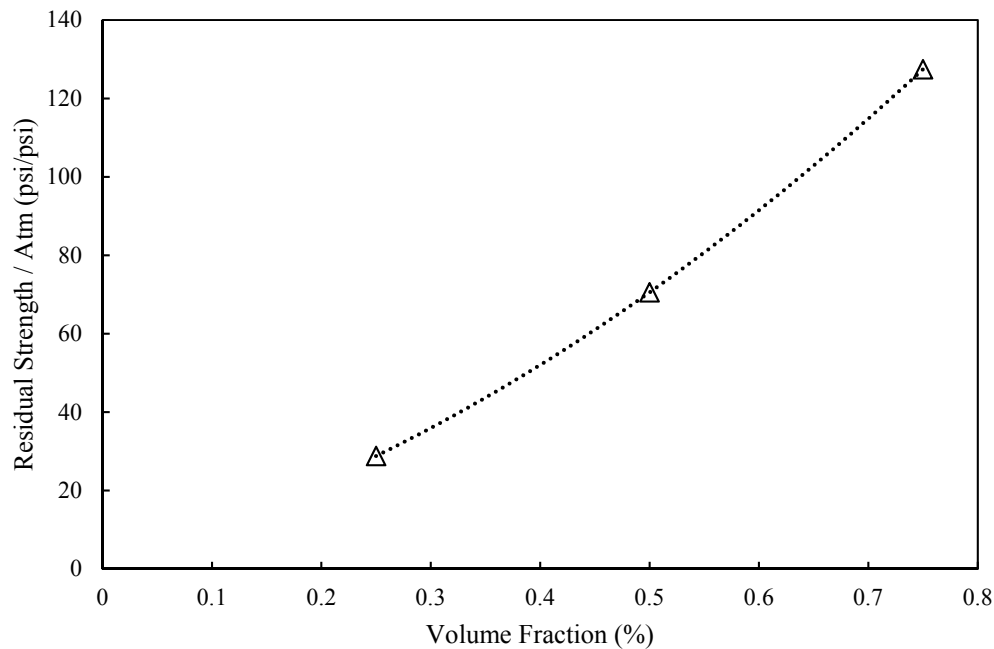


Figure 3-2. Residual strength versus Reinforcement Index Plot is plotted for a typical fiber.

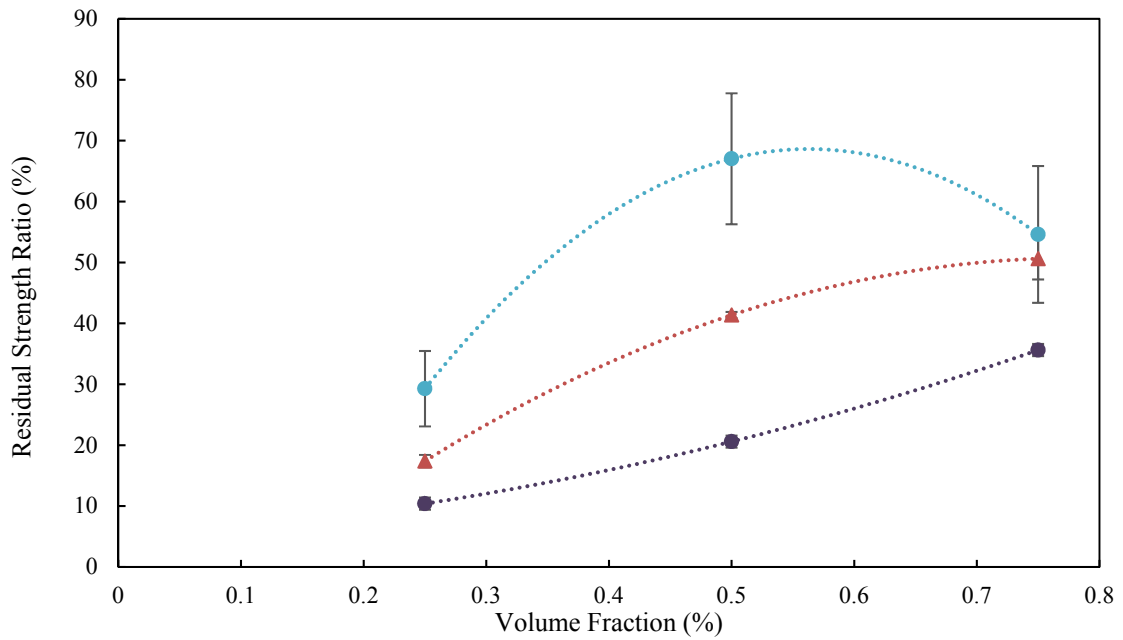


Figure 3-3. RSR is displayed as a function of volume fraction of fibers in the mixture.

### 3.3 Presentation of a Mechanistic Estimation Method

To the best of the author's knowledge, there are no appropriate methods are currently available for mechanistically estimating flexural performance of FRC or maximum fiber tensile stress based on concrete strength, fiber type, geometry, or dosage. For this reason, fibers are difficult to account for in the design without extensive trial testing. This work will seek to provide a solution to this problem in the cracked state of a FRC specimen in flexure.

This method will also create an additional tool for comparing fibers performance and behavior. From this method, an effective working stress (EWS) of the fibers can be calculated. EWS refers to the amount of stress that fibers can be subjected to, prior to pulling from the concrete, which leads to plastic deformation. Chapter 5.4 will provide derivations, explanations of unknowns, assumptions, and solutions to this problem.

### 3.4 Experimental Laboratory Testing Plan

In order to complete the objectives associated with this work, eleven fibers were selected for testing, later described in Section 4.2.1, to observe the effect of fiber length, geometry and type on FRC performance. These fibers were tested at three dosages (0.25%, 0.5%, and 0.75% volume fraction) to evaluate the fibers behavior at various fiber dosages. In a final stage of testing, four fibers were selected and cast into concrete that was tested 24 hours after casting in order to observe the fibers behavior in lower strength concrete. In total, 38 mixtures were cast, tested, and reported in this work and are summarized as follows: 33 FRC mixtures (11 fibers x 3 dosages) and one plain mixture at a single compressive strength and 4 additional FRC mixtures tested at 24 hours after testing. Figure 3-4 shows the flow of work conducted, while Table 3-1 shows a summary of the work conducted in this report.

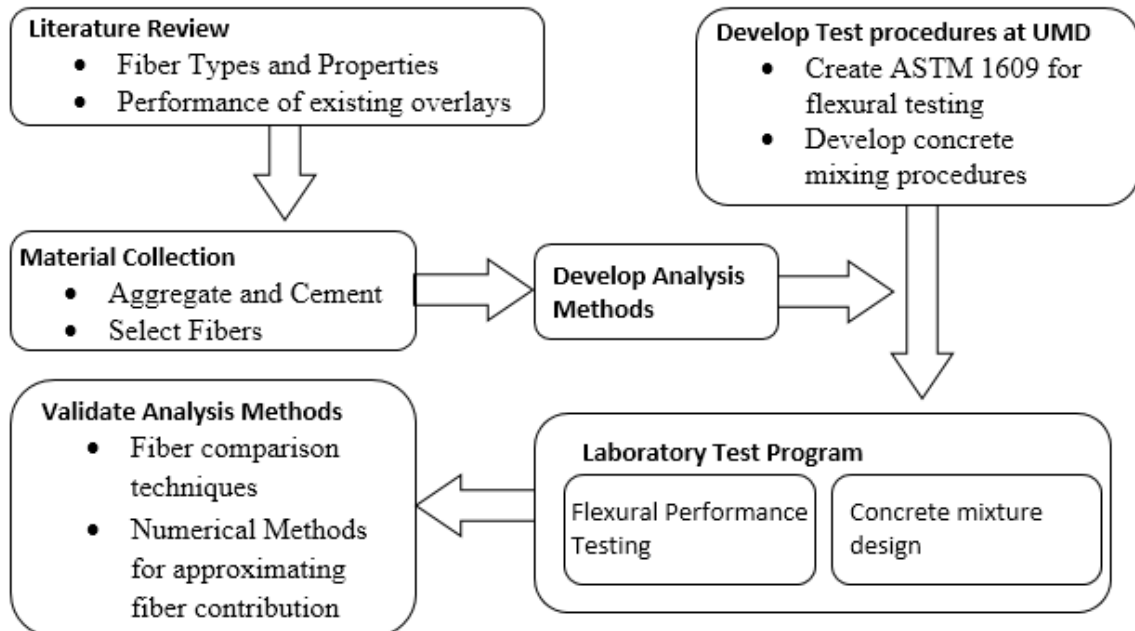


Figure 3-4. Flow chart of work conducted.

Table 3-1. Testing matrix for the work conducted.

			Tests to be Conducted		
Phase	# of Fibers	Dosages	Compressive Strength	Modulus of Elasticity	Flexural Performance
1) High Strength	11	3	3	3	5
2) 18 Hours After Casting	4	1	3	-	5
Total Number of Samples	-	-	111	99	185

### 3.5 Conclusion

This chapter discusses the development of laboratory analysis methods, presents mechanistic estimation method and lays out the experimental laboratory plan. The laboratory analysis methods included post-crack toughness and the post-crack performance (PCP) index. The mechanistic estimation method creates a tool for approximating the effective working stress (EWS) of fibers and allows for post-crack flexural performance to be estimated. Finally, the experimental laboratory plan details the scope of work conducted in this study, which includes four-point flexural testing, compressive testing and modulus of elasticity testing for 38 mixtures.

## **4 MATERIALS, TESTING, AND PROCEDURES**

### **4.1 Introduction**

After the literature review was conducted, an experimental testing plan was established, concrete materials such as, cement, aggregates, structural fibers, and admixtures were collected, and the mixing procedures for laboratory concrete mixing, specifically for FRC, were established. Proportioning and batching was performed for a large number of concrete mixtures that varied with fiber types and dosages. Fresh concrete tests such as slump and air content by pressure method were conducted for each mixture considered in this research. Hardened concrete testing consisted of compression testing, flexural testing, and chord modulus of elasticity testing. With exception to the testing conducted at 24 hours after casting for lower strength concrete, the tests related to the hardened concrete properties were conducted after curing the concrete for 28 days in an environmental chamber at a 95% relative humidity and 70° F temperature.

### **4.2 Material**

This section presents the details of the materials used in the laboratory study. Description is provided on the fibers type and their properties, aggregates and their gradations, cement, and admixtures, such as air entrainer and water reducer. Concrete mixture proportions are also presented in this section.

#### **4.2.1 Fibers**

A wide variety of fibers are commercially available; however, the fibers used in this study will be restricted to structural macro fibers made from either steel or polypropylene. From the literature review three fibers dosages were selected: 0.25, 0.50 and 0.75 percent volume fraction ( $V_f$ ) of the total volume of concrete. The 0.25 percent

$V_f$ (approximately 3 to 3.5 pounds per cubic yard for synthetic fibers) represents a low, but common dosage implemented in concrete. The 0.75 percent  $V_f$  was selected because it is likely the maximum dosage that could be implemented without experiencing significant fiber balling, while 0.50 percent  $V_f$  represents an intermediate dosage between 0.25 and 0.75 percent  $V_f$ .

Eleven different types of fibers were included for this work based on variables to be considered including fiber type, geometry, length, aspect ratio, and manufacturer. Nine of the fibers selected were synthetic polypropylene, while only one fiber was steel. Of the eleven fibers in this study, four fibers were flat and straight in cross section, three were embossed, two were twisted, one fiber was continuously crimped, and one was end crimped. Photographs of the fibers used in this study can be found in Appendix B. See Table 4-1 for other descriptive information related to the fibers selected. The main differences between the four straight synthetic fibers (Fiber 1 through 4) are the manufacturer, length and aspect ratio; stiffness's of these fibers were similar. Fiber 6 and 11 varied in length and aspect ratio. Fiber 7 and 9 of the three embossed fibers were of same length and manufacturer, except Fiber 7 was chemically enhanced for improved bonding to cementations matrices.

Table 4-1. Description of fibers investigated in this research

Fiber Serial Number	Geometry / Type	Length (inch)	Aspect Ratio, Specific Gravity, Modulus of Elasticity (ksi), Tensile Strength (ksi)
Fiber 1	Straight / Synthetic	1.5 or 2	*94, 0.91, N/A, 70
Fiber 2	Straight / Synthetic	1.5 or 2	*100, 0.91, N/A, 70
Fiber 3	Straight / Synthetic	1.55	90, 0.92, 1378, 90
† Fiber 4	Straight / Synthetic	*1.625	96.5, 0.91, N/A, 70
† Fiber 5	Twisted Straight / Synthetic	2	74, 0.92, 1380, 87-94
† Fiber 6	Continuously Crimped / Synthetic	2.0	*60, 0.91, N/A, N/A
Fiber 7	Embossed / Synthetic	2.1	70, 0.91, N/A, 85
Fiber 8	Embossed / Synthetic	1.89	*66, 0.90-0.92, 1450, 93
† Fiber 9	Embossed / Synthetic	2.1	70, 0.91, N/A, 85
Fiber 10	End Crimped / Steel	2.4	65, 7.8, 29000, N/A
Fiber 11	Twisted / Synthetic	*1.5-2.25	*150-200, 0.91, N/A, 90

Photographs of these fibers are provided in the Appendix B.

N/A: Information not available

\*Approximate measurement, not by manufacturer

† Phase 2 fibers

#### 4.2.2 Aggregate

The fine and coarse aggregates used in this project were collected from a quarry, operated by Duluth Ready Mix, near Canyon Minnesota and can be seen in Figure 4-1.

The fine aggregate was washed sand; the gradation can be seen on Figure 4-2 and Table 4-2. The bulk specific gravity of the fine aggregate was 2.68. The coarse aggregate was a rounded to sub rounded gravel with a bulk specific gravity of 2.75. See the gradation in Figure 4-2 and Table 4-2. A Los Angeles Abrasion test was conducted on the coarse aggregate that resulted in a mass loss of 9.2 percent.



Figure 4-1. Coarse aggregate and fine aggregate used in this project.

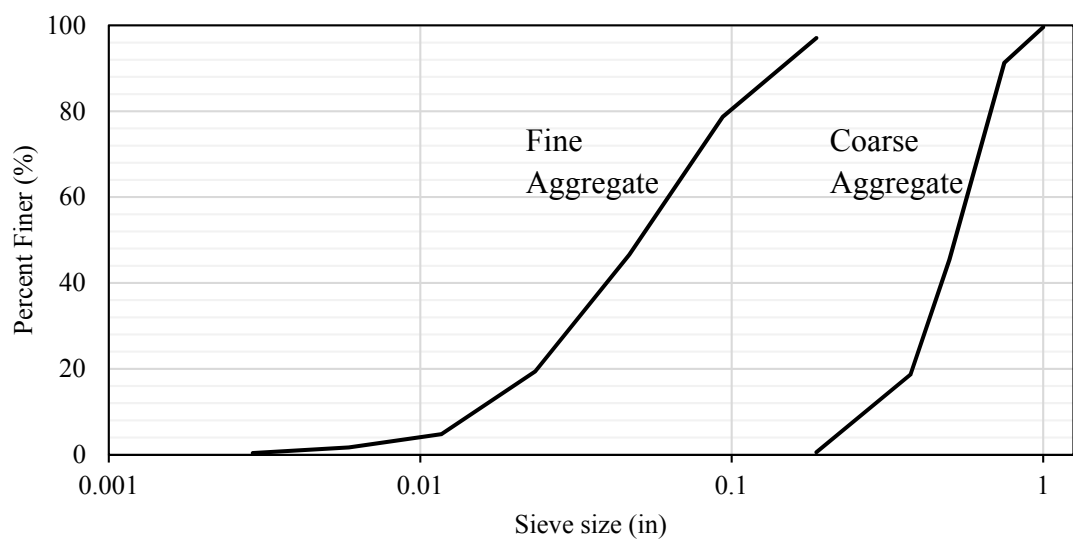


Figure 4-2. Gradations for the coarse and fine aggregates used in this project.

Table 4-2. Percent passing table for fine and coarse aggregate in this study.

Sieve Number	Passing (%)	
	Fine	Coarse
1"	-	99.6
3/4"	-	91.3
1/2"	-	45.4
3/8"	100	18.7
4	97.1	0.7
8	78.7	-
16	46.6	-
30	19.4	-
50	4.8	-
100	1.7	-
200	0.4	-
Pan	0	0.1

#### 4.2.3 Mixture Design

The mixture design used in this work was developed after numerous trial batches.

Initial trial batching was performed with 580 lb/yd<sup>3</sup> of cement; however, the workability and consolidation issues when using higher fiber dosages encouraged the use of a higher content of cement (615 lb/yd<sup>3</sup>). ASTM Type I cement was used. Table 4-3 shows the base concrete design for the mixtures used in this study. Both the volume fraction and mass of the ingredients are provided in this table. As the fiber dosage was increased, the sand content was slightly decreased (volume of sand per volume of fibers) to make up the volume difference. No volume change was made in coarse aggregate fraction and cement content as a result of changing the fiber volume fraction. The air entraining admixture (AEA) was increased for an increase in fiber dosage in order to maintain an entrained air content in the range of 5.5 percent to 9 percent by volume. AEA dosage ranged between 0.98 to 1.06 ounces per 100 lb of cement. The mid-range water reducer (WR) was also

increased for an increase in fiber dosage (slump was maintained to a range of 0.5 inches to 3 inches) and ranged between 5.93 to 7.25 ounces per 100 lb of cement.

Table 4-3. Base mixture design for concrete mixes for this study.

	<b>Volume (%)</b>	<b>Approx. Mass (lb/yd<sup>3</sup>)</b>
Cement (Type I)	11.6	615.0
Coarse Aggregate	42.0	2024.0
Fine Aggregate	25.1	1188.8
Potable Water	13.9	233.7
Fibers	varied	varied
BASF MasterAir® 400 (fl. Oz)	-	6.08
MasterPolyheed® 1020 (fl. Oz)	-	36.5

#### **4.2.4 Mixture Designations**

In order to properly and concisely designate the thirty-eight different mixtures in this report, all of the mixtures were given designations. The designations describe each mixture according to the fibers material type, geometry, fiber designation and fiber dosage (percentage of total volume) used in the respective mixture. Table 4-4 describes the nomenclature in the mixture designation. For an example, the mixture designation ‘H.S.S.1.25’ represents a mixture comprised of a higher strength concrete (H), synthetic fibers (S), a fiber with a straight (S) geometry, a fiber with a serial number of 1 (see Table 4-1 for the length, aspect ratio, density, etc.), and a fiber dosage in terms of volume fraction of 0.25 percent.

Table 4-4. Nomenclature for the mixture designation

<b>Concrete Strength</b>	<b>Fiber Material</b>	<b>Fiber Geometry</b>	<b>Fiber Number</b>	<b>Dosage (<math>V_f \%</math>)</b>
High (H)	Synthetic (S)	Crimped (C)	See Table 3.1	0.25
18 hour - Low (L)	Steel (L)	End Crimped (EC)		0.5
		Embossed (E)		0.75
		Straight (S)		
		Twisted (T)		

### **4.3 Concrete Mixing Procedure**

In order to efficiently and consistently produce the concrete required for this work, a mixing procedure needed to be developed. Initial trial mixtures were conducted per ASTM C192, the procedure for making and curing concrete specimens in the laboratory, in which all of the materials are added to the mixer, the concrete mixture was mixed for three minutes, allowed to rest for three minutes, and then finally mixed for an additional 2 minutes. This procedure was conducted after mixing a butter batch (small batch of concrete to condition the inside of the mixer, and wheel barrow). Figure 4-3 shows an image of the concrete mixer used in this project. The following observations were made:

- Fibers were not properly dispersed.
- It was difficult to consistently obtain the required air entrainment.
- Fibers had a tendency to ball and mat. Figure 4-4 shows an image of fiber balling.



Figure 4-3. Concrete mixer used in this study.



Figure 4-4. Fiber balling in a concrete mixture.

From the above-mentioned observations, an extended procedure was adopted that provided more consistent slump, air entrainment, and fiber distribution. The mixing procedure was conducted after the implementation of a butter batch, and is as follows:

1. All fine aggregate and air entraining admixture (AEA) were added to the mixer with 1/3 of the mixing water and mixed for 2 minutes.
2. The coarse aggregate was added to the stopped mixer.
3. The mixer was turned on and the fibers placed in the mixer by hand with care to pull apart balls or mats, mixing for a total of 3 minutes.
4. With the mixer still turning, the cement, remaining mixing water and water reducer were added to the mixer and mixed for 3 minutes.
5. The mixer was stopped and the mixture allowed to rest for 3 minutes.
6. The mixture was mixed for two final minutes.

#### **4.4 Plastic (Fresh) Concrete Testing**

In this work, multiple fresh concrete tests were performed. The tests included slump and air content (by pressure method). These tests were conducted as quality control measurements to ensure that hardened concrete results were comparable. The following subsections briefly describe those tests and the target values for this study.

##### **4.4.1 Slump Test**

A slump test was conducted in accordance to ASTM C143 after the concrete mixing procedure was completed and again after any additional admixture was added to the mixture (ASTM C143, 2015) to attain the desired workability. The target slump range was 0.5 inches to 3 inches which is common for slabs -on -grade. Figure 4-5 shows a

photograph of slump test conducted on a low workability fiber reinforced concrete mixture.



Figure 4-5. Slump test on FRC mixture.

#### 4.4.2 Air Content by Pressure Method

Air content was measured by pressure method and was conducted after the mixing procedure was completed and again after any additional admixture was added to the mixture (ASTM C231, 2017). The target air content was 6% with an acceptable range of 5.5% to 9%. Figure 4-6 shows an air content test being conducted.



Figure 4-6. The air content by pressure method test is in progress.

#### 4.5 Hardened Concrete Testing

In this research, three hardened concrete tests were conducted: compressive strength, static modulus of elasticity of concrete in compression, and flexural performance of fiber reinforced concrete, also referred to as a RSR test in this report. The following subsections briefly describe those test procedures.

##### 4.5.1 Compressive Strength Testing

Concrete compression testing was conducted on 6-inch diameter by 12-inch height cylindrical specimens to avoid preferential fiber alignment in smaller cylinders. It may also be stated that the size of the test cylinders depends on the length of the fibers, where the minimum cylinder diameter should be equal to or greater than three times the maximum fiber length (ACI 544.2R, 1999). A minimum of 4 cylinders were cast for each mixture. The specimens were tested as per ASTM C 39 (ASTM C39, 2017). Figure 4-7 is

an example of a compression test taking place at the University of Minnesota Duluth (UMD).



Figure 4-7. An example of a concrete compression test per ASTM C39.

#### 4.5.2 Modulus of Elasticity

The modulus of elasticity procedure was conducted on 4 inches by 8 inches specimens to accommodate the testing equipment available at UMD. It may be mentioned here that conducting this test with 6-inches by 12-inches specimens would be the most appropriate; however, UMD's civil engineering lab currently does not have the equipment for conducting the test with 6-inch by 12-inch specimens. At least three specimens were tested per mix (ASTM C469, 2014). After conducting the modulus of elasticity test, specimens were then broken for ultimate compressive strength per ASTM

C39. As 4-inch by 8-inch specimens were used, modulus of elasticity of concrete was also computed based on the compressive strength, obtained using 6 inch by 12 inch specimens; the ACI Equation used for this purpose.

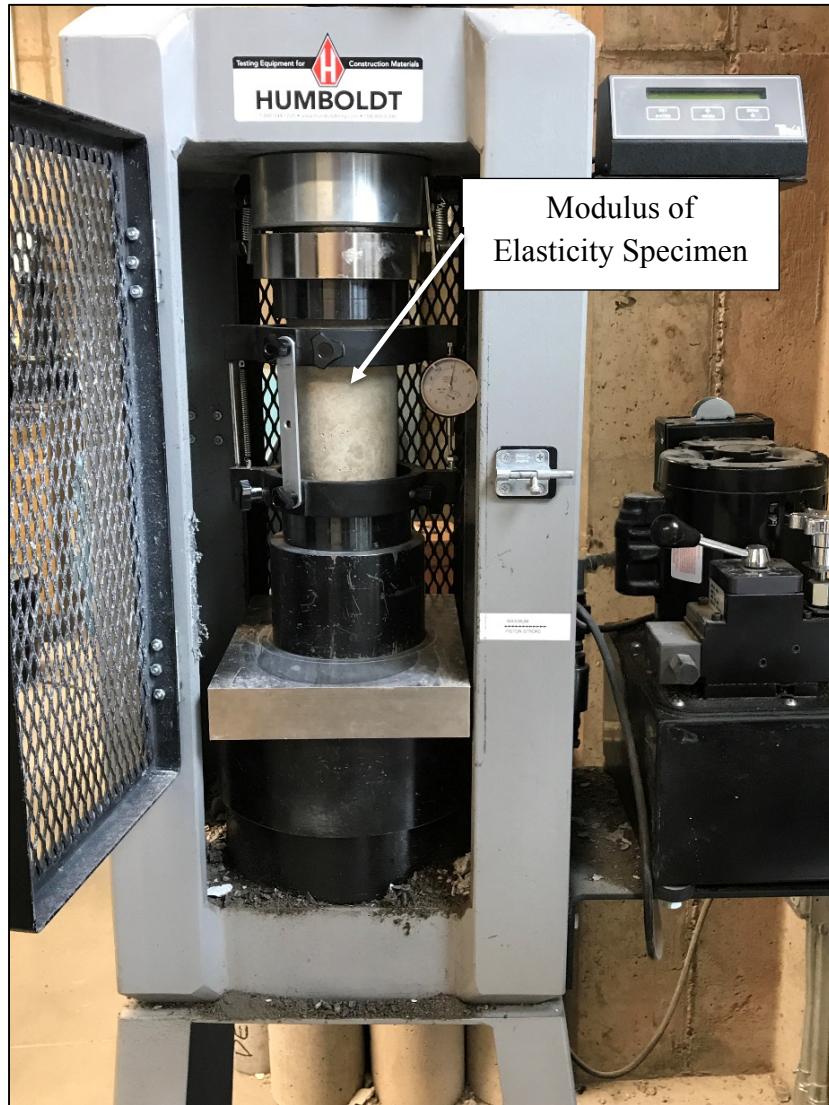


Figure 4-8. An example of a Modulus of Elasticity test per ASTM C469.

#### 4.5.3 Flexural Testing per ASTM C1609

The flexural performance test was conducted as per ASTM 1609 (standard test method for flexural performance of fiber-reinforce concrete). MOR, RS, RSR, and toughness was determined from the flexural performance test as mentioned in 2.3.1. The

dimensions of the beam specimens were 21 inches x 6 inches x 6 inches. The length of the span was 18 inches. For each mix, five beam specimens were tested. Figure 4-9 shows a photograph of this test being conducted at UMD and Figure 4-10 shows fibers restraining a crack during a flexural performance test. For this work, a total of 175 good beams and dozens of trial beams were tested for flexural performance.

In this test, mid-span deflection and applied force are collected in order to generate the load vs displacement curves as shown in Figure 4-11. These plots can be used to compute the MOR, RS, RSR, toughness, post-crack toughness, and the PCP index. Figure 4-11 provides examples of load vs displacement curves for synthetic and steel fiber reinforced concrete prepared with a 0.5 percent  $V_f$  fiber dosage, more comparisons will be made in Chapter 5. In both of the curves, it can be seen that the applied load does not drop to zero immediately after the peak load, fibers restrain the crack and carry residual load while the displacement increases. In general, the post-peak load drop for synthetic fibers is greater than for steel fibers.

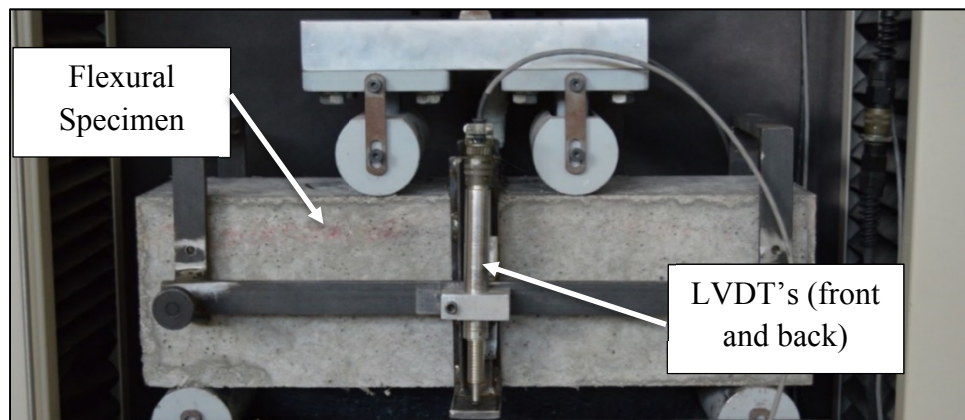


Figure 4-9. An example of a flexural performance test for fiber-reinforced concrete per ASTM C1609.



Figure 4-10. An example of a crack developed after peak load was achieved in a flexural performance test.

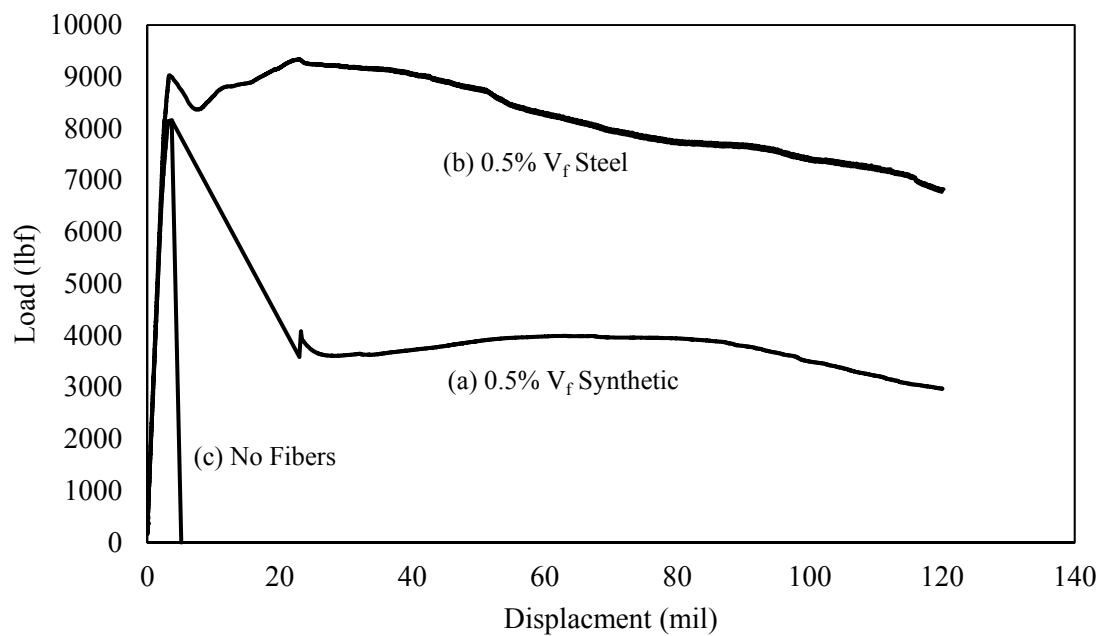


Figure 4-11. Typical displacement versus load plots: (a) synthetic (b) steel fiber, (c) no fibers.

#### **4.6 Conclusion**

The fourth chapter provided information related to the materials, concrete mixing procedure, and the concrete testing procedures implemented in the experimental testing plan. The materials in this work included eleven different fibers, coarse aggregate, fine aggregate, cement and admixtures. The concrete mixing procedure section discussed the progression of the mixing procedure and provided a detailed description of its final version. The plastic concrete tests in this work only included the slump and air by pressure method tests, while the hardened concrete tests included modulus of elasticity, compressive strength and four-point flexural testing.

## **5 ANALYSIS AND DISCUSSION OF LABORATORY RESULTS**

### **5.1 Introduction**

The behavior of fiber reinforced concrete is dependent on various fiber properties, such as, length, aspect ratio, and dosage. These properties influence the hardened properties of concrete such as, RSR, RS, toughness, post-crack toughness, and PCP index. This chapter will analyze the results of the tests conducted in this study and discuss the effects of fiber aspect ratios, geometries, dosages, and lengths on the above-mentioned hardened concrete properties. Also, the properties of the fresh concrete that were used to prepare the specimens will be discussed in this chapter.

### **5.2 Plastic (Fresh) Concrete Properties**

Since the main objective of this work was to investigate the effect of fiber properties on the flexural performance of the hardened concrete, it was required to keep the fresh concrete properties consistent among the mixtures. In order to consistently create concrete with an acceptable slump and air entrainment, the admixture contents and fine aggregate proportions were altered for each mixture, as required. Since the range of fresh concrete properties is purposefully kept narrow, it would not be appropriate to draw strong quantitative conclusions based on the fresh concrete properties. Qualitatively, some observations can be made regarding air content and slump.

In general, fiber geometry, aspect ratio (mostly diameter of the fiber) in combination with dosage appeared to play the largest role in the fresh concrete properties. Due to these observations, the fresh concrete properties are plotted and analyzed with respect to a parameter called reinforcement index (RI), which is the product of aspect

ratio (AR) and volume fraction of fibers ( $V_f$ ). As RI is function of both AR and  $V_f$ , the influence of fibers on the concrete properties can be presented in a more rational way.

### 5.2.1 Air Content by Pressure Method

The average of the air content for all the mixtures was 6.9 percent and ranged from 5.5 to 9 percent. Figure 5-1 presents the plot of the air content for all the mixtures. In these figures, the average air content is plotted as a dashed line, while plus and minus one standard deviations are plotted as solid lines. Because of admixture dosage changes with increases in fiber dosages, it is not appropriate to make quantitative conclusions on how fiber dosage or geometry affect air content; however, as a side effect to an increase in dosage, it is apparent that it becomes more difficult to obtain proper air entrainment, likely due to the increase in difficulty mixing the concrete.

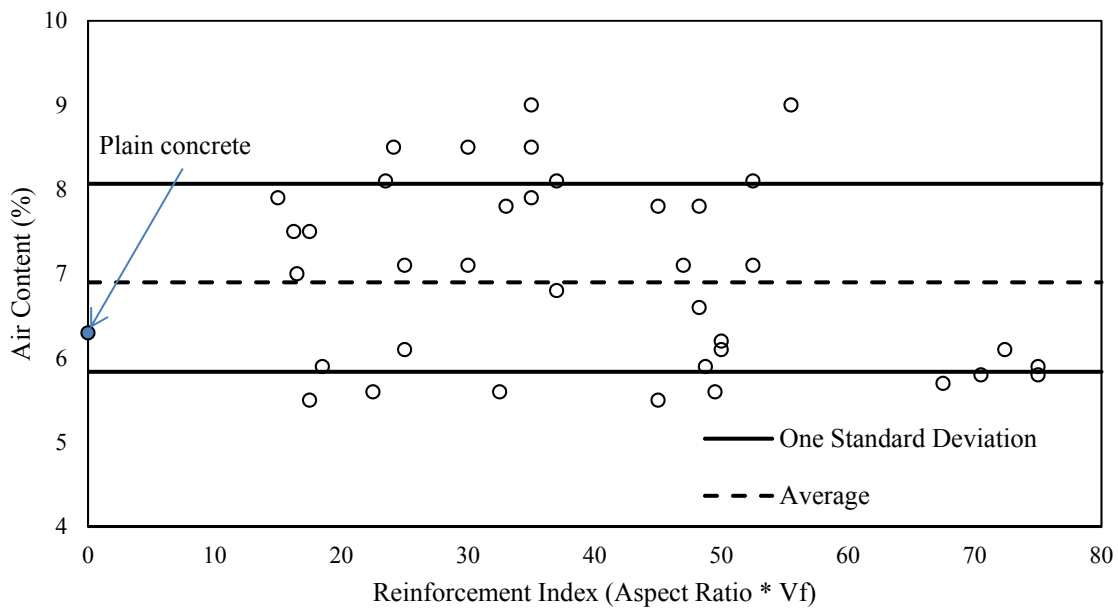


Figure 5-1. Air content as a function of reinforcement index.

### **5.2.2 Slump and Workability**

The average slump in this work was 1.6 inches and ranged from 0.5 inches to 3 inches. Figure 5-2 shows the average slump plotted as a dashed line, while plus and minus one standard deviation are plotted as solid lines. Since admixture dosage changes occurred after increases in fiber dosages, it is not possible to make quantitative conclusions as to how fiber dosage or geometry affect the slump or box test results, qualitative results are as follows:

- Achieving good workability with smaller effective diameter fibers (coincidentally having a higher aspect ratio) was difficult, especially at higher dosages, meaning more water reducing admixture was required. This observation is similar to what was reported in ACI 544, 2010 where it stated that the workability decreases with the increase in reinforcement index.
- Finishing and consolidating were difficult when smaller effective diameter fibers were used.
- Trial batches showed that increasing mixing time typically broke up fiber matts and balls.

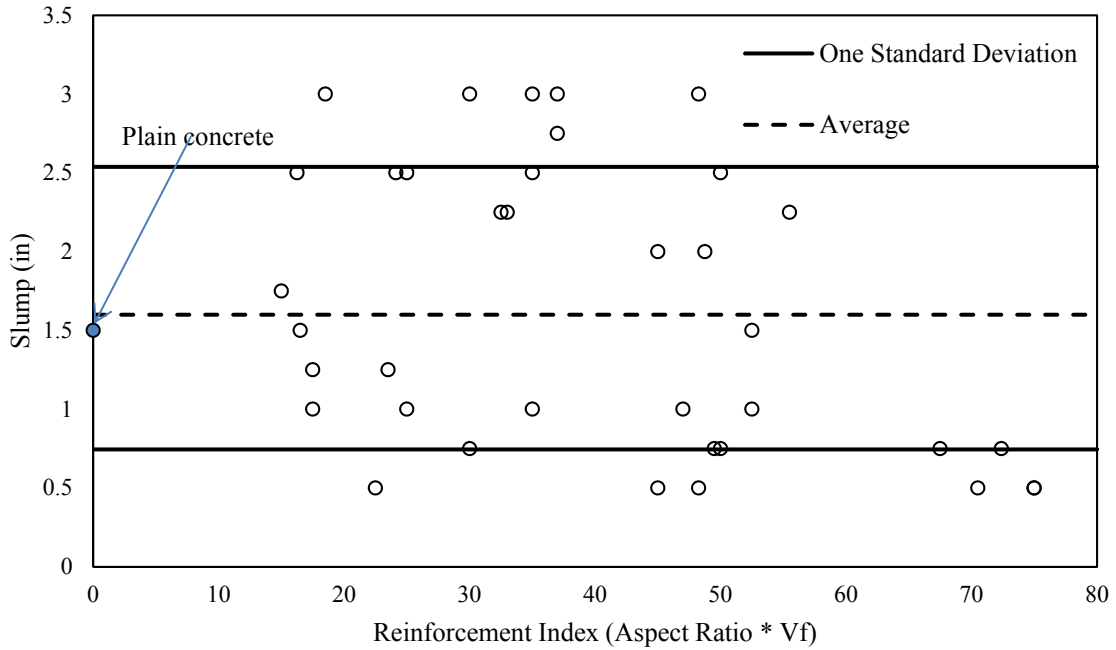


Figure 5-2. Slump as a function of reinforcement index.

### 5.3 Hardened Concrete Results

The following sections discuss the effects of fiber dosage, type, and geometry on the properties of hardened FRC; specifically, the results will be discussed in terms of uncracked and cracked properties. The uncracked properties include compressive strength, modulus of elasticity, and MOR, while the cracked properties pertain to the flexural performance after the first crack was achieved and variations of residual strength. It is important to discuss them separately because, as previously stated, concrete typically exists either in the cracked or uncracked state.

#### 5.3.1 Uncracked Concrete Properties

##### 5.3.1.1 Compressive Strength and Modulus of Elasticity

Figure 5-3 and Figure 5-4 show trends for both steel and synthetic FRC mixtures tested in this study for compressive strength and modulus of elasticity (based on the lab test) as a function of RI. These figures show that the change in reinforcement index ( $V_f \times$

AR) did not significantly influence the compressive strength or modulus of elasticity for synthetic fibers. The average compressive strength for synthetic FRC was 6,810 psi with a standard deviation and coefficient of variation of 323 psi and 4.74 percent, respectively. The average modulus of elasticity for synthetic FRC was 4,742 ksi with a standard deviation and coefficient of variation of 241 ksi and 5.08 percent, respectively. The compressive strengths of the PCC (6,960 psi) and synthetic FRC were comparable. On the contrary, the one steel FRC tested showed a dramatic increase in compressive strength and a relatively small increase in modulus of elasticity when the RI was increased. The compressive strength for the steel FRC increased from 7,330 psi to 9,320 psi for a change of fiber  $V_f$  from 0.25 to 0.75 percent. This particular finding is in accordance with the study conducted by Mahadik & Kamane, 2014 where it stated that the compressive strength of steel FRC increases with the increase in fiber content until 0.75 percent  $V_f$  and then decreases. It is theorized that the unusual behavior of the steel fiber mixture is due to forced orientation in the undersized specimens being used for Modulus of elasticity testing. Since limited samples were gathered for steel fibers, this was not investigated further.

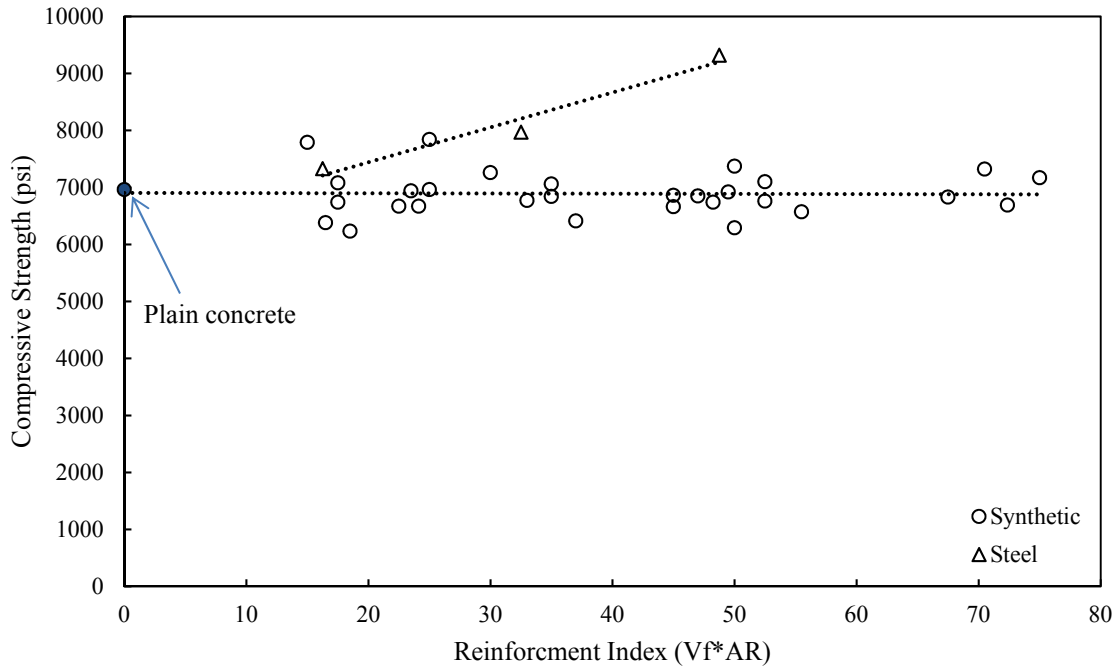


Figure 5-3. Compressive strength as a function of reinforcement index.

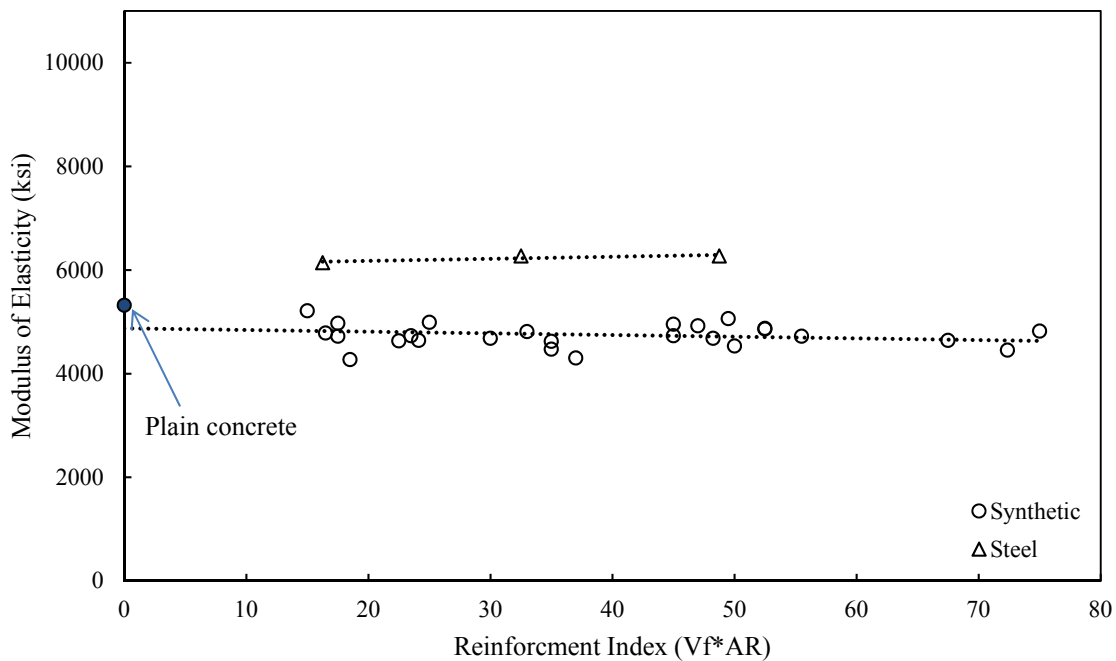


Figure 5-4. The modulus of elasticity as a function of reinforcement index.

### **5.3.1.2 Modulus of Rupture (MOR)**

The MOR vs RI is plotted in Figure 5-5. As similar to the compressive strength, the MOR is also not significantly influenced by the RI for the synthetic FRCs. The average and standard deviation of the MOR for all the synthetic FRC mixtures is 738 psi and 35 psi, respectively, with a coefficient of variation equal to 4.79 percent. The MOR for the plain concrete was 720 psi which is comparable to MOR of the synthetic FRC mixtures. The MOR for the steel FRCs was however found to increase with the increase in RI, especially when the RI exceeded 32.5. Figure 5-6 shows the MOR as a function of  $V_f$  of fibers in the mixture. As anticipated, it can be seen that the MOR also remained minimally influenced by the volume fraction of synthetic fibers. The MOR for the steel FRC increased with the increase in the  $V_f$  of fibers. It may be stated that the AR of all fibers considered in this study varied between 65 and 150, which is a relatively narrow range, but includes a large variety of commercially available fibers typically used in concrete.

Since the  $V_f$ , AR and RI of the synthetic fibers did not influence the MOR significantly, Figure 5-6 was plotted to investigate the influence of individual fibers on the MOR. It appeared that synthetic straight fiber, S.S.3 has shown consistently greater MOR for all the three dosages. The MOR for straight synthetic fiber, S.S.4 was moderate and was minimally influenced by the fiber  $V_f$ . The straight synthetic fiber, S.S.1 experienced gain in MOR with the increase in fiber  $V_f$ . The MOR of the synthetic continuously crimped, S.C.6 fiber has increased with the increase in fiber content. The MOR for this particular FRC was the lowest when the fiber  $V_f$  was 0.25 percent and significantly increased with the increase in fiber  $V_f$ . Among the embossed fibers, the

MOR of S.E.8 was not significantly influenced by the fiber  $V_f$ , and showed the maximum MOR at 0.5 percent  $V_f$ ; and exactly an opposite trend was noticed for the fiber S.E. 7. The MOR of synthetic fiber S.S.2 and twisted fiber, S.T.5 were found to be decreasing with the increase in fiber volume fraction. The MOR of the steel FRC, L.E.C.10, was found to be increasing with the increase in fiber volume fraction. Lastly, it can be stated that for all the synthetic FRC mixtures, the MORs approximately lied between 700 psi and 800 psi, meaning a variation of 100 psi, which may not be a significant variation when considering the large variation in fibers and fiber dosage. So, consideration of MOR to compare the contribution of fibers may not be the most appropriate hardened concrete property.

It should be noted that on average, an increase in synthetic fiber dosage led to a slight decrease in MOR. Given that polypropylene has a lower modulus than concrete, this trend is appropriate. On the other hand, the steel fibers had a significantly greater modulus of elasticity, making it appropriate that the MOR increased significantly with an increase in dosage. This trend can be considered a function of not only modulus of elasticity of the fibers but transformed section properties, where an increase in fiber dosage of a low modulus of elasticity fiber leads to a decrease in section properties; as follows, a high modulus fiber would increase the section properties.

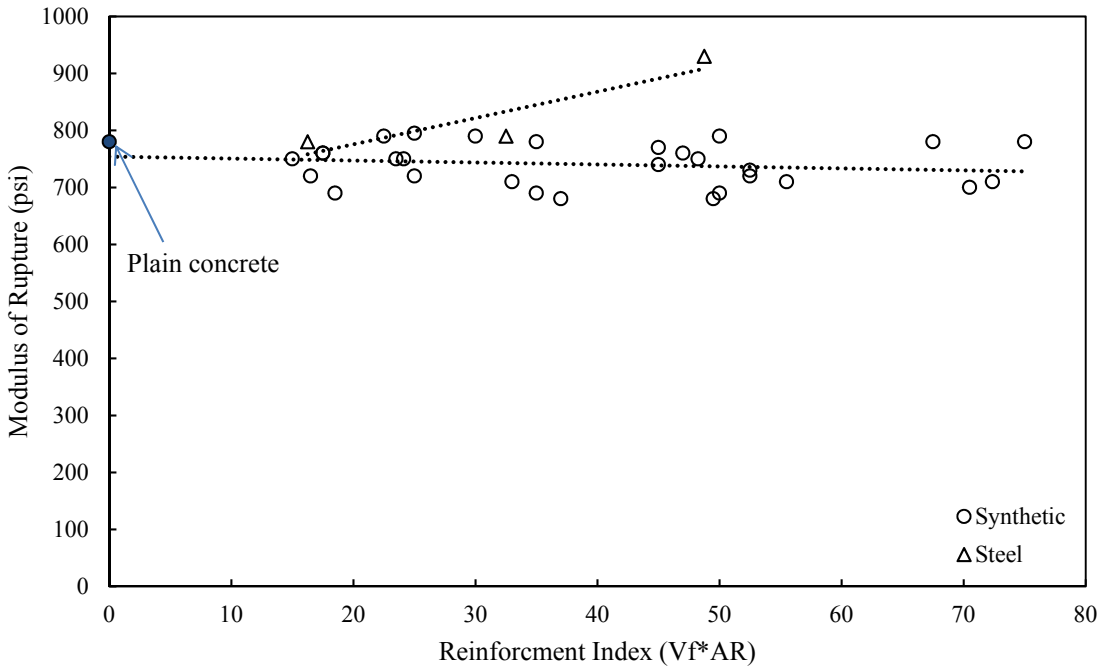


Figure 5-5. Modulus of rupture as a function of volume fraction for FRC mixtures together.

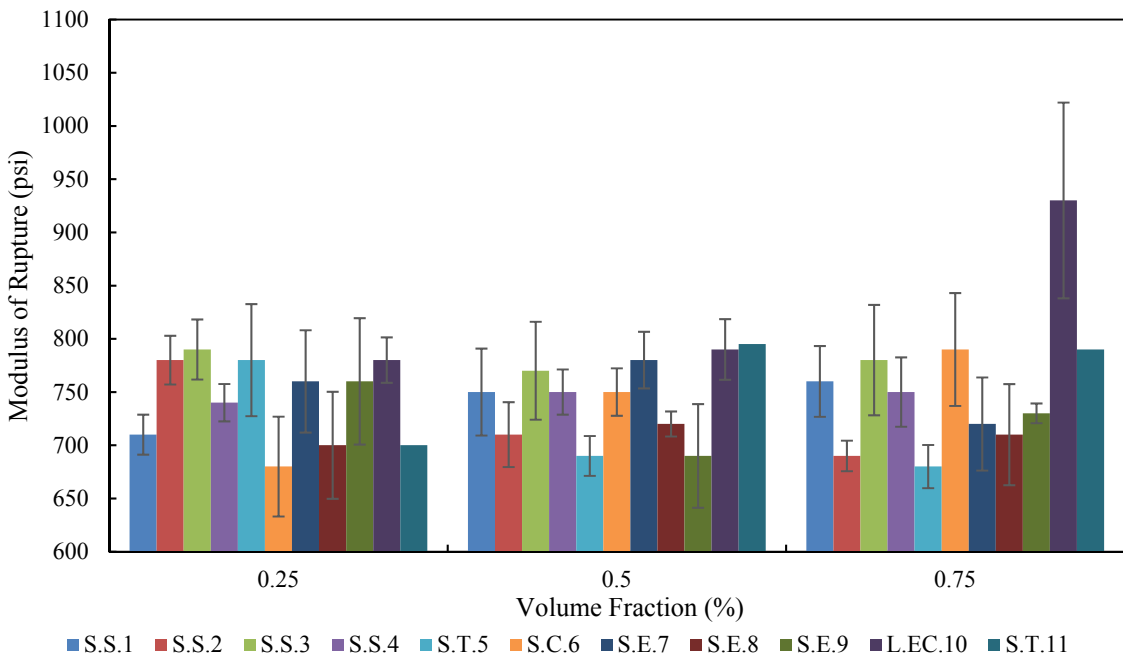


Figure 5-6. The volume fraction versus the modulus of rupture for each fiber considered in this work.

### **5.3.2 Cracked Concrete Properties**

#### ***5.3.2.1 General Fiber Behavior***

The general behavior for all fibers evaluated in this work can be seen in Figure 5-7 and Figure 5-8 individually. From these plots, it appears that the synthetic embossed fiber S.E.9 has shown consistently greater RS and post crack toughness for all three dosages for synthetic fibers. The other synthetic embossed fiber, S.E.7, and synthetic crimped fiber, S.C.6, also resulted in above average performance values with slightly less incremental increase in performance beyond 0.5 V<sub>f</sub>.

The behavior trends of S.T.5 and S.S.4 were similar in comparison and performed near the overall average for all synthetic fibers considered. The S.E.8 fiber resulted in good behavior at 0.25 percent V<sub>f</sub>, but shows less of an increase at higher dosages. The synthetic straight fiber S.S.2 has shown almost an opposite trend. For fiber S.S.3, the behavior values at 0.25 V<sub>f</sub> was among the lowest of all the values obtained in this study, but showed moderated behavior at 0.75 V<sub>f</sub>. Fiber S.S.1 and S.E.8 have resulted in good values at the 0.25 V<sub>f</sub> but was among the lowest RSR values at 0.75 percent V<sub>f</sub>. From these plots, it is also apparent that steel fibers perform significantly better than any synthetic fibers.

From these two plots, it is also apparent that shorter fibers performed worse when considering post-crack toughness against residual strength. This may be due to reduced strength towards the end of the flexural performance test as the shorter fibers began to pull from the concrete.

When considering Figure 5-9, the previously stated difficulties of RSR can be seen, particularly with the steel fiber (L.EC.10). The use of RSR in this instance gives the

impression that L.EC.10 decreased in post-crack performance between 0.5% and 0.75% volume fraction; however, this is not the case. From Figure 5-6 it can be seen that an increase in volume fraction lead to relatively no change in performance from 0.5% volume fraction to 0.75% volume fraction. This finding is in accordance to the findings of Mahadik and Kamane (2014).

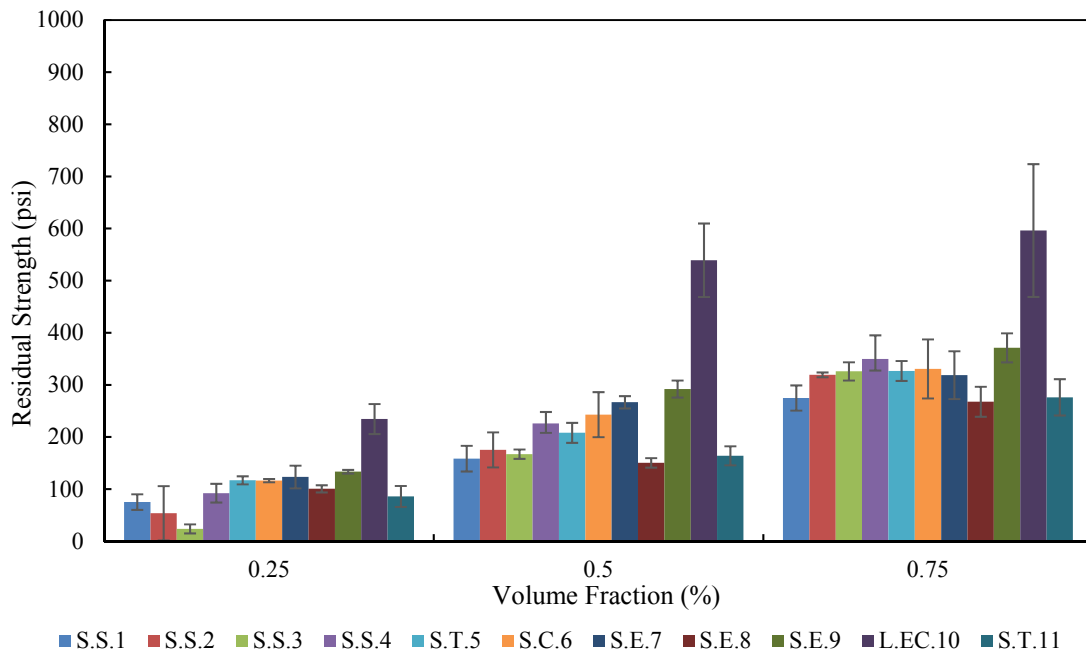


Figure 5-7. The residual strength as a function of volume fraction.

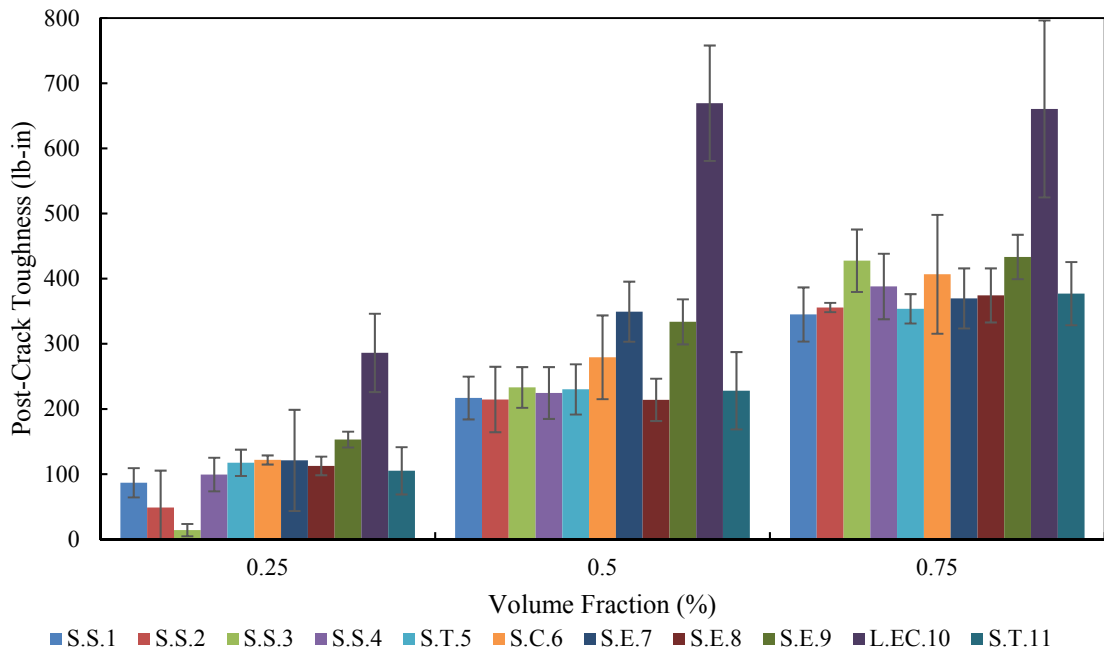


Figure 5-8. Post-crack toughness as a function of volume fraction.

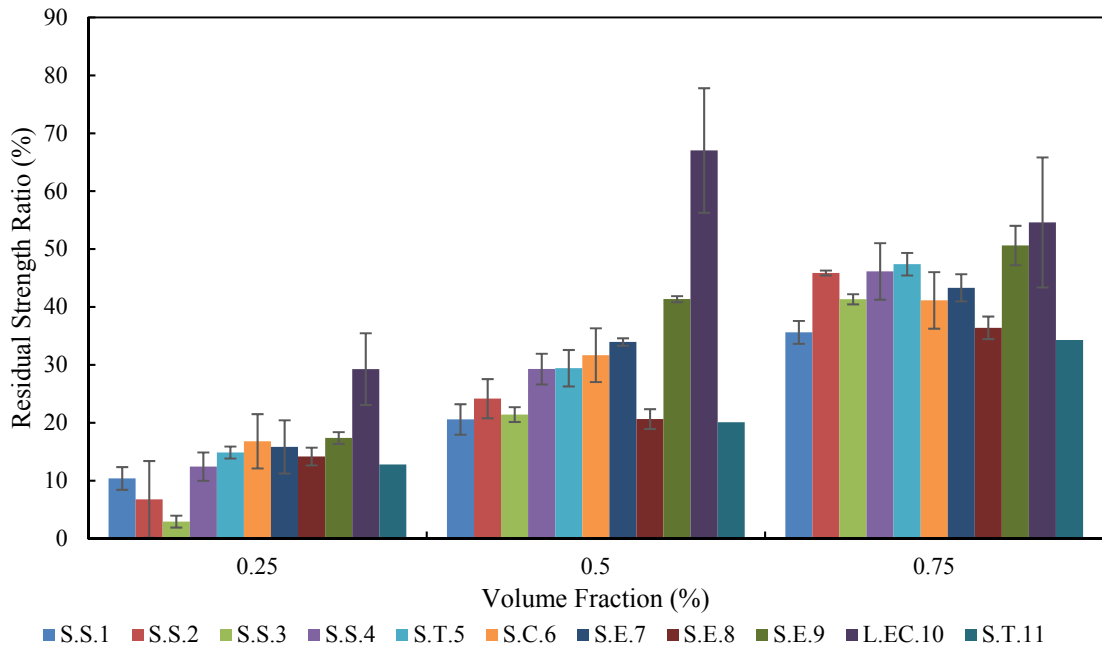


Figure 5-9. The residual strength ratio as a function of volume fraction.

### **5.3.2.2 Effect of Fiber Type and Dosage on Cracked Concrete Behavior**

For synthetic fibers in the dosage range tested, it can be seen that an increase in fiber dosage typically leads to a linear increase in performance (Figure 5-10). However, this statement does not stand true when considering the steel fiber tested in this work. From Figure 5-10 it appears that the steel fiber performance increased linearly between 0.25%  $V_f$  and 0.5%  $V_f$ , but then increased at a significantly lesser rate up to 0.75%  $V_f$ . It is likely that the higher dosage steel fiber mixture altered the failure mechanism when a certain crack face stress was achieved from a fiber pullout failure to a mechanism related to the concrete pullout strength, which explains this behavior. Overall, the RS and  $V_f$  has an excellent correlation as can be seen in Figure 5-10;  $R^2$  is equal to 0.85. Steel fibers were not considered in this correlation.

From Figure 5-11, the post-crack toughness is shown as a function of volume fraction of fibers in each mixture. This plot also has a strong correlation ( $R^2$  equal to 0.90), slightly better than RS versus volume fraction. Fiber geometry and length may have a greater effect on this property, which are not directly considered in volume fraction or post-crack toughness.

Regarding the influence of the material on the fiber behavior, the steel fibers outperformed the synthetic fibers by a significant margin. Table 5-1 presents a comparison of the fiber performance values between the synthetic fiber and steel fibers obtained for different ranges of fibers dosages. It can be seen that steel fibers at a dosage of 0.25%  $V_f$  provided a greater performance than the synthetic fibers at 0.5%  $V_f$ .

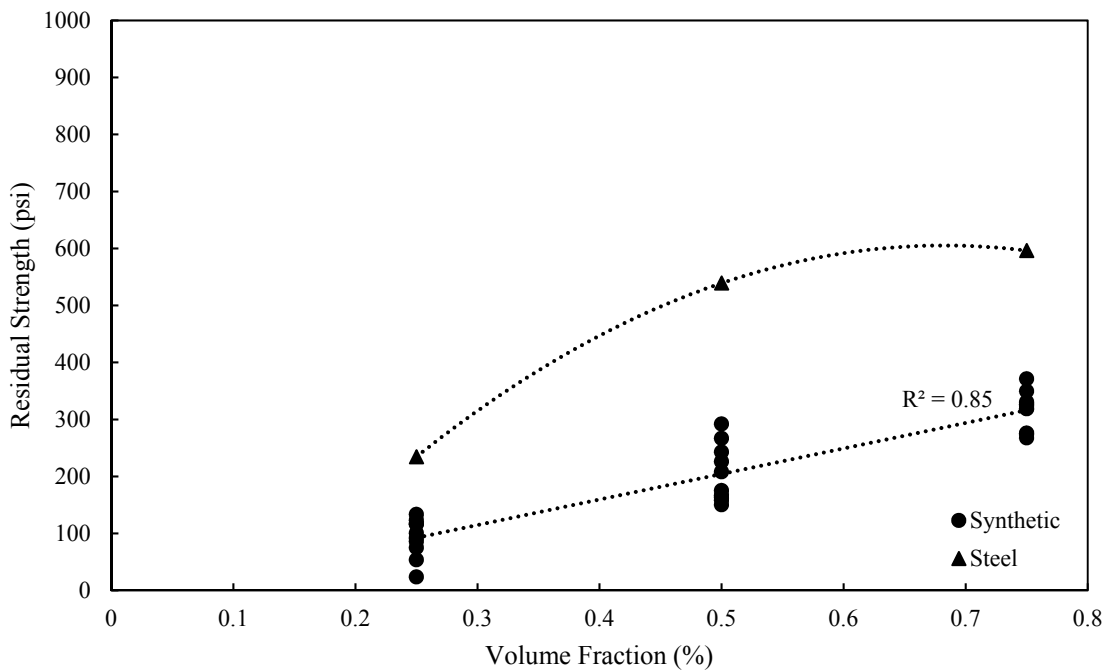


Figure 5-10. Residual strength as a function of volume fraction for all synthetic and steel fibers separately.

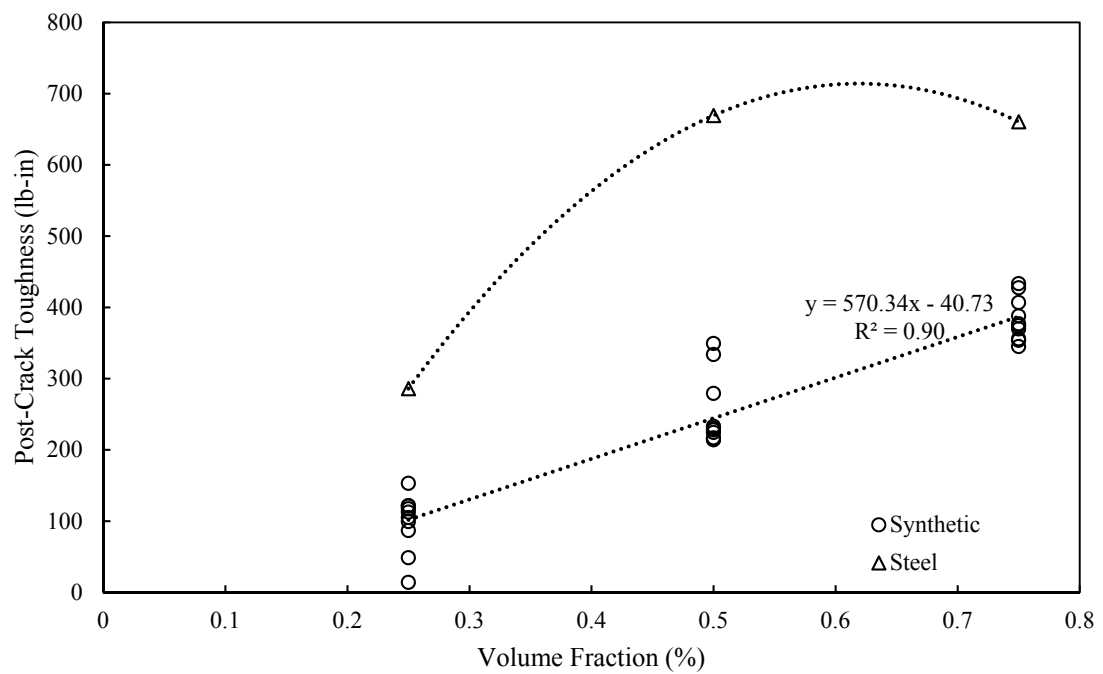


Figure 5-11. Post-crack toughness ad a function of volume fraction.

Table 5-1. Dosage and average 28 day RSR values are presented for synthetic fibers and steel fibers respectively

Dosage (V <sub>f</sub> – lb/yd <sup>3</sup> )	Synthetic RS (psi)	Synthetic PC Toughness (lb-in)	Dosage (V <sub>f</sub> – lb/yd <sup>3</sup> )	Steel RS (psi)	Steel PC Toughness (lb-in)
0.25 – 3.8	112	123	0.25 - 33	234	286
0.5 – 7.6	205	252	0.5 - 66	539	669
0.75 – 11.8	324	387	0.75 - 99	596	661

### 5.3.2.3 *Effect of Fiber Geometry on Cracked Concrete Behavior*

Figure 5-12 and Figure 5-13 shows how the geometry and cross section of the fibers effect the RS and post-crack toughness respectively. These plots show that on average, embossed and continuously crimped fibers perform better than twisted and straight fibers at low and intermediate dosages: however, have little difference at high dosages. The end crimped steel fibers greatly outperformed the others; however, because the end crimped fibers were steel, a comparison cannot be made to the other geometries. It should be noted that the fiber length may also play a large role in these results.

When testing, it was noted that almost all of the synthetic fibers tested pulled out of the concrete without yielding or tearing. In the case of the hooked end fibers, it was seen that the hooks did not fully engage in the concrete since the hooks were often partially flattened from there originally shape. It is likely that with more dramatic geometry, better post-crack behavior can be achieved.

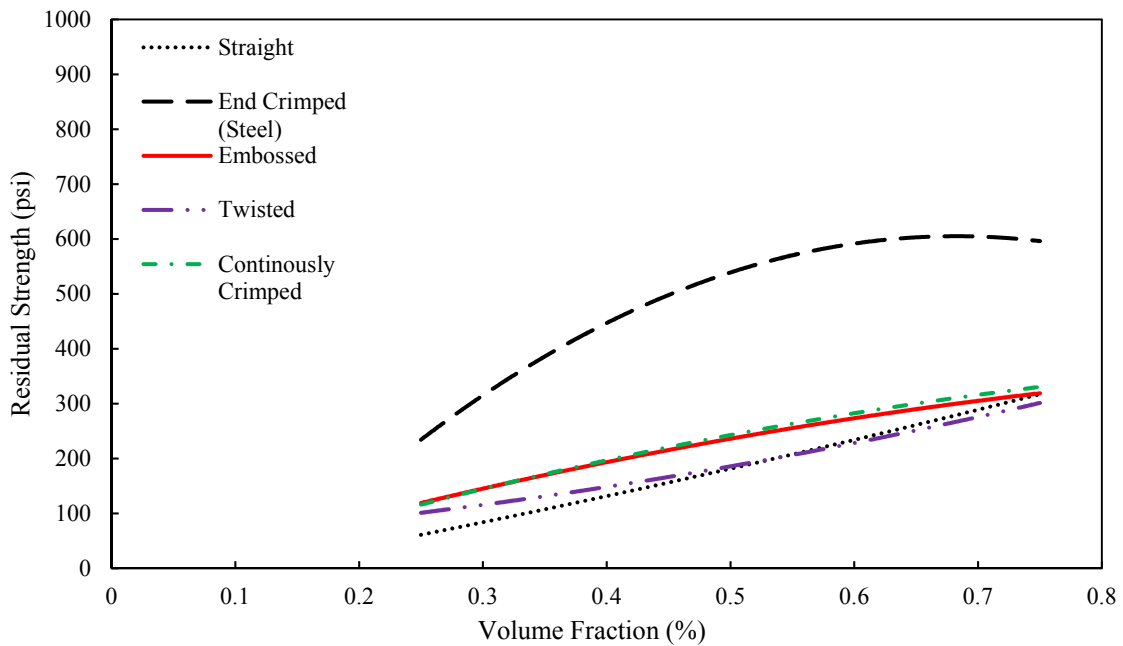


Figure 5-12. The residual strength as a function of dosage and geometry of fibers.

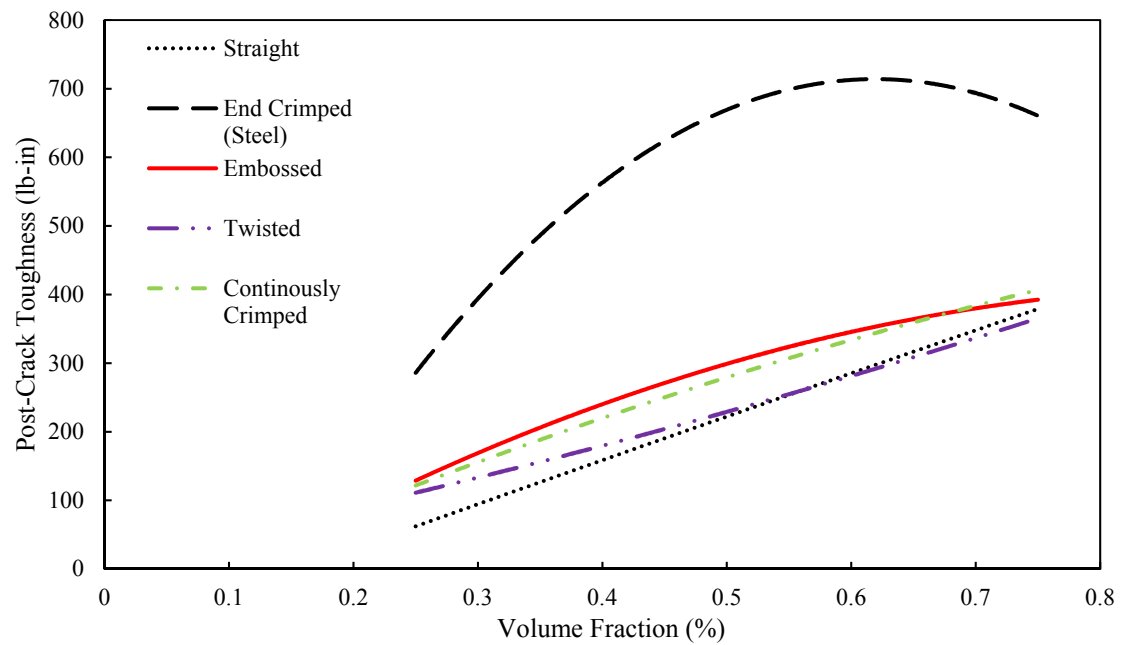


Figure 5-13. The post-crack toughness as a function of dosage and geometry of fibers.

#### **5.3.2.4 Effect of Fiber Length on Cracked Concrete Behavior**

In order to see the effect of fiber length and aspect ratio on the performance values of different FRC mixtures, these parameters were plotted in terms of one another. Figure 5-14 and Figure 5-15 show the relationship between fiber length and fiber behavior (RS and post-crack toughness, respectively). From these two plots, the effect of dosage and fiber length can be observed. As the dosage increases, it is apparent that an increase in fiber length has a much smaller effect than at smaller dosages. This may be related to the total stress being absorbed by the concrete at the crack face, reaffirming what was found by (Mahadik & Kamane, 2014) that at some point increasing fiber dosage leads to a decrease in performance. Generally speaking, this study shows that an increase in fiber length from 1.5 inches to 2.5 inches leads to an approximate increase in RS of 50 psi and post-crack toughness of 100 lbf-inches. These results may be deceiving due to the fact that the longer fibers in this work were typically embossed or physically deformed, while the shorter fibers were straight in geometry; however, since fiber S.E.8 was similar to fibers S.E.7 and S.E.9 in geometry and effective diameter and performed poorly compared to the later mentioned, a conclusion would be that due to the relatively narrow range of fiber lengths studied, fiber geometry was seen to play a large role in FRC behavior than fiber length.

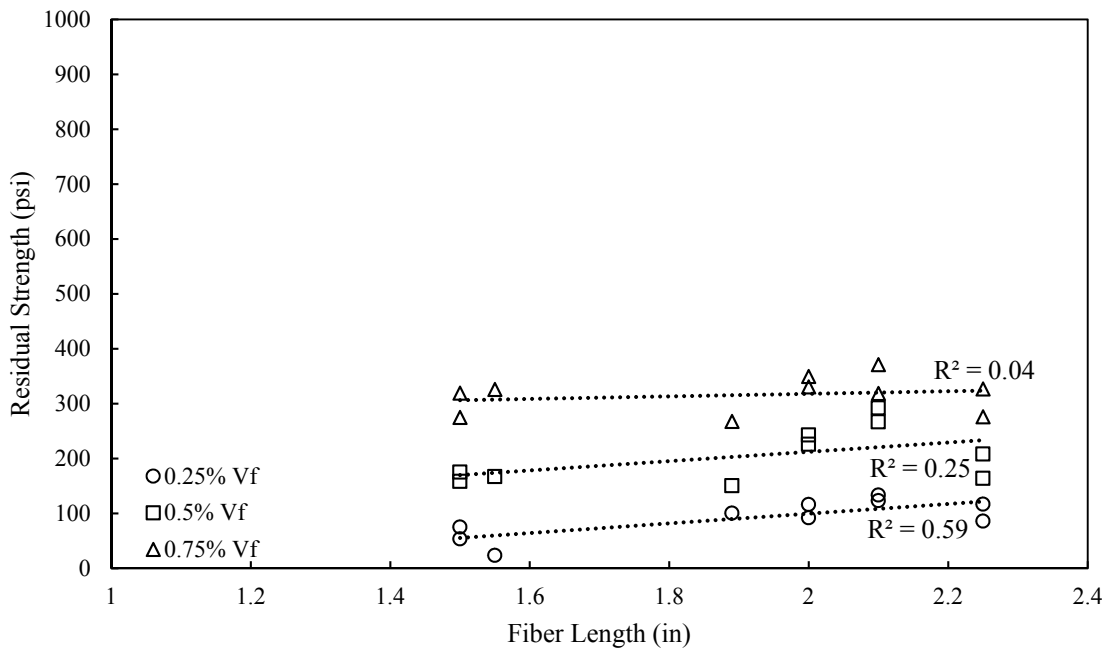


Figure 5-14. Residual strength as a function of fiber length for synthetic fibers at different dosages implored.

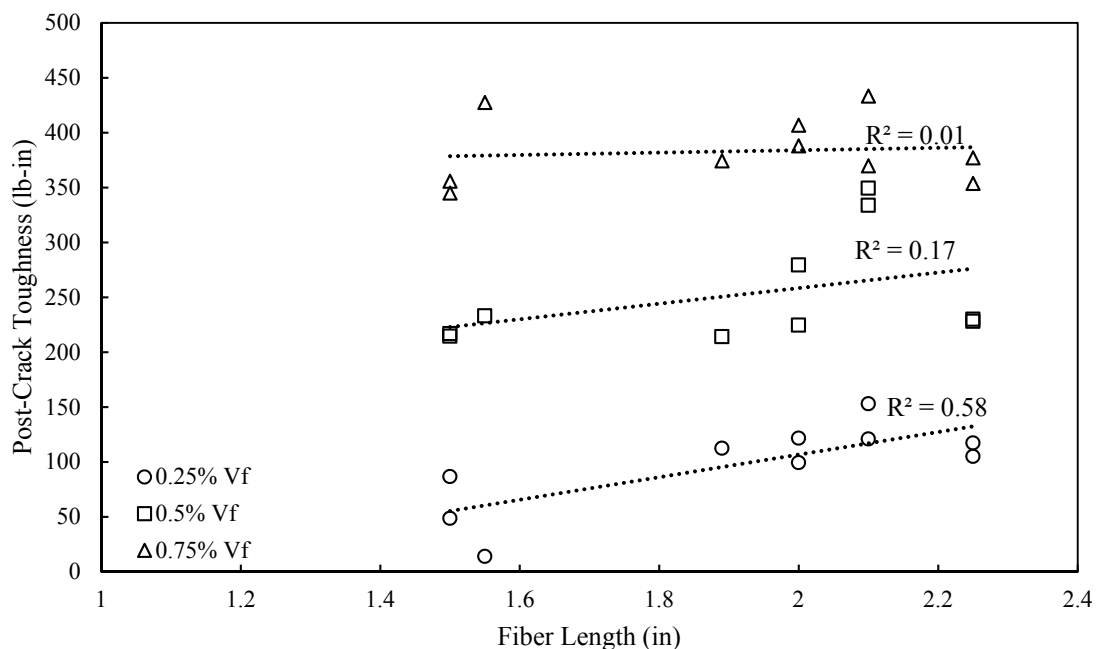


Figure 5-15. Post-crack toughness as a function of fiber length for synthetic fibers at different dosages implored.

### 5.3.2.5 Effect of Aspect Ratio on Cracked Concrete Behavior

To explore the effect of aspect ratio on post-crack behavior properties, Figure 5-16 and Figure 5-17 show aspect ratio plotted as a function of RS and post-crack toughness respectively. Opposite to fiber length, an increase in fiber dosage decreases the effect of fiber properties on the post-crack behavior. This work shows that for an increase in aspect ratio, fiber properties typically decreased very similarly to fiber length. Since it is known that longer fibers perform better than shorter fibers (5.3.2.4), this finding may be due to the fact that larger aspect ratio fibers have significantly smaller effective diameters. This may again be deceptive do to the fact that the lower aspect ratio fibers in this study had surface deformations, unlike the large aspect ratio fibers which were straight in geometry.

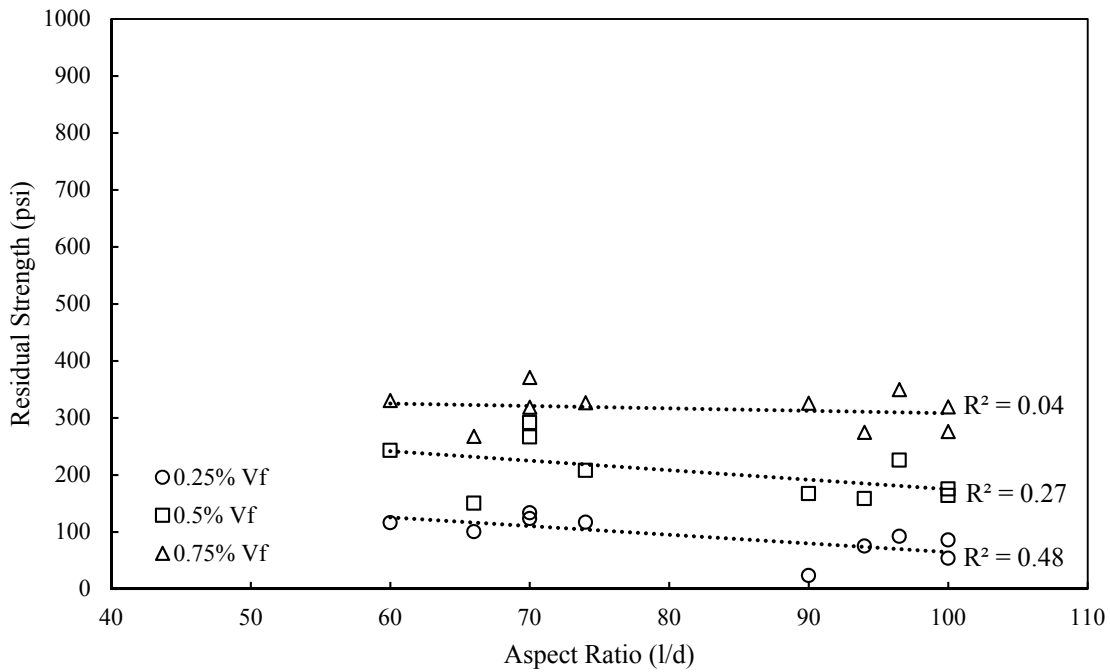


Figure 5-16. Residual strength as a function of aspect ratio for synthetic fibers at different dosages implored.

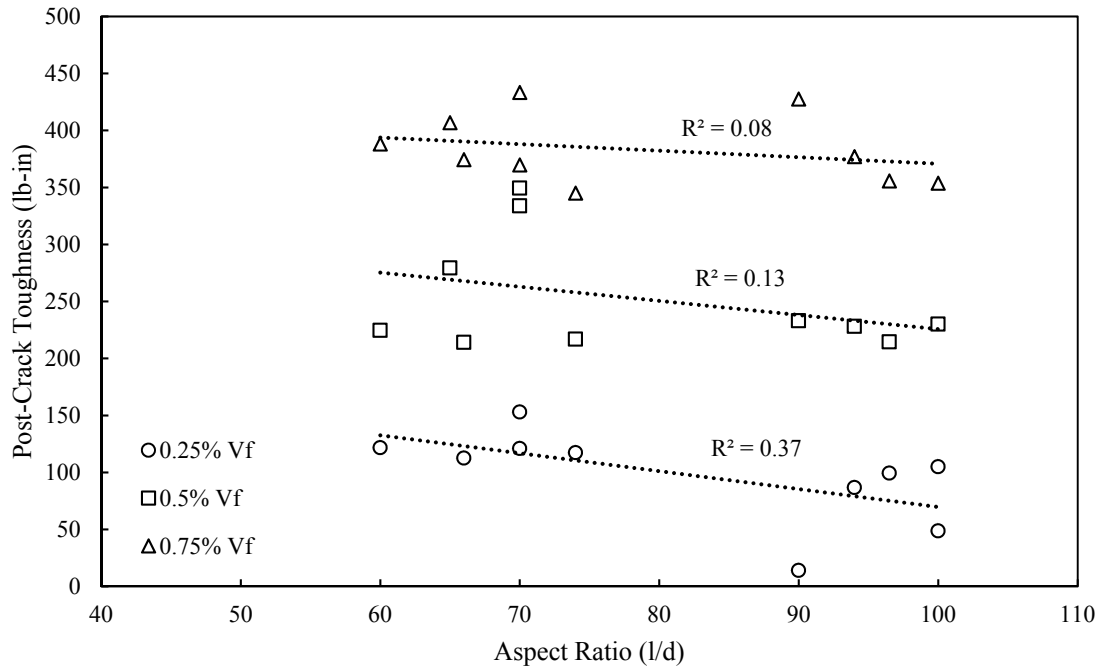


Figure 5-17. Post-crack toughness as a function of aspect ratio for synthetic fibers at different dosages implored.

### 5.3.2.6 Effect of Concrete Compressive Strength on Fiber Behavior

To evaluate the effects of compressive strength on the behavior of fibers, four mixtures were cast at 0.5% volume fraction and tested for compressive strength and per ASTM C1609 at 24 hours after casting to achieve a lower compressive strength. Plots in Figure 5-18 and Figure 5-19 show how each fiber performed respective of concrete compressive strength. Little increase was observed over this range of concrete strengths (approximately 4000 psi to 7000 psi), with the increases occurring with general uniformity.

For comparison purposes, the MOR and the RS are plotted in Figure 5-20. This plot shows a significantly greater increase in MOR than RS for the concrete strength range explored. These plots, along with Figure 5-21 show trends for fiber performance as a function of concrete strength and their respective  $R^2$  (0.21 for post-crack toughness and

0.06 for RS). These low  $R^2$  values are evidence that concrete compressive strength has little effect on the post-crack behavior of fibers in FRC.

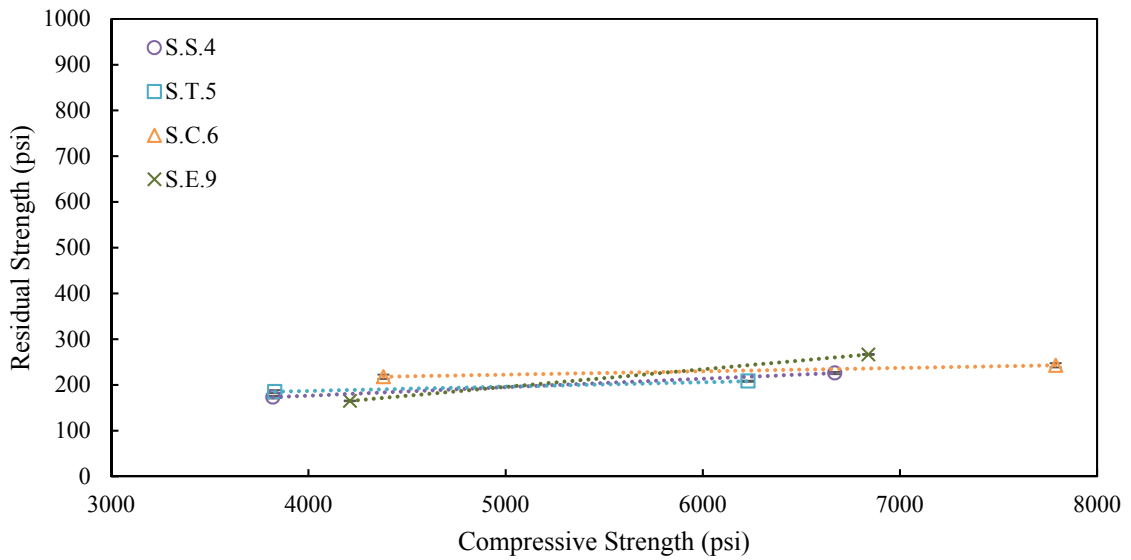


Figure 5-18. Residual strength as a function of concrete compressive strength for selected synthetic fibers at 0.5% volume fraction.

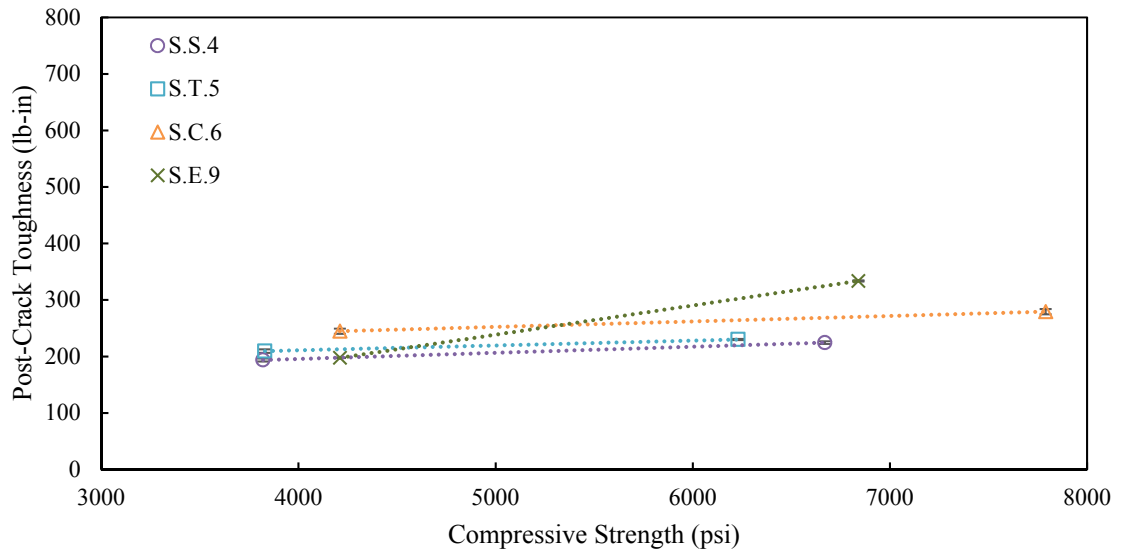


Figure 5-19. Post-crack toughness as a function of concrete compressive strength for selected synthetic fibers at 0.5% volume fraction.

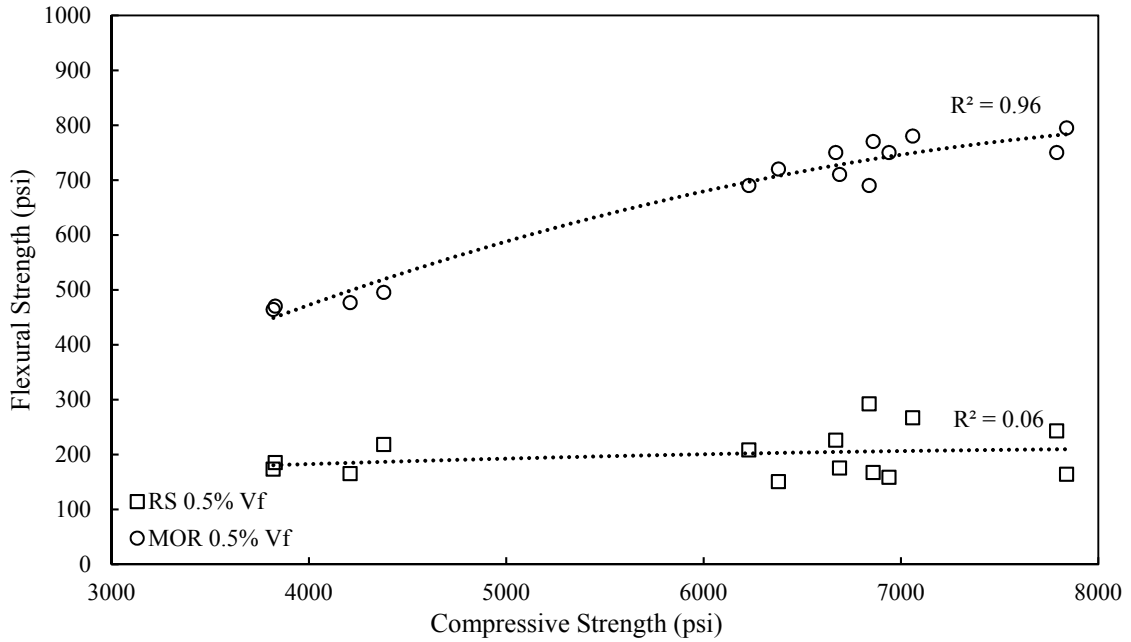


Figure 5-20. Modulus of rupture and residual strength as a function of concrete compressive strength for synthetic fibers at 0.5% volume fraction.

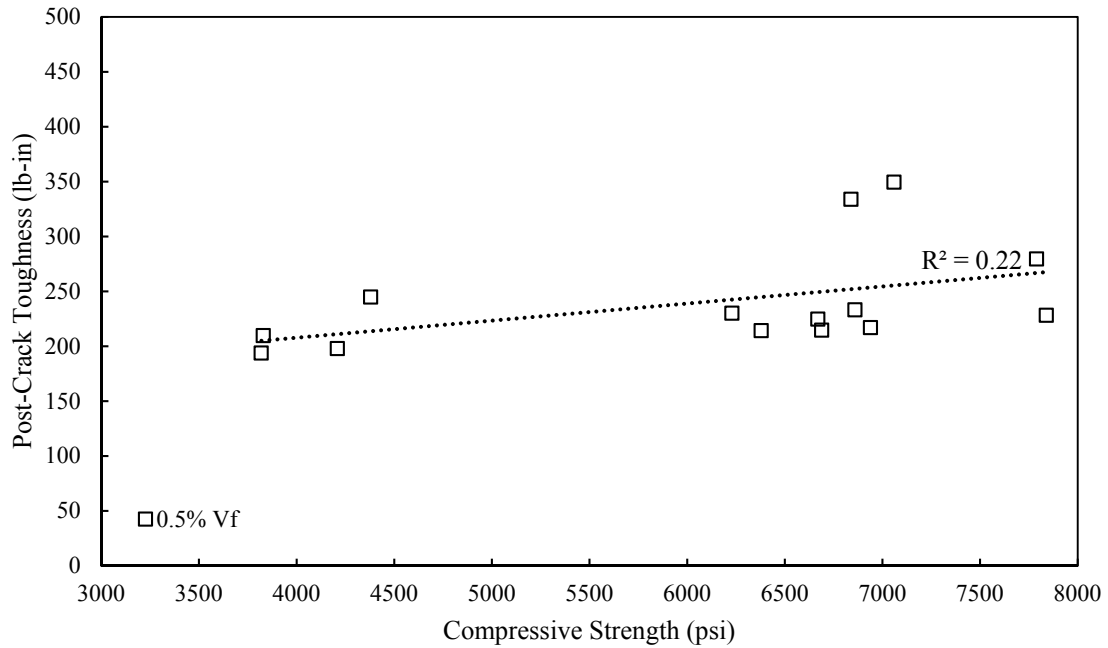


Figure 5-21. Post-crack toughness as a function of concrete compressive strength for synthetic fibers at 0.5% volume fraction.

### **5.3.2.7 ANOVA and t-test Statistical Comparisons**

In order to explore the statistical significance and difference of this work, a single factor ANOVA test was conducted on the 28-day synthetic fiber flexural results, specifically the residual strength at each dosage was investigated. Table 5-2 shows the results from the statistical analysis. Using an alpha of 0.05, the statistical analysis shows that the flexural results were significantly different in each instance. Additional single factor ANOVA tests were conducted to compare the fibers geometry at 0.75% volume fraction. 0.75% volume fraction was selected because it was the least significant dosage as per Table 5-2. Again, using an alpha equal to 0.05, we see in

Table 5-3 that the F values are greater than F Critical values, meaning that these results are significant, even when the straight fibers are removed from the analysis. When comparing the results of just the straight fibers (Table 5-3), it can be seen that these fibers are statistically the same (F value less than the F critical value). A final single factor ANOVA test was also conducted between the straight fibers and all of the other results. As per Table 5-2 it can be seen that this test showed that the straight fibers are not statistically different from all other fibers

A t-test was also conducted with an alpha of 0.05 on the 0.75% volume fraction mixtures to compare the two embossed fibers (fibers 7 and 9) having the same manufacturer, length, effective diameter, etc., but the one (Fiber 7) having a chemical coating. The previous results showed that fiber 9 slightly out performed fiber 7; however, the t-test resulted in a P two-tail of 0.190, meaning that these two fibers are statistically the same.

Table 5-2. Single factor ANOVA statistical comparisons of the synthetic fibers for each dosage investigated in this study.

Volume Fraction (%)	0.25	0.5	0.75
F	24.94	10.85	4.78
p-Value	$5.6 \times 10^{-9}$	$1.18 \times 10^{-6}$	0.00133
F Critical	2.393	2.282	2.342

Table 5-3. Factor statistical comparisons of synthetic fiber geometries at 0.75% volume fraction.

Factor Levels	Straight, Embossed, Twisted, and Crimped	Embossed, Twisted, and Crimped	Straight	Straight, all other results
F	3.61	4.02	3.12	0.81
p-Value	0.027	0.044	0.081	0.375
F Critical	2.99	3.81	3.8	4.21

### 5.3.2.8 *Fiber Effectiveness in terms of PCP index*

The post-crack performance (PCP) index, as described in 3.2.2, can be used to compare the effectiveness of fibers and to serve as a quality control or a preapproving measure for use in any application. As was previously described, PCP index is the area under the normalized RS versus  $V_f$  curve for a specific fiber. Figure 5-22 presents the normalized residual strength vs  $V_f$  relations for all the FRCs used in this study. The results of the PCP index are in Table 5-4. These results are used in Figure 5-23 to see the effects of fiber length on post-crack behavior. These results show a better correlation ( $R^2 = 0.55$ ) to fiber length than previously shown in Figure 5.14 in Section 5.3.2.4 ( $R^2 = 0.04$  for 0.75%  $V_f$  and to 0.58 for 0.25%  $V_f$ ). This indicates that even though the influence of the fibers length was not observed when the results were compared with respect to RSR or RS, the PCP index could provide a better discrimination between the fibers.

The average PCP index for straight fibers was 6.3, crimped 8, twisted 6.5, and embossed 7.8. That being said, the crimped and embossed fibers clearly performed better

than the others, but because no straight fibers having a length similar to the embossed or crimped fibers were tested, it is difficult to clearly determine whether length or geometry plays a larger role. A safe assumption is that longer fibers having a crimped or embossed geometry will outperform short fibers having straight or twisted geometry.

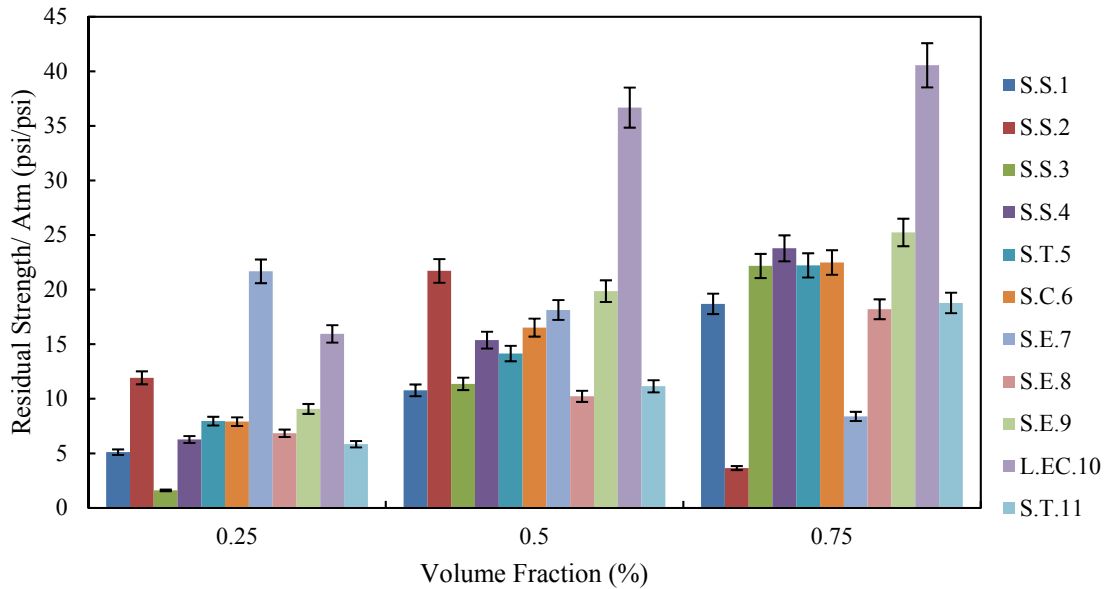


Figure 5-22. Post-crack performance in terms of normalized RS and volume fraction.

Table 5-4. Post-crack behavior in terms of the PCP index.

Fiber Designation	PCP Index
S.S.1	5.7
S.S.2	6.1
S.S.3	5.8
S.S.4	7.6
S.T.5	7.2
S.C.6	8.0
S.E.7	8.6
S.E.8	5.5
S.E.9	9.5
L.EC.10	16.9
S.T.11	5.8

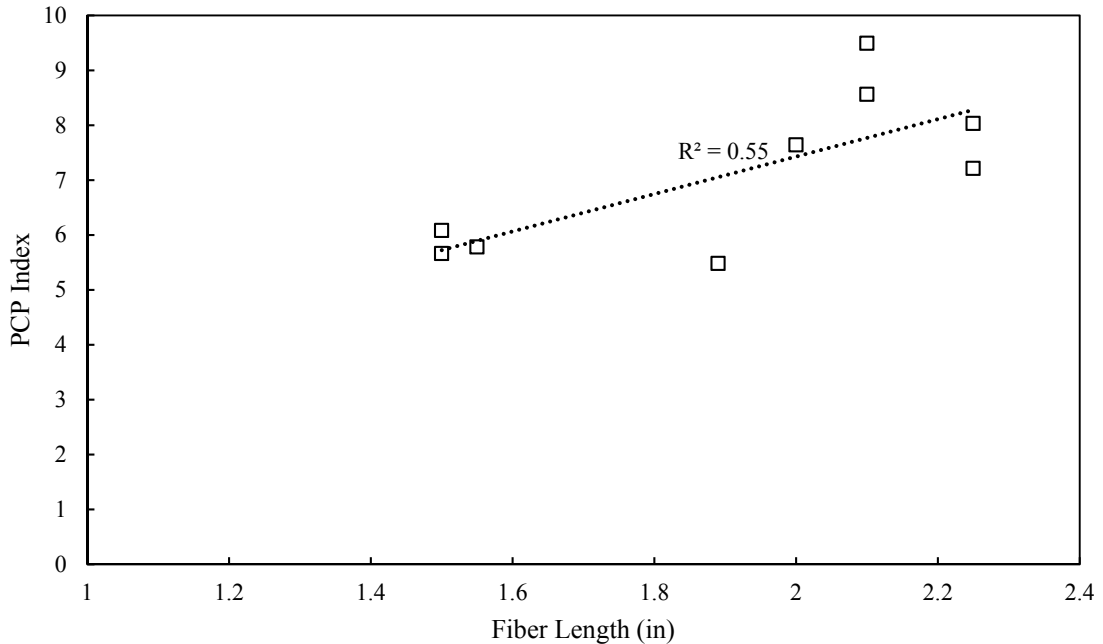


Figure 5-23. PCP index as a function of fiber length.

#### 5.3.2.9 Predicting Post-Crack Fiber Behavior

Predicting post-crack behavior of FRC is a difficult task, due to the large number of variables to be considered (geometry, length, dosage, effective diameter, material, etc.); therefore, any prediction attempt (mechanistically or empirically) should consider these variables. Currently, there is not an option for accounting for fiber geometry, because of this, correlations are typically relatively poor. A correlation involving RI seems reasonable because it includes dosage, length and effective diameter as variables; however, stills neglects fiber geometry. Plots including post-crack performance and RI are seen in Figure 5-24 and Figure 5-25 with low  $R^2$  values (0.62 and 0.68 respectively).

Since overall fiber behavior was quantified in 5.3.2.7 in the form of the PCP Index, that can be used to account for fiber length, geometry, aspect ratio, type, or another fiber property. PCP Index will be utilized to normalize post-crack strength parameters (post-crack toughness, RS, etc.) by dividing the parameter in question by the

volume fraction. Figure 5-26 and Figure 5-27 show this method to produce strong correlations for RS and post-crack toughness ( $R^2 = 0.91$  and  $R^2 = 0.85$  respectively). This correlation includes all fibers, synthetic and steel.

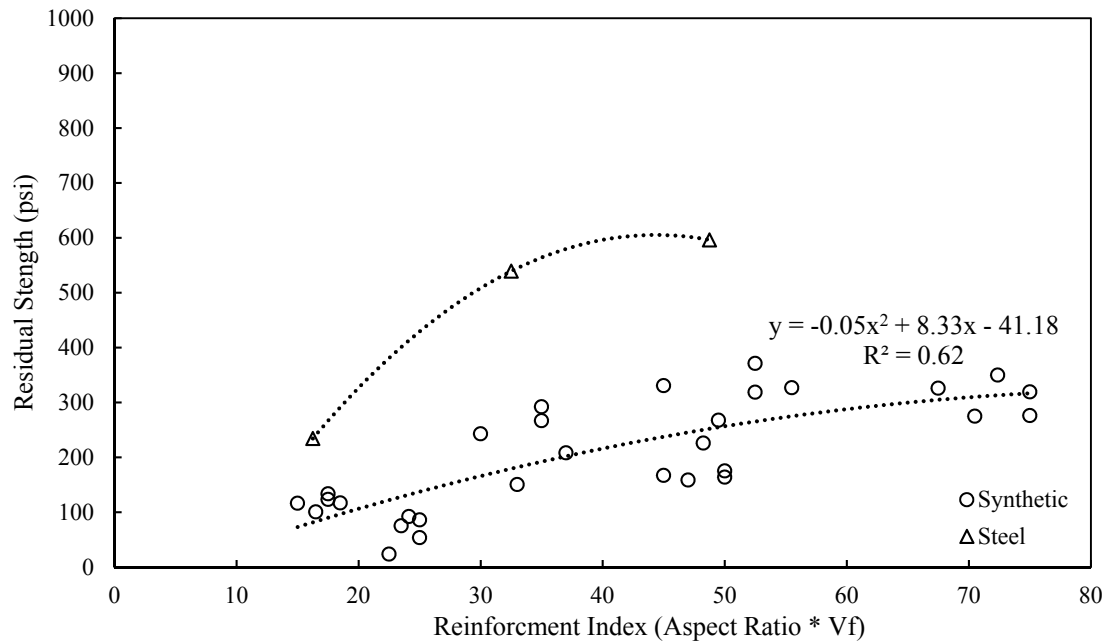


Figure 5-24. RS as a function of RI.

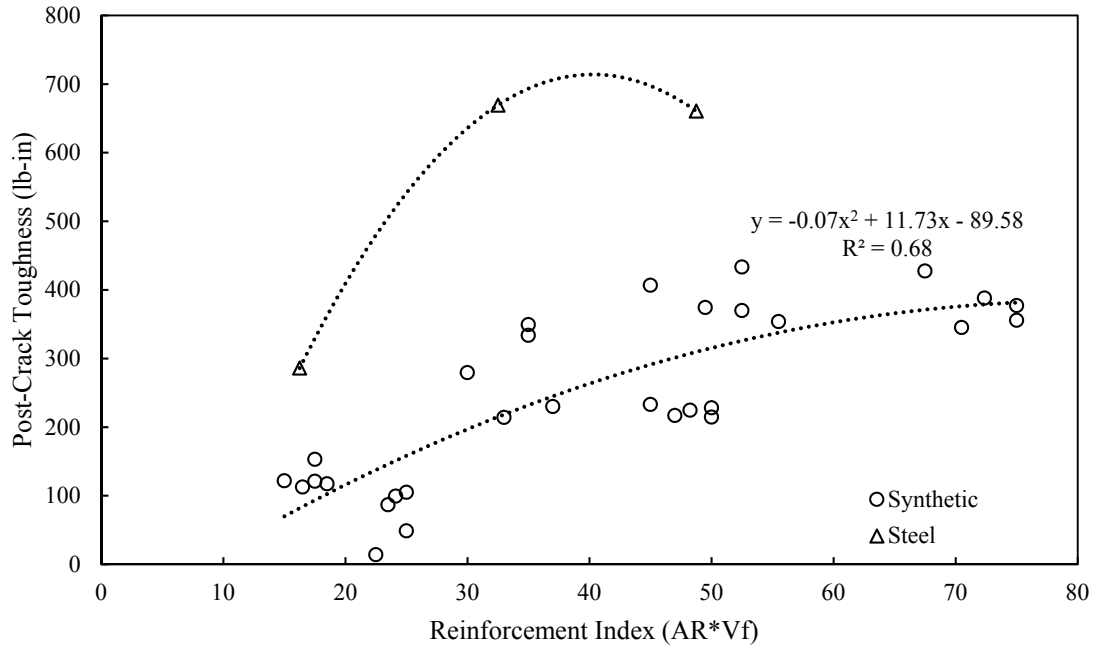


Figure 5-25. Post-crack toughness as a function of RI.

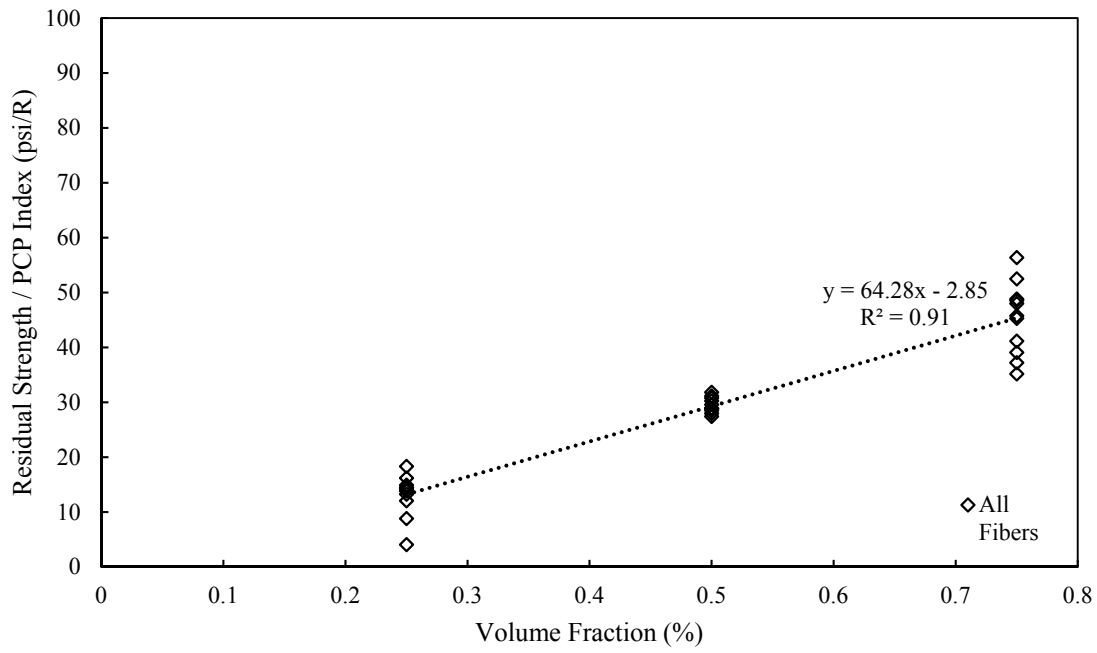


Figure 5-26. RS and PCP Index ratio as a function of volume fraction.

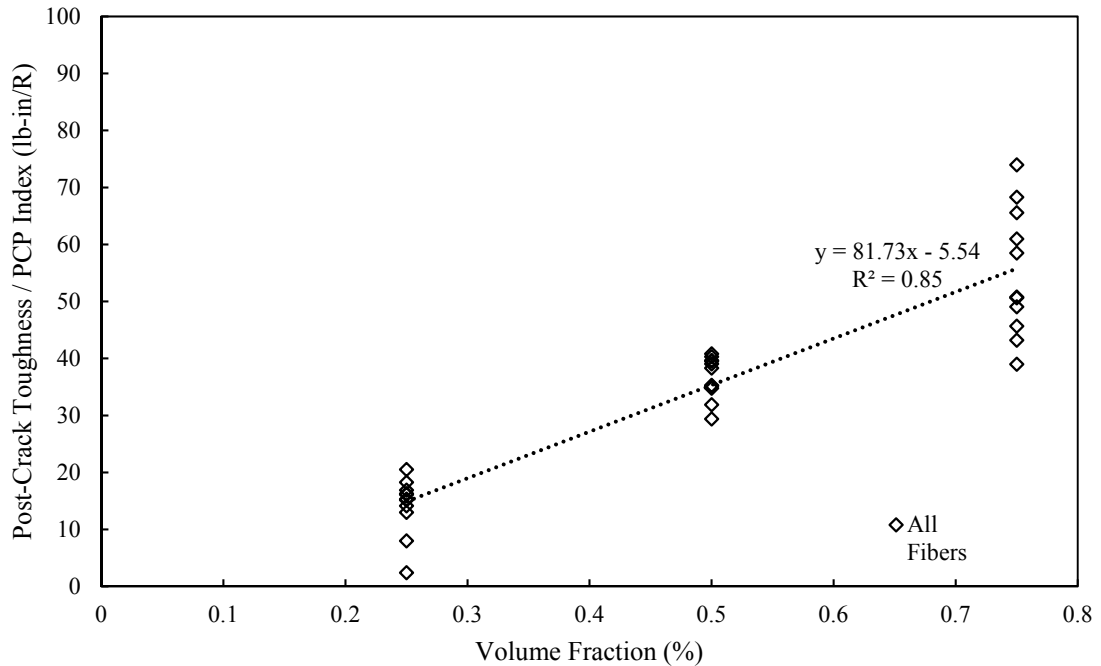


Figure 5-27. Post-crack toughness and PCP Index ratio as a function of volume fraction.

#### 5.4 Conclusion

The purpose of this chapter was to discuss and analyze the results of the experimental program. In this chapter, plastic, uncracked and cracked FRC properties were examined in terms of fiber properties (length, aspect ratio, and geometry) and fiber dosage. Since admixtures and fine aggregate quantities varied with an increase in fiber dosage, it was not possible to draw quantitative correlations; however, it was qualitatively observed that an increase in reinforcement index decreased the workability (slump) and made it more difficult to obtain proper air entrainment.

When considering uncracked synthetic FRC properties, little change in behavior was observed, on average, for an increase in fiber volume fraction; however, steel FRC significantly improved in performance for an increase in fiber volume fraction.

The majority of this chapter discussed cracked concrete properties, particularly in four-point flexural testing. It was found that fiber length, aspect ratio, and concrete compressive strength affect the post crack behavior; however, fiber geometry has the most dramatic effect on post crack performance. That being said, twisted, crimped, and embossed fibers performed nearly 50% better than straight fibers.

In this section, the post crack toughness parameter and the PCP index were utilized. The post crack toughness continuously gave stronger correlations than RS and RSR. The post crack performance (PCP) index also proved valuable in directly comparing results.

## **6 PRESENTATION OF A MECHANISTIC ESTIMATION METHOD FOR EFFECTIVE FIBER TENSILE STRENGTH**

### **6.1 Introduction**

FRC is also used in many civil engineering structures other than the concrete pavement or overlays. Currently, accounting for the mechanistic benefits of fibers in concrete is difficult because of the unavailability of an analysis procedure to estimate the stresses induced into the fibers. Unlike reinforced concrete, it is not possible to accurately determine an appropriate minimum fiber dosage for applications such as slabs -on -ground, foundations, etc., because the allowable tensile strength of fibers cannot be determined due to the fact that fibers typically pullout of the concrete instead of yielding. The following section will discuss this problem and propose a method for determining the effective allowable tensile strength of fiber for concrete. This section is for academic purposes and is not intended for application.

### **6.2 Approximate Calculations of Residual Strength**

Reinforced concrete (RC) design concepts utilize several assumptions that allow for relatively accurate designs for shear and flexural strength. Those assumptions include the following:

- Reinforcement is perfectly bonded to the concrete.
- Concrete stress-strain curve is non-linear.
- Once the composite section has cracked, tensile stresses in concrete are neglected.
- Reinforcement stress-strain curve is elastic.

In FRC, it cannot be assumed that the fibers are perfectly bonded to the concrete or that the fibers stress-strain curve is elastic when in concrete; therefore, it is difficult to

determine an allowable stress in the fibers. Due to this, FRC is typically not used as primary reinforcement in structural systems (beams, columns, elevated slabs, etc.).

Because the yield strength of fibers in FRC is typically not developed into the concrete, Equation 2 cannot currently be utilized in a similar manner for FRC. Since an extensive laboratory study is currently being conducted for this thesis, it is possible to calculate an effective working stress that corresponds to fiber types, geometries, dosages, and concrete strength. This method could also be used in an opposite order, where a designer assumes an effective allowable stress, and then specifies the corresponding residual strength or strength in the ASTM C1609 test procedure.

$$M_n = A_s \times f_y \times (d - a/2)$$

Equation 2

Where:

- $M_n$  is the nominal flexural strength at a given section (lb – in).
- $A_s$  is the area of longitudinal tension reinforcement, replaced with  $A_f$  (area of fibers) when used for FRC ( $\text{in}^2$ ).
- $f_y$  is the specified yield strength for reinforcement, replaced with  $f_{ew}$  (effective working stress) when used for FRC (psi).
- $d$  is the distance from the extreme compression flange to the centroid of the longitudinal tension reinforcement (in).
- $a$  is the depth of the equivalent stress block (in).

### 6.2.1 Assumptions Considered in this Method

To utilize Equation 2 for FRC, a number of assumptions need to be defined that relate to fiber area ( $A_f$ ), depth to tension fibers ( $d$ ), how to consider fibers in compression, and the effective working stress of the fibers. For this method to work, it is assumed that

the fibers are uniformly, not randomly, distributed in the flexural specimen and then idealized as seen in Figure 6-1 in order to simplify calculations.

The cross-sectional area of fiber in tension can be assumed to be the area of fibers in the tension zone of the beam, this numerical definition is defined in Equation 3 and is not equal to the total volume fraction of fibers, but rather the cross-sectional area of fibers between the neutral axis and the extreme tension flange.

The distance from the extreme compression flange to the centroid of the idealized tension fiber location ( $d$ ) is idealized in Equation 4. This idealization assumes a linear strain relationship from the compression flange to the tension flange; therefore, the tension fibers are located at two-thirds the distance from the neutral axis to the extreme tension flange, which is the centroid of the force.

In this situation, as is idealized in Figure 6-1 and Figure 6-2, it would be intuitive to consider this beam a doubly-reinforced member, since it has reinforcement in the compression and tension zone. However, this is not accurate when the compressive strength is determined or specified with the fibers in the concrete, meaning that considering this member doubly-reinforced would consider the fibers twice. Also, neglecting the fibers in compression in this method would have a negligible effect for synthetic fibers since they give little benefit to the compressive strength of the concrete. Equation 5 shows the definition of the depth of the equivalent compression stress block. Equation 6 and Equation 7 provide definitions for the remaining variables (depth of equivalent stress block and depth to neutral axis) required for completing these calculations.

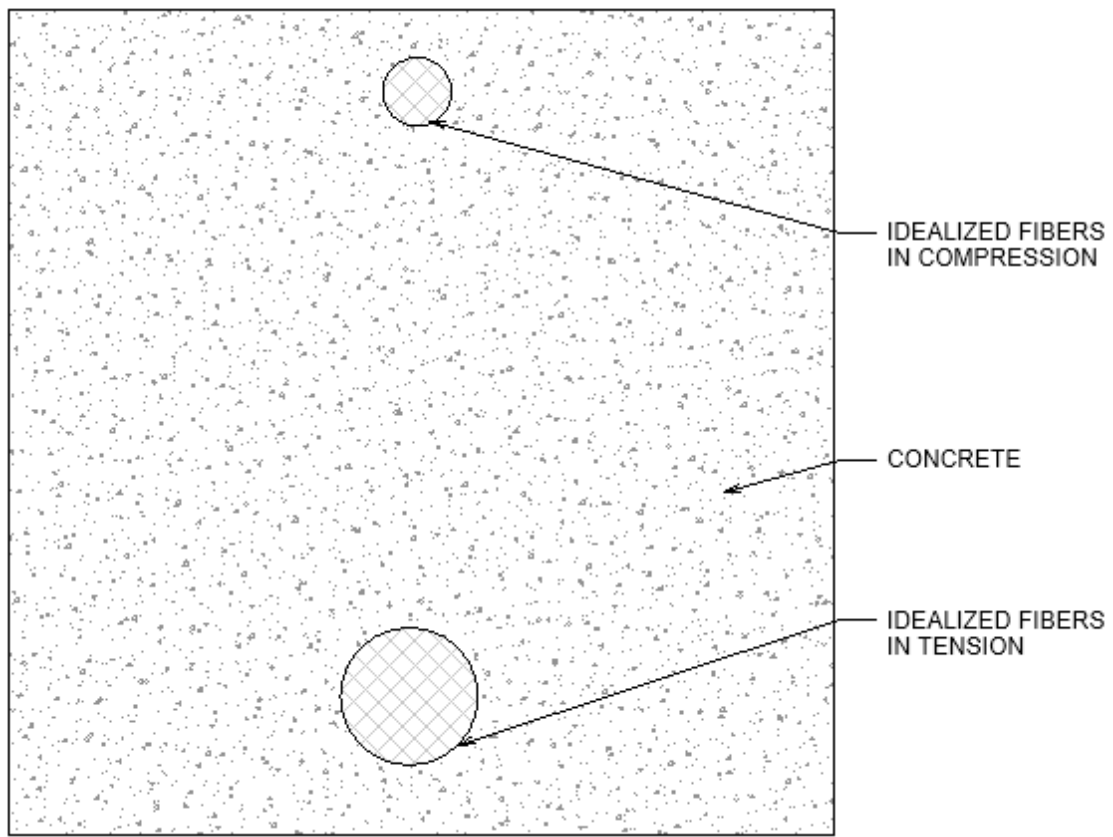


Figure 6-1. Idealized fiber layout in a flexural specimen.

$$A_f = A_b * \frac{V_f}{100} * (h - c) \quad \text{Equation 3}$$

Where:

- $A_f$  is the cross-sectional area of fibers considered to be in tension when the FRC beam is experiencing flexure ( $\text{in}^2$ ).
- $A_b$  is the cross-sectional area of the beam in question ( $\text{in}^2$ ).
- $V_f$  is the fraction of cross-sectional area of fibers to the cross-sectional area of concrete in a given beam section (%). This is assumed to be the volume fraction of fibers in the concrete mixture.
- $h$  is the height of beam cross-section (in).
- $c$  is the distance from the neutral axis to the extreme compression flange.

$$d = \left( \left( \frac{2}{3} \right) * (h - c) \right) + c \quad \text{Equation 4}$$

Where:

- d is the distance from the extreme compression flange to the centroid of the idealized tension fiber location (in).
- h is the height of beam cross-section (in).
- c is the distance from the neutral axis to the extreme compression flange.

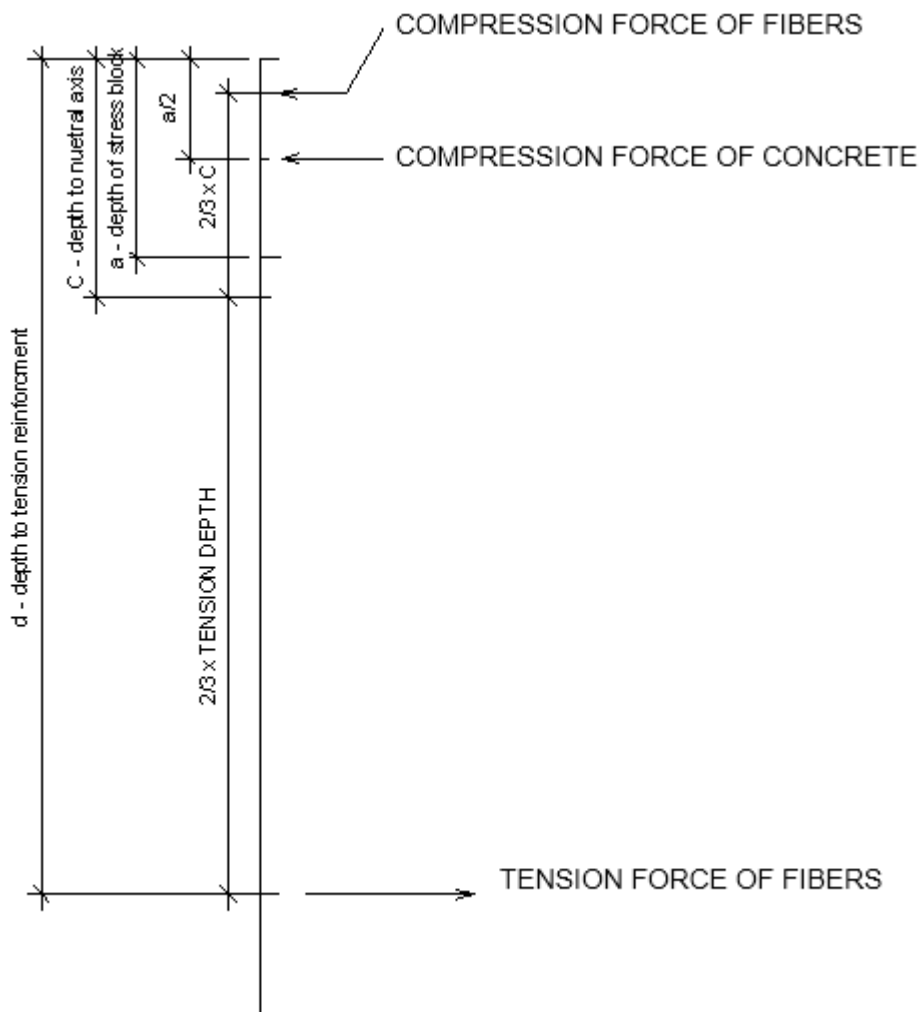


Figure 6-2. Diagram showing the location of forces about a beam cross section.

$$a = \frac{A_f * f_{ew}}{0.85 * f'_c * b} \quad \text{Equation 5}$$

Where:

- a is the depth of the equivalent stress block (in)
- $A_f$  is the cross-sectional area of fibers considered to be in tension when the FRC beam is experiencing flexure ( $\text{in}^2$ ).
- $f_{ew}$  is the effective working stress (tensile) of the fibers (psi).
- $f'_c$  is the compressive strength of the concrete ( $\text{lb/in}^2$ )
- b is the width of the compression block (in).

$$c = \frac{a}{\beta_1} \quad \text{Equation 6}$$

Where:

- c is the depth to the neutral axis (in).
- a is the depth of the equivalent stress block (in).
- $\beta_1$  is factor relating depth of equivalent rectangular stress block to depth of neutral axis. This factor is defined by ACI 318-14

### 6.2.2 Calculation of Effective Working Stress

With the previously described assumptions, the effective working stress (EWS) of the fibers can be calculated using residual strength data from this work. To determine EWS, the applied moment can be calculated using Equation 7, then setting the applied moment equal to Equation 2 can allow for  $f_{ew}$  to be solved for. This method requires iteration because Equation 5 also requires the use of  $f_{ew}$ . It is recommended to calculate the applied moment from applied load data collected at 120 mils of mid-span deflection.

$$Total\ Applied\ Load\ (lbf) = \frac{M_n}{\frac{1}{3} * l} * 2 \quad \text{Equation 7}$$

- Equation for four-point bending configuration

Where:

- $M_n$  is the nominal flexural strength at a given section (lb – in).
- $l$  is the span of the beam, for ASTM C1609 it is 18 inches

### 6.3 Effective Working Stress (EWS) of Fibers

From the laboratory study conducted in this work, a number of plots were generated to explore how fiber properties affect the fibers EWS. Figure 6-3 shows the EWS for all the fibers tested in this work. In general, the fiber behavior is similar to other forms of behavior comparisons, where the steel fiber greatly outperformed the synthetic fibers.

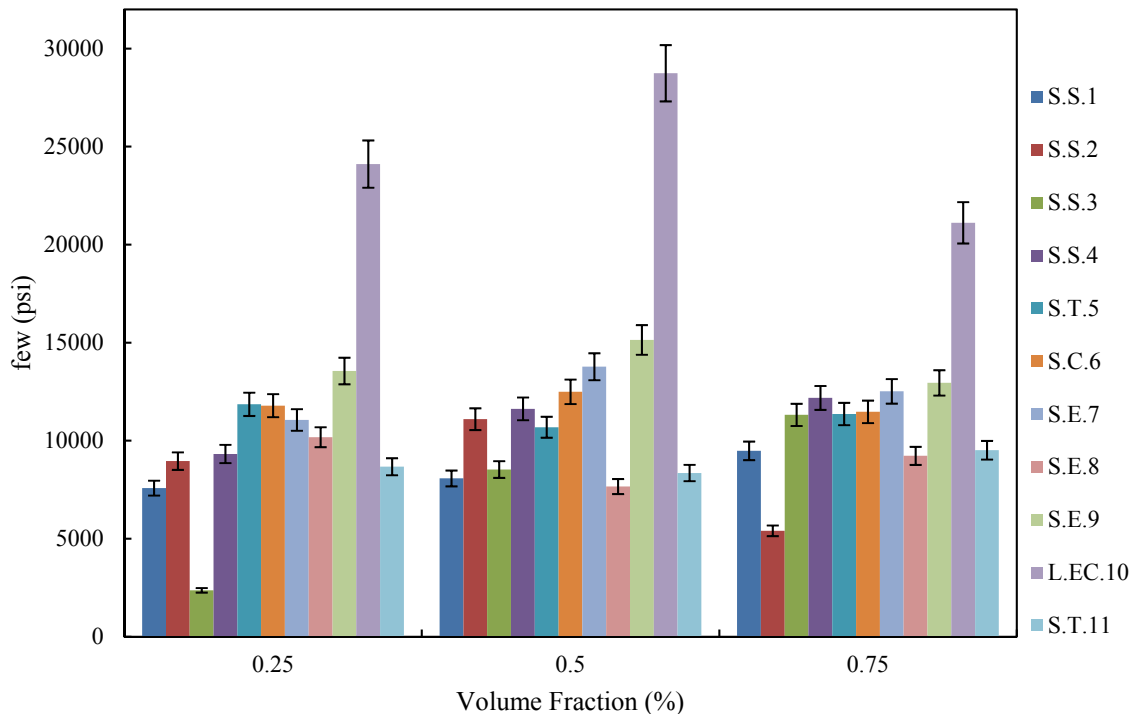


Figure 6-3. EWS as a function of volume fraction.

### 6.3.1 Effect of Fiber Type and Dosage on EWS

As previously seen, the steel fiber tested in this work greatly outperformed all of the synthetic fibers by a large margin. Figure 6-4 shows the EWS of the synthetic and steel fibers tested as a function of volume fraction. From this plot, it can be seen that increasing the  $V_f$  has little effect of the EWS of synthetic fibers; however, this is not true for the steel fiber tested. The steel fiber saw a significant decrease in performance between 0.5% and 0.75%  $V_f$  leading to the conclusion that the optimum dosage for this steel fiber is near 0.5%  $V_f$ .

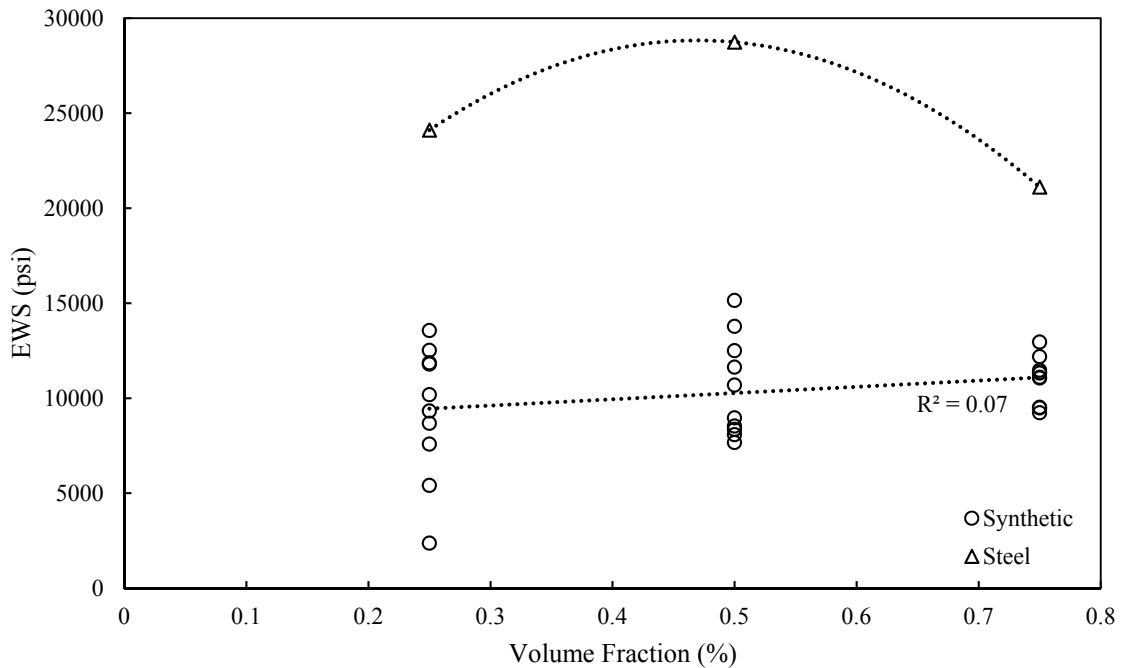


Figure 6-4. EWS as a function of volume fraction

### 6.3.2 General Estimates for EWS

The trends for post-crack behavior are nearly identical to those equated with EWS; therefore, they will not be presented. Like stated in Section 5.3.2.3, the embossed and

crimped synthetic fibers outperformed the straight and twisted fibers. Along that same point, longer, lower aspect ratio fibers also performed stronger than the others.

Since it was seen that nearly all fibers pulled from the concrete in each specimen, the values obtained give reasonable results as compared to the tensile strengths of the materials. Table 6-1 shows a comparison of average EWS values obtained in this work. These values could be used as initial estimates for the method previously presented in Section 6.2.2; however, proper testing should be implemented to verify these values.

Table 6-1. Comparison of fiber geometries at various fiber dosages in terms of EWS.

Dosage (V <sub>f</sub> %)	Fiber geometry EWS (psi)				
	Hooked-End (Steel)	Embossed	Twisted	Crimped	Straight
0.25	24107	12080	10262	11785	6165
0.5	28741	12189	9516	12492	9294
0.75	21112	11074	10435	11470	11017

### 6.3.3 Direct Tension (DT) Test

To verify the EWS calculations direct tension testing was conducted on a few FRC beams. Since this experiment was auxiliary to the study as a whole only two mixtures were cast. The two mixtures included repetitions of H.S.S.4.25 and H.S.E.9.25. Three beams (6 inches x 6 inches x 24 inches) were cast per mixture with threaded rod anchored into both ends. The beams were cracked in the ASTM 1609 frame at 18 hours after casting and then tested at 24 hours. The beams were cracked at 18 hours because pulling this specimen apart in tension uncracked would be rather difficult and would likely generate high loads that would likely lead to the threaded rod pulling from the concrete instead of creating a tensile failure. The test setup (shown in Figure 6-5) shows a load cell for collecting tensile loads and Linear voltage displacement transducers (LVDT's) for measuring the resulting crack width. These specimens were pulled apart by

manually by tightening a nut on the threaded rod while data was continuously collected.

Care was taken to conduct this test at a relatively slow rate. Figure 6-6 shows the plots of the results from this experiment.



Figure 6-5. Direct tension test conducted as an extra step to this work.

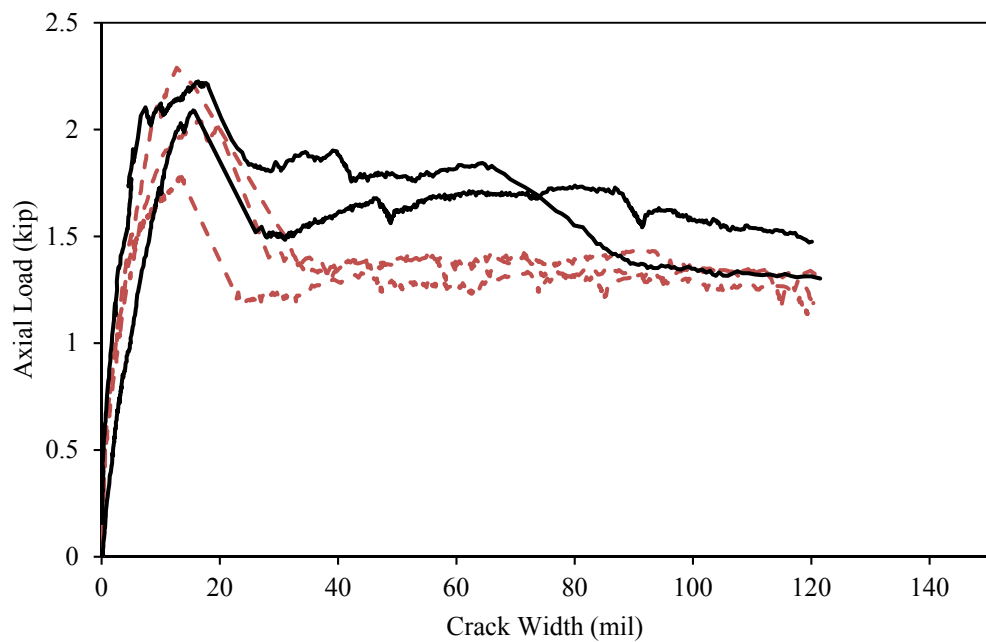


Figure 6-6. DT test specimen results.

### **6.3.4 Comparison of DT and EWS**

DT is the tension forces achieved when a specimen is being directly put into tension, while EWS is a back calculation of the effective tensile stress of the fibers from a flexure test. Table 6-2 presents a comparison of fiber tensile stresses for DT and EWS. Of the two mixtures compared it can be seen that EWS is conservative by 32% and 19% respectively as compared to DT. This relatively large difference is likely due to the assumptions utilized in the calculations of EWS, especially uniform fiber distribution, fiber orientation and fiber count at the crack. If adjustments are made to the d, depth of the idealized tension force in the fibers, it is relatively simple to reduce the difference significantly; however, this undermines previous assumptions.

Table 6-2. A comparison of fiber tensile forces in terms of fiber cross-sectional area not concrete cross-sectional area.

	H.S.S.4.25	H.S.E.9.25
Direct Tension (DT) (ksi)	13780	15440
Effective Working Stress (EWS) (ksi)	9319	12515

## **6.4 Conclusion**

This chapter discusses the mechanistic estimation method. This method is a tool that utilizes many of the assumptions associated with steel reinforced concrete design and allows for the estimation of flexural performance and effective working stress (EWS). As a comparison, direct tension testing was conducted as a comparison to EWS. The direct tension testing showed relatively different results, with differences likely resulting from variations in fiber dispersion, angle and uniformity.

## 7 CONCLUSION

The main objective of this work was to characterize and investigate the behavior of FRC as a function of fiber properties and to provide new parameters to aid in fiber selection and analysis. Eleven different fibers were tested at three different dosages each, after 28 days of curing. Four FRC mixtures were also evaluated at 24 hours of curing to evaluate performance at a lower compressive strength. In total 37 different FRC mixtures and 1 plain concrete mixture were reported in this laboratory study to investigate the effect of fiber dosage, type and geometry on the compressive strength, modulus of elasticity, MOR, RS, RSR, post-crack toughness, EWS and, PCP index.

This study found a number of conclusions related to general fiber properties, post-crack toughness, PCP index, and EWS. The following are some major conclusions drawn on the behavior of fiber reinforced concrete

- Qualitatively, the addition of fibers to concrete reduces workability and makes it more difficult to obtain a proper air entrainment. (Section 5.2)
- Synthetic fibers have very little effect on the uncracked properties (compressive strength, modulus of elasticity and, MOR). (Section 5.3.1)
- Fiber type (material) appears to play a large role in the fibers ability of enhance the concrete in cracked and uncracked states. Steel fibers showed higher performance in terms of cracked and uncracked properties versus the synthetic polypropylene fibers used in this work. This is likely related to the fibers modulus of elasticity and the fibers ability to remain anchored into the concrete. (Sections 5.3.1.2 and 5.3.2.2)

- Fiber dosage generally increased the fiber performance linearly in the dosage range explored (0.25%  $V_f$  to 0.75%  $V_f$ ) for the synthetic fibers; however, the steel fibers experienced a significant decrease in performance with dosage increase after 0.5%  $V_f$ . It is likely that the higher dosage steel fiber mixture altered the failure mechanism when a certain crack face stress was achieved from a fiber pullout failure to a mechanism related to the concrete strength. (Section 5.3.2.2)
- Embossed, twisted and crimped fibers performed better on average than straight flat synthetic fibers when comparison is made in terms of cracked concrete properties. (Section 5.3.2.3)
- $V_f$ , stiffness and geometry of the fibers significantly influence the post-crack (cracked) behavior of FRC. Evidence suggests that fiber geometry plays the largest role in behavior. (Sections 5.3.2.4 and 5.3.2.5)
- PCP index is an appropriate tool in comparing fiber efficiency across several dosages and works well for comparing fibers behavior directly. (Sections 3.2.2 and 5.3.2.7)
- Several strong correlations were developed relating cracked concrete behavior with  $V_f$  and RI. Of the correlations, the strongest correlation used the PCP index to account for fiber properties (type, geometry, length, aspect ratio, etc) and predicted RS as a function of  $V_f$  ( $R^2 = 0.9054$ ). (Section 5.3.2.9)
- Post-crack toughness better represents the fibers contribution to the composite because it does not include the pre-crack toughness, which typically remains constant for low modulus fibers. This is beneficial because it is not artificially

increased by a constant, especially when design already expects for the concrete to be cracked when the fibers are needed for strength.

- Some of the fibers resulted in low MOR's but have shown high RS which resulted in higher RSR's. So, consideration of only MOR, RSR, RS or post-crack toughness alone for characterizing crack resistance of fiber reinforced concrete may be misleading. Consideration should be given to FRC parameters in the cracked and uncracked states separately, since the properties in each state can vary so greatly independent of one another. (Section 5.3)

## 8 BIBLIOGRAPHY

- ACI 544.1R, (2009). *State-of-the-Art Report on Fiber Reinforced Concrete*. Farmington Hills, MI, American Concrete Institute.
- ACI 544.1R, (2002). *State-of-the-Art Report on Fiber Reinforced Concrete*. Farmington Hills, MI, American Concrete Institute.
- ACI 544.2R, (1999). *Measurement of Properties of Fiber Reinforced Concrete*. Detroit, MI, American Concrete Institute.
- ACI 544.3R, (2008). *Guide for Specifying, Proportioning, and Production of Fiber-Reinforced Concrete*. Farmington Hills, MI, American Concrete Institute.
- ACI 544.5R, (2010). *Report on the physical properties and durability of fiber reinforced concrete*. Farmington Hills, MI, American Concrete Institute.
- Altoubat, S., Lange, D., (2001). “Creep, Shrinkage, and Cracking of Restrained Concrete at Early Age.” *ACI Materials Journal*, American Concrete Institute.
- ASTM A820, (2016). *Standard Specification for Steel Fibers for Fiber Reinforced Concrete*. West Conshohocken, PA, ASTM International.
- ASTM C39, (2017). *Standard Test Method for Compressive Strength of Cylindrical Concrete Specimens*. West Conshohocken, PA, ASTM International.
- ASTM C143, (2015). *Standard Test Method for Slump of Hydraulic-Cement Concrete*. West Conshohocken, PA, ASTM International.
- ASTM C1609, (2012). *Standard Test Method for Flexural Performance of Fiber-Reinforced Concrete (Using Beam with Third-Point Loading)*. West Conshohocken, PA, ASTM International.
- ASTM C231, (2017). *Standard Test Method for Air Content of Freshly Mixed Concrete by Pressure Methods*. West Conshohocken, PA, ASTM International.
- ASTM C469, (2014). *Standard Test Method for Static Modulus of Elasticity and Poisson’s Ratio of Concrete in Compression*. West Conshohocken, PA, ASTM International.
- ASTM C1666, (2015). *Standard Specification for Fiber-Reinforced Concrete*. West Conshohocken, PA, ASTM International.
- Balaguru et. al., (1992). “Flexural Toughness of steel fiber reinforced concrete.” *ACI Materials Journal*, American Concrete Institute, 541-546.
- Balaguru, P., Ramakrishnan, V. (1985). “Freeze-Thaw Durability of Fiber Reinforce Concrete”. *ACI Materials Journal*, American Concrete Institute.

- Barborak, R. (2011). "Fiber reinforced Concrete (FRC)" *Construction and Materials TIPS*, <[ftp://ftp.dot.state.tx.us/pub/txdpt-info/cst/tips/frc\\_4550.pdf](ftp://ftp.dot.state.tx.us/pub/txdpt-info/cst/tips/frc_4550.pdf)>
- Banithia, N., Sappakittipakorn, M. (2007). *Toughness enhancement in steel fiber reinforced concrete through fiber hybridization*. Elsevier.
- Barman, M., (2014). "Joint Performance Characterization of Bonded Whitetopping Overlays." Pittsburgh: University of Pittsburgh.
- Colley, B. E. & Humphrey, H. A., 1967. Aggregate Interlock at Joints in Concrete Pavements. *Highway Research Record*, Issue 198, pp. 1-18.
- Gaddam. (2016). "Fiber reinforced concrete and behavior properties and applications and advantages." <[civiline.blogspot.com](http://civiline.blogspot.com)> (Sept. 6, 2016)
- Hannant, D., (1978). *Fibre Cements and Fibre Concretes*. John Wiley & Sons Ltd., Chichester, United Kingdom, 53.
- Kosa, K., Naaman, A. E. (1990). "Corrosion of Steel Fiber Reinforced Concrete". *ACI Materials Journal*, American Concrete Institute, 27-37.
- Ludirdja, D., Yougn, J., (1992). *Synthetic Fiber Reinforcement for Concrete*. Champaign, IL: U.S. Army Construction Engineering Research Laboratories.
- Mahadik, S., Kamane, A., (2014). "Effect of steel fibers on compressive and flexural strength on concrete". International Journal of Advanced structures and Geotechnical Engineering.
- Mangat, P., Gerusamy, K. (1987). Long Term Properties of Steel Fiber-Reinforce Marine Concrete. *Materials and Constructions (RILEM)*, 273-282.
- Portland Cement Association (PCA), (2015). *Design and Control of Concrete Mixtures 15<sup>th</sup> edition*. PCA, Skokie, IL.
- Prince, R. (2016). "Basalt Fiber Properties". <<http://www.build-on-prince.com/basalt-fiber>> (September, 2016).
- Ramakrishnan, V., (1987). "Materials and Properties of Fibre Concrete." *Proceedings of the international symposium on Fibre Reinforced Concrete*, Madras, India.
- Rasmussen, R., Rozycki, D. (2004). *Thin and Ultra-Thin Whitetopping. NCHRP Synthesis of Highway Practice 338*. Washington, DC: National Cooperative Highway Research Program.
- Raja, Z. I., Snyder, M. B., 1995. *Factors Affecting the Deterioration of Transverse Cracks in JRCP*. East Lansing, MI: Michigan State University, Department of Civil and Environmental Engineering, Michigan Department of Transportation

and Great Lakes Center for Truck Transportation Research University of Michigan.

Roesler, J., A. Bordelon, A. Ioannides, M. Beyer, and D. Wang. *Design and Concrete Material Requirements for Ultra-Thin Whitetopping*. Publication FHWA- ICT-08-016. Illinois Center for Transportation, IL, 2008.

Tavakoli, M., (1994). “Tensile and Compressive Strengths of Polypropylene Fiber Reinforced Concrete.” Section in *Fiber reinforced concrete: Developments and innovations SP-142*. American Concrete Institute, Detroit, MI, 61-72.

Vasile, C. (2000). “Polyolefin fibers”. *Handbook of Polyolefins*. New York: Marcel Dekker. (773-808).

Vandenbossche Julie M., M. B. (2015). Characterization of Load Transfer Behavior for Bonded Concrete Overlays on Asphalt. *Transportation Research Record: Journal of the Transportation Research Board*, 143-151.

Vondran, G. (1987). “Making More Durable Concrete with Polymeric Fibers”. *Concrete Durability: Kathrine and Bryant Mather International Conference SP-100*. American Concrete Institute, Farmington Hills, MI, 377-396.

Zollo, R., (1984). “Collated Fibrillated Polypropylene Fibers in FRC.” In *SP-81* Detroit, MI, American Concrete Institute, 397-409.

## A APPENDIX: LITERATURE REVIEW

Table A-1. General properties of selected fiber types (after PCA, 2015).

Fiber type	Relative density (specific gravity)	Diameter, $\mu\text{m}$ (0.001 in.)	Tensile strength, MPa (ksi)	Modulus elasticity, MPa (ksi)	Strain at failure, %
Steel	7.80	100–1000 (4–40)	500–2600 (70–380)	210,000 (30,000)	0.50–3.5
Glass	E	8–15 (0.3–0.6)	2000–4000 (290–580)	72,000 (10,400)	3.0–4.8
		12–20 (0.5–0.8)	1500–3700 (220–540)	80,000 (11,600)	2.5–3.6
	AR				
<b>Synthetic</b>					
Acrylic	1.18	5–17 (0.2–0.7)	200–1000 (30–145)	17,000–19,000 (2500–2800)	28–50
Aramid	1.44	10–12 (0.4–0.47)	2000–3100 (300–450)	62,000–120,000 (9000–17,000)	2–3.5
Carbon	1.90	8–9 (0.3–0.35)	1800–2600 (260–380)	230,000–380,000 (33,400–55,100)	0.5–1.5
Nylon	1.14	23 (0.9)	1000 (140)	5200 (750)	20
Polyester	1.38	10–80 (0.4–3.0)	280–1200 (40–170)	10,000–18,000 (1500–2500)	10–50
Polyethylene	0.96	25–1000 (1–40)	80–600 (11–85)	5000 (725)	12–100
Polypropylene	0.90	20–200 (0.8–8)	450–700 (65–100)	3500–5200 (500–750)	6–15
<b>Natural</b>					
Wood cellulose	150	25–125 (1–5)	350–2000 (51–290)	10,000–40,000 (1500–5800)	
Sisal			280–600 (40–85)	13,000–25,000 (1900–3800)	3.5
Coconut	1.12–1.15	100–400 (4–16)	120–200 (17–29)	19,000–25,000 (2800–3800)	10–25
Bamboo	1.50	50–400 (2–16)	350–500 (51–73)	33,000–40,000 (4800–5800)	
Jute	1.02–1.04	100–200 (4–8)	250–350 (36–51)	25,000–32,000 (3800–4600)	1.5–1.9
Elephant grass		425 (17)	180 (26)	4900 (710)	3.6

Table A-2. Typical properties of natural fibers (after ACI 544.1R, 2009).

Fiber type	Coconut	Sisal	Sugar cane Bagasse	Bamboo	Jute	Flax	Elephant grass	Water reed	Plantain	Musamba	Wood fiber (kraft pulp)
Fiber length, in.	2-4	N/A	N/A	N/A	7-12	20	N/A	N/A	N/A	N/A	0.1-0.2
Fiber diameter, in.	0.004- 0.016	N/A	0.008- 0.016	0.002- 0.016	0.004- 0.008	N/A	N/A	N/A	N/A	N/A	0.001-0.003
Specific gravity	1.12-1.15	N/A	1.2-1.3	1.5	1.02-1.04	N/A	N/A	N/A	N/A	N/A	1.5
Modulus of elasticity, ksi	2750- 3770	1880- 3770	2175-2750	4780- 5800	3770-4640	14,500	710	750	200	130	N/A
Ultimate tensile strength, psi	17,400- 29,000	40,000- 82,400	26,650- 42,000	50,750- 72,500	36,250- 50,750	145,000	25,800	10,000	13,300	12,000	101,500
Elongation at break, percent	10-25	3-5	N/A	N/A	1.5-1.9	1.8-2.2	3.6	1.2	5.9	9.7	N/A
Water absorption, percent	130-180	60-70	70-75	40-45	N/A	N/A	N/A	N/A	N/A	N/A	50-75

Note: N/A = properties not readily available or not applicable.  
Metric equivalents: 1 in. = 25.4 mm; 1 ksi = 1000 psi = 6.895 MPa

Table A-3. Range of proportions for normal weight steel fiber reinforced concrete (after ACI 544.1R, 2009).

Mix parameters	3/8 in. maximum-size aggregate	3/4 in. maximum-size aggregate	1-1/2 in. maximum-size aggregate
Cement, lb/yd <sup>3</sup>	600-1000	500-900	470-700
w/c	0.35-0.45	0.35-0.50	0.35-0.55
Percent of fine to coarse aggregate	45-60	45-55	40-55
Entrained air content, percent	4-8	4-6	4-5
Fiber content, vol. percent			
Deformed fiber	0.4-1.0	0.3-0.8	0.2-0.7
Smooth fiber	0.8-2.0	0.6-1.6	0.4-1.4

## B APPENDIX: FIBER IMAGES



Figure B-1. Image of Fiber 1.



Figure B-2. Image of Fiber 2.



Figure B-3. Image of Fiber 3.



Figure B-4. Image of Fiber 4.



Figure B-5. Image of Fiber 5.



Figure B-6. Image of Fiber 6.

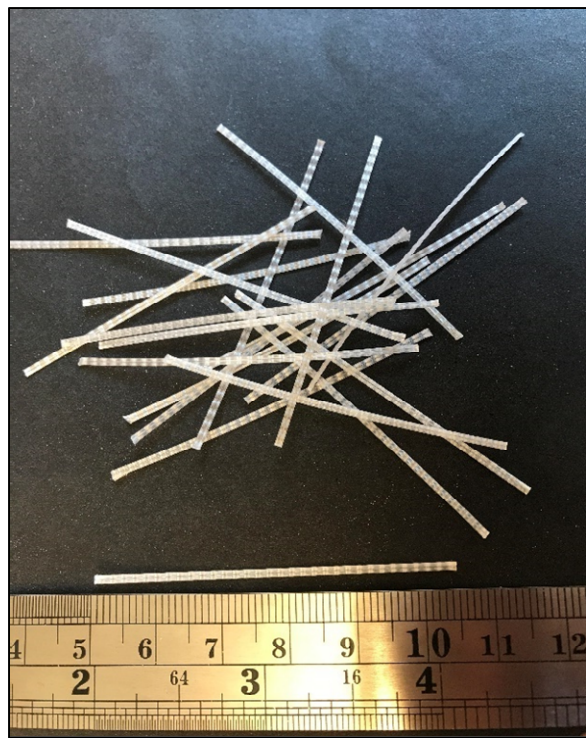


Figure B-7. Image of Fiber 7.



Figure B-8. Image of Fiber 8.

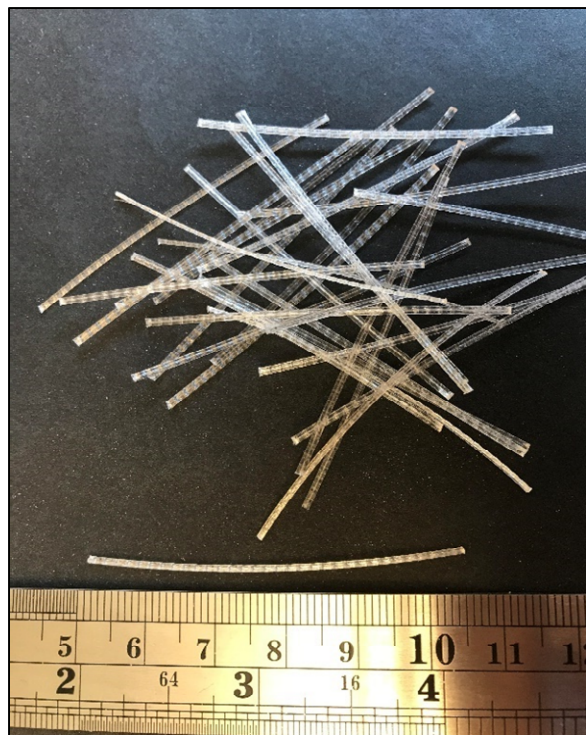


Figure B-9. Image of Fiber 9.

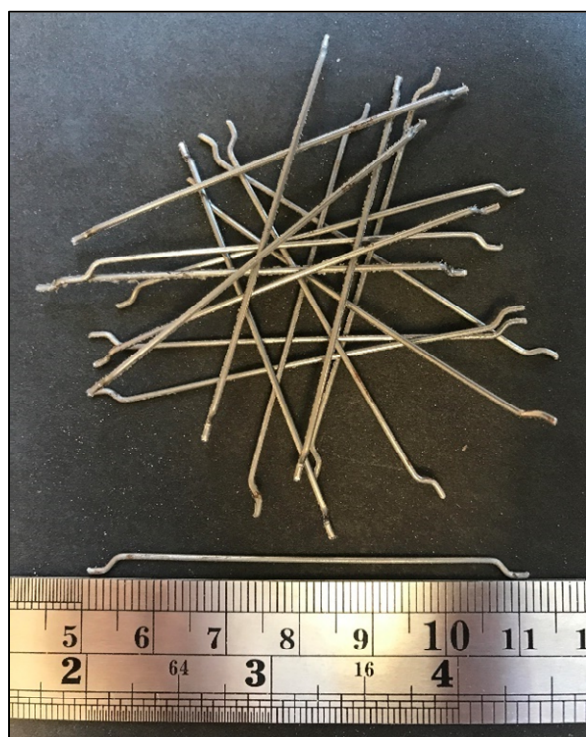


Figure B-10. Image of Fiber 10.



Figure B-11. Image of Fiber 11.

## C APPENDIX: MIXTURE RESULTS

Table C-1. Properties collected from ASTM 1609 testing.

Designation	MOR (psi)	RSR L/180 (%)	RSR L/600 (%)	Toughness (lb-in)	Post-Crack Toughness (lb-in)
H.S.S.1.25	710	10.4	8.8	246	122
H.S.S.1.5	750	20.6	30.5	397	279
H.S.S.1.75	760	35.6	43.2	519	407
H.S.S.2.25	710	6.8	0	266	49
H.S.S.2.5	690	24.2	26	376	215
H.S.S.2.75	780	45.9	45	520	356
H.S.S.3.25	790	2.9	0	364	14
H.S.S.3.5	770	21.4	33	399	233
H.S.S.3.75	780	41.3	53	626	428
H.S.S.4.25	740	12.4	8	256	99
H.S.S.4.5	750	29.3	25	391	225
H.S.S.4.75	750	46.1	48	570	388
H.S.T.5.25	780	14.9	8	308	117
H.S.T.5.5	690	29.4	28	391	230
H.S.T.5.75	680	47.4	45	521	354
H.S.C.6.25	680	16.8	4	282	122
H.S.C.6.5	750	31.7	28	473	279
H.S.C.6.75	790	41.1	42	594	407
H.S.E.7.25	720	15.8	6	334	121
H.S.E.7.5	780	34.0	43	548	349.3
H.S.E.7.75	760	43.3	51	553	370
H.S.E.8.25	700	14.2	7	297	113
H.S.E.8.5	720	20.6	27	396	214
H.S.E.8.75	710	36.4	52	546	374.3
H.S.E.9.25	760	17.4	12	343	153
H.S.E.9.5	690	41.4	41	502	334
H.S.E.9.75	730	50.6	55	615	43
H.L.EC.10.25	780	29.3	37	481	286
H.L.EC.10.5	790	67	89	924	669
H.L.EC.10.75	930	54.6	80	955	661
H.S.T.11.25	700	12.4	9.3	267	105
H.S.T.11.5	795	20.1	28.6	421	228
H.S.T.11.75	790	34.3	47.5	576	377
(H) Control	720	N/A	N/A	N/A	N/A
L.S.E.9.5	480	34.1	39.2	309	198
L.S.C.6.5	500	43.4	40.8	354	245
L.S.S.4.5	460	36.7	40.4	295	134
L.S.T.5.5	470	40.3	38.8	315	210

Table C-2. Compressive Properties of FRC tested in this work.

Designation	Compressive Strength (psi)	Modulus of Elasticity (ksi)	
		Lab Test	Approx.
H.S.S.1.25	6,570	4,720	4,620
H.S.S.1.5	6,940	4,730	4,748
H.S.S.1.75	6,850	4,920	4,718
H.S.S.2.25	6,690	4,450	4,662
H.S.S.2.5	6,290	4,530	4,521
H.S.S.2.75	7,170	4,820	4,827
H.S.S.3.25	6,670	4,630	4,655
H.S.S.3.5	6,860	4,730	4,721
H.S.S.3.75	6,830	4,640	4,711
H.S.S.4.25	6,660	4,950	4,652
H.S.S.4.5	6,670	4,640	4,655
H.S.S.4.75	6,740	4,680	4,680
H.S.T.5.25	6,960	5,320	4,755
H.S.T.5.5	6,230	4,270	4,499
H.S.T.5.75	6,410	4,300	4,564
H.S.C.6.25	6,920	5,060	4,742
H.S.C.6.5	7,788	5,210	5,030
H.S.C.6.75	7,260	4,680	4,857
H.S.E.7.25	6,740	4,970	4,680
H.S.E.7.5	7,060	4,470	4,789
H.S.E.7.75	6,760	4,860	4,686
H.S.E.8.25	6,610	4,650	4,634
H.S.E.8.5	6,380	4,780	4,553
H.S.E.8.75	6,770	4,810	4,690
H.S.E.9.25	7,080	4,720	4,796
H.S.E.9.5	6,840	4,620	4,714
H.S.E.9.75	7,100	4,870	4,803
H.L.EC.10.25	7,330	6,140	4,880
H.L.EC.10.5	7,970	6,270	5,089
H.L.EC.10.75	9,320	5,940	5,503
H.S.T.11.25	7320	x	4,877
H.S.T.11.5	7840	x	5,047
H.S.T.11.75	7370	x	4,893
(H) Control	6,960	4,990	4,755
L.S.E.9.5	4210	x	3,698
L.S.C.6.5	4380	x	3,772
L.S.S.4.5	3820	x	3,523
L.S.T.5.5	3830	x	3,527

x Information unavailable

Table C-3. Fresh concrete properties for the mixtures evaluated in this work.

<b>Designation</b>	<b>Slump (in)</b>	<b>Air (%)</b>
H.S.S.1.25	1.25	8.1
H.S.S.1.5	1	7.1
H.S.S.1.75	0.5	5.8
H.S.S.2.25	0.75	6.5
H.S.S.2.5	0.5	5.9
H.S.S.2.75	1	6.1
H.S.S.3.25	0.5	5.6
H.S.S.3.5	2	7.8
H.S.S.3.75	0.75	5.7
H.S.S.4.25	2.5	8.5
H.S.S.4.5	0.5	7.8
H.S.S.4.75	0.75	6.1
H.S.T.5.25	3	5.9
H.S.T.5.5	2.75	8.1
H.S.T.5.75	2.25	9
H.S.C.6.25	1.75	7.9
H.S.C.6.5	3	8.5
H.S.C.6.75	0.5	5.5
H.S.E.7.25	1	5.5
H.S.E.7.5	1	9
H.S.E.7.75	1	7.1
H.S.E.8.25	1.5	7
H.S.E.8.5	2.25	7.8
H.S.E.8.75	0.75	5.6
H.S.E.9.25	1.25	7.5
H.S.E.9.5	3	7.9
H.S.E.9.75	1.5	8.1
H.L.EC.10.25	2.5	7.5
H.L.EC.10.5	2.25	5.6
H.L.EC.10.75	2	5.9
H.S.T.11.25	2.5	8.1
H.S.T.11.5	2.5	6.1
H.S.T.11.75	0.5	5.8
(H) Control	1.5	6.3
L.S.E.9.5	2.5	8.5
L.S.C.6.5	0.75	7.1
L.S.S.4.5	3	6.6
L.S.T.5.5	3	6.8

## D APPENDIX LOAD VERSUS DISPLACEMENT PLOTS

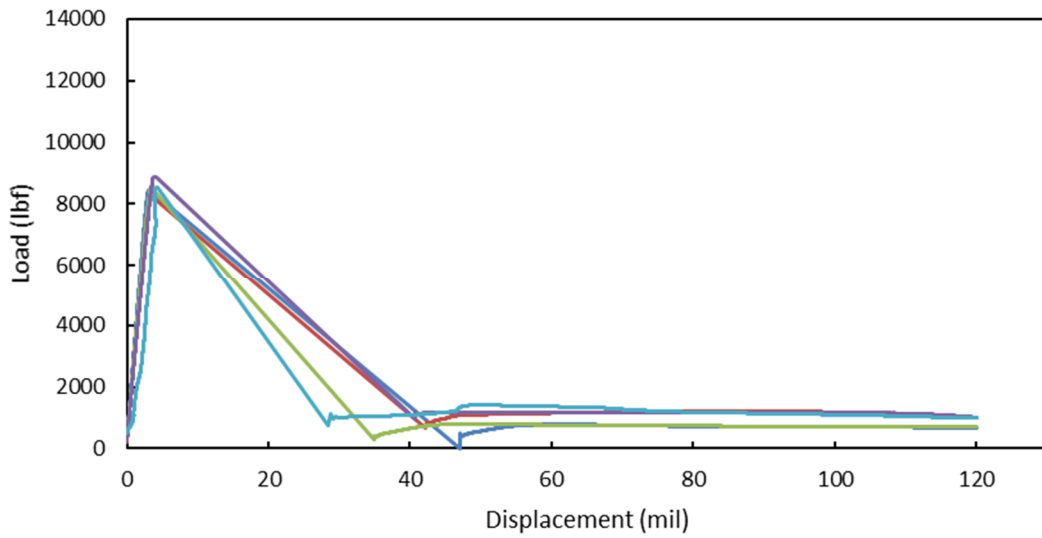


Figure D-1. Load versus displacement curves for H.S.S.1.25.

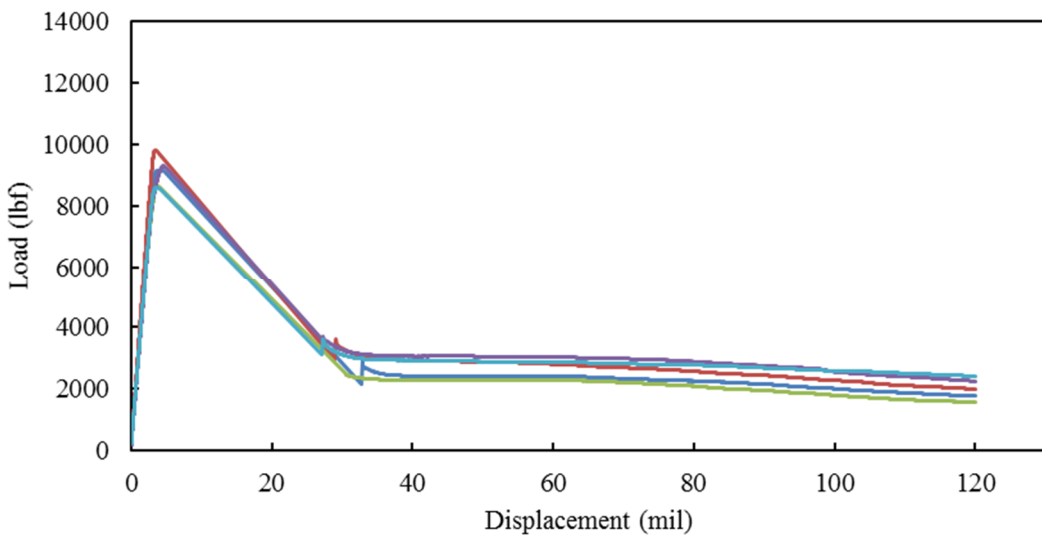


Figure D-2. Load versus displacement curves for H.S.S.1.5.

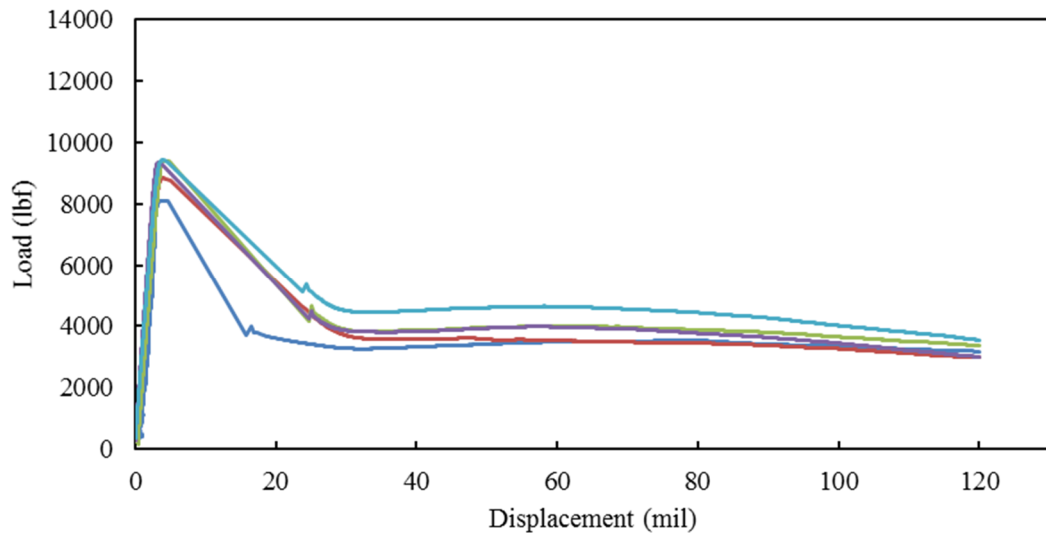


Figure D-3. Load versus displacement curves for H.S.S.1.75.

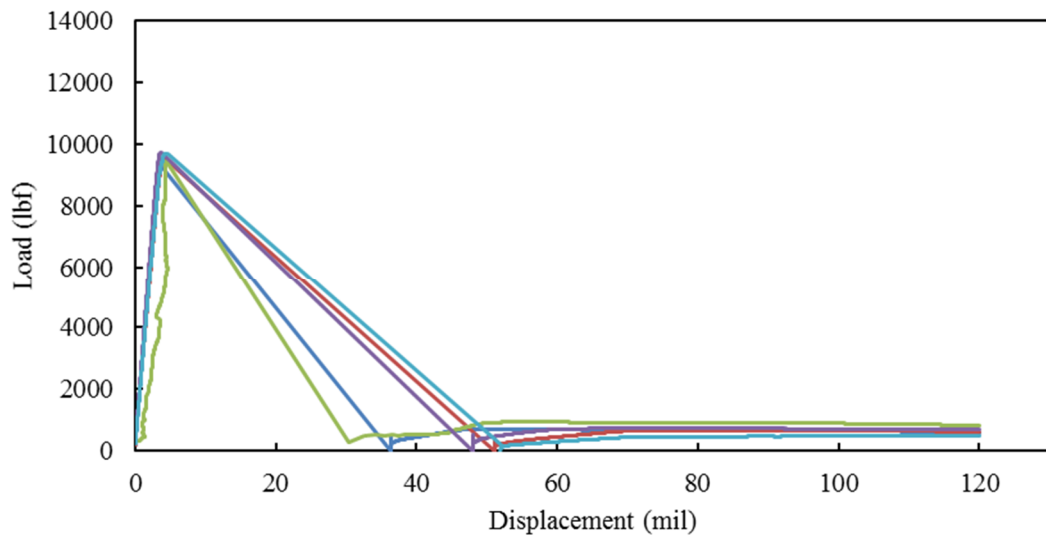


Figure D-4. Load versus displacement curves for H.S.S.2.25.

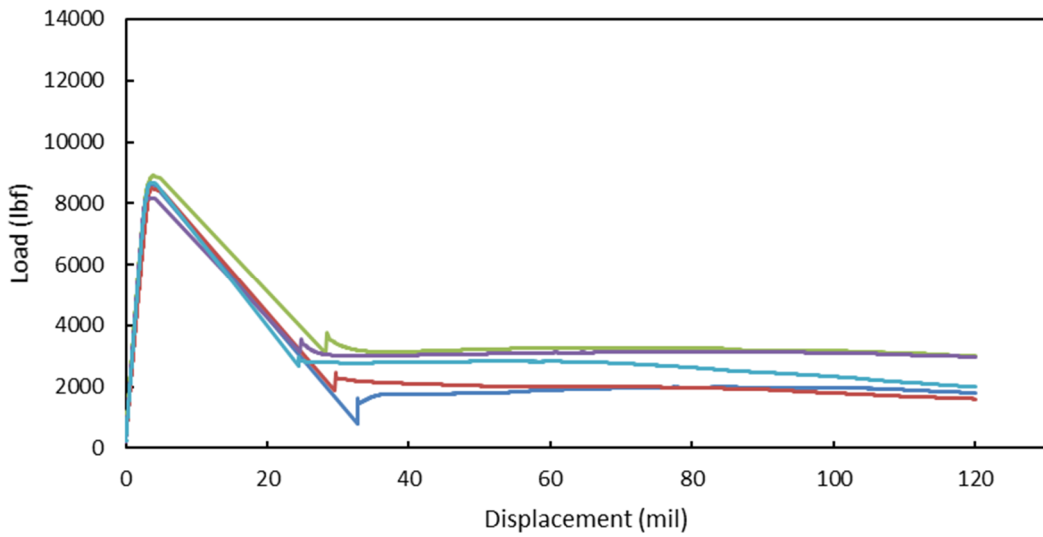


Figure D-5. Load versus displacement curves for H.S.S.2.5.

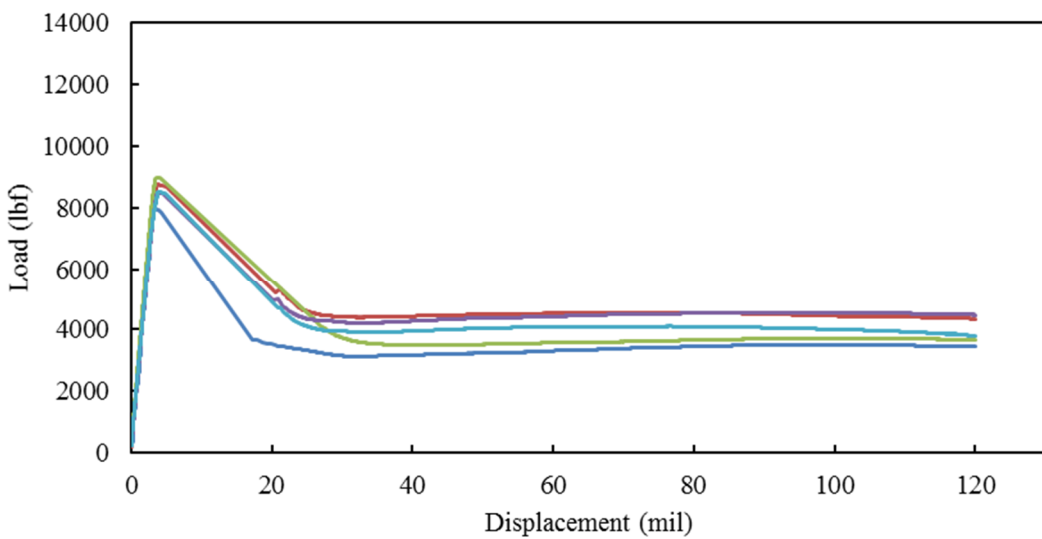


Figure D-6. Load versus displacement curves for H.S.S.2.75.

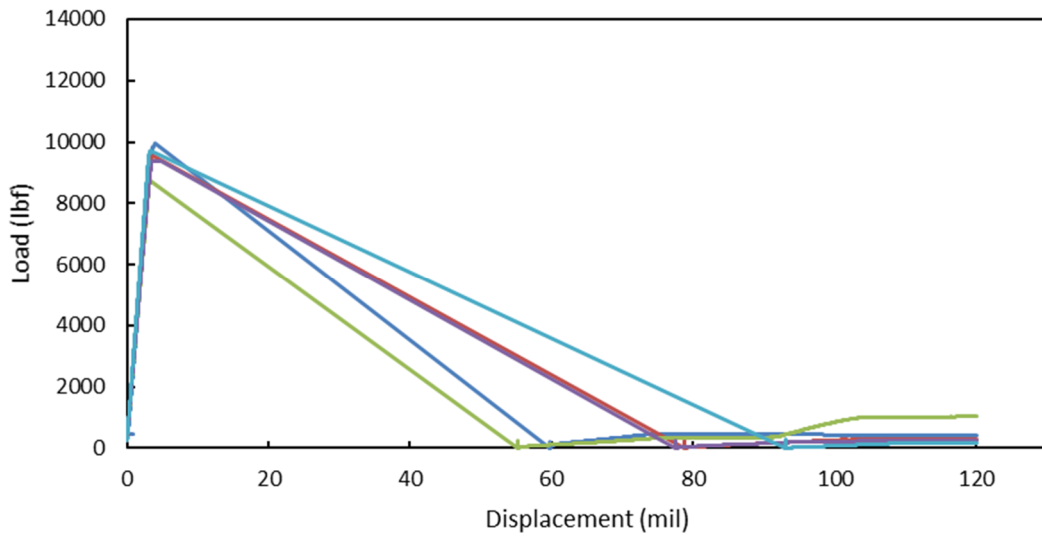


Figure D-7. Load versus displacement curve for H.S.S.3.25.

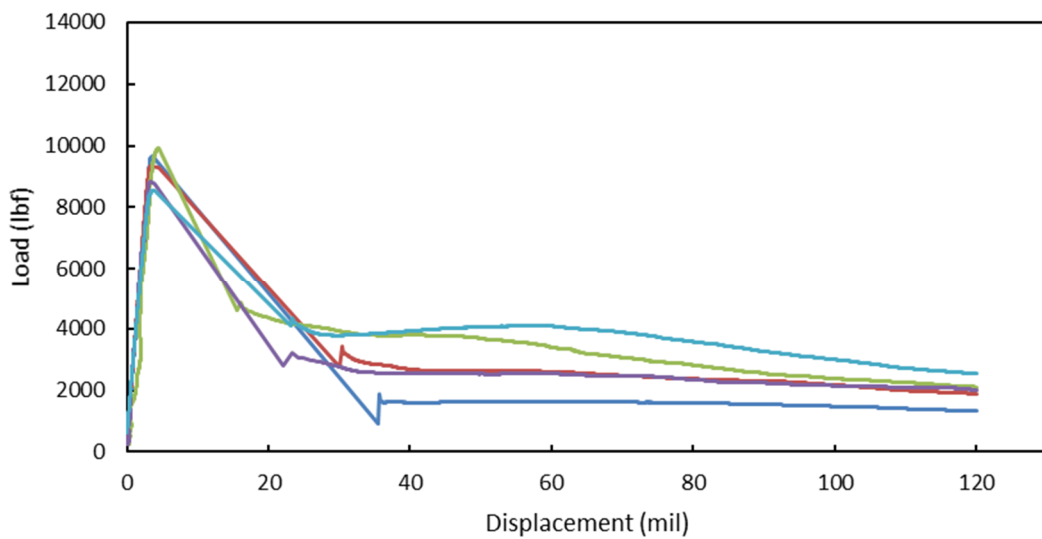


Figure D-8. Load versus displacement curves for H.S.S.3.5.

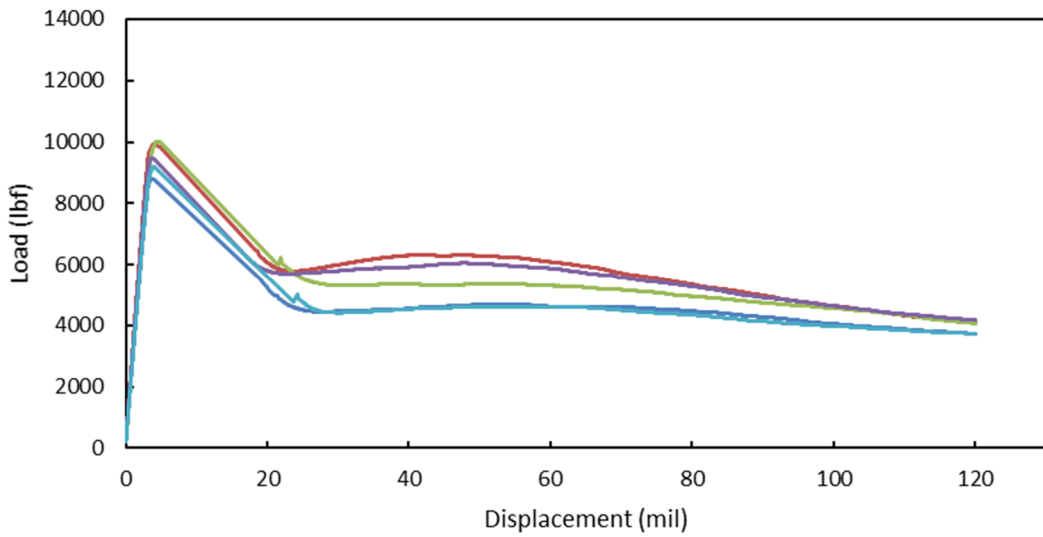


Figure D-9. Load versus displacement curves for H.S.S.3.75.

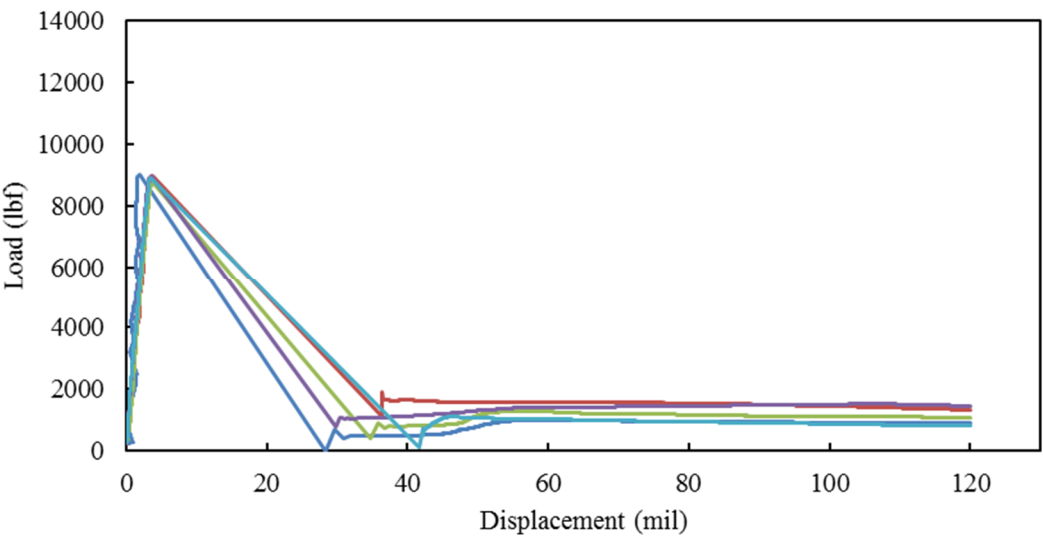


Figure D-10. Load versus displacement curves for H.S.S.4.25.

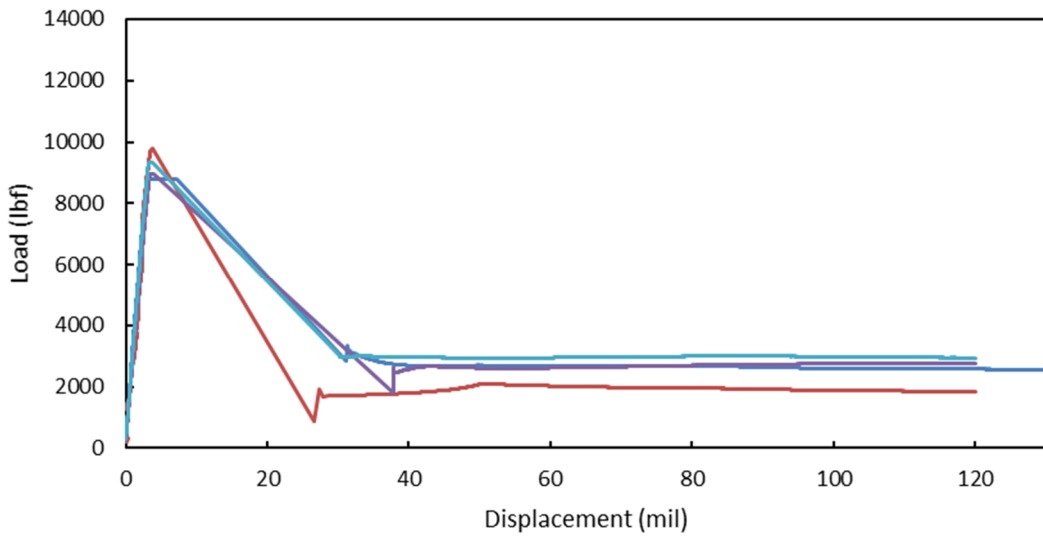


Figure D-11. Load versus displacement curves for H.S.S.4.5.

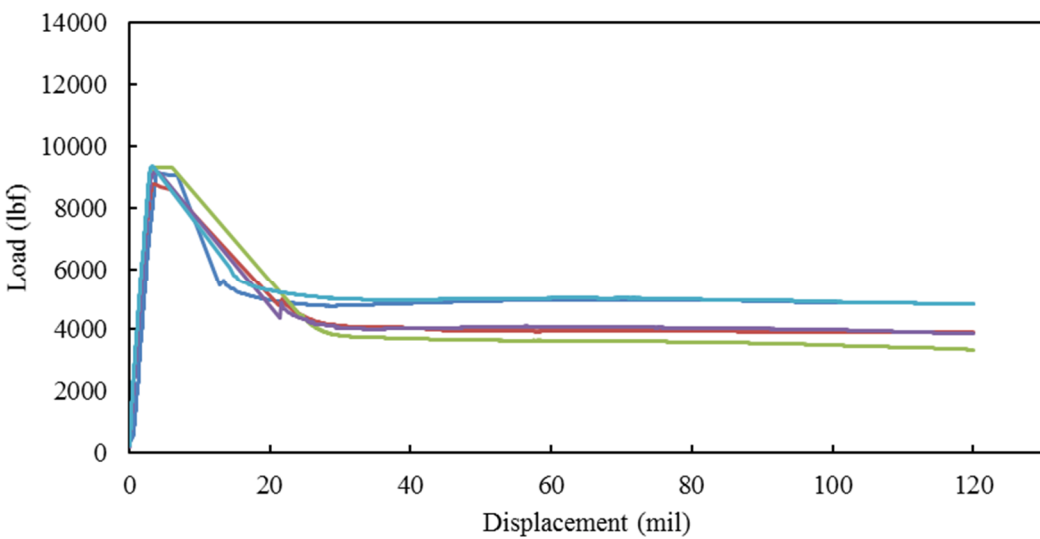


Figure D-12. Load versus displacement curves for H.S.S.4.75.

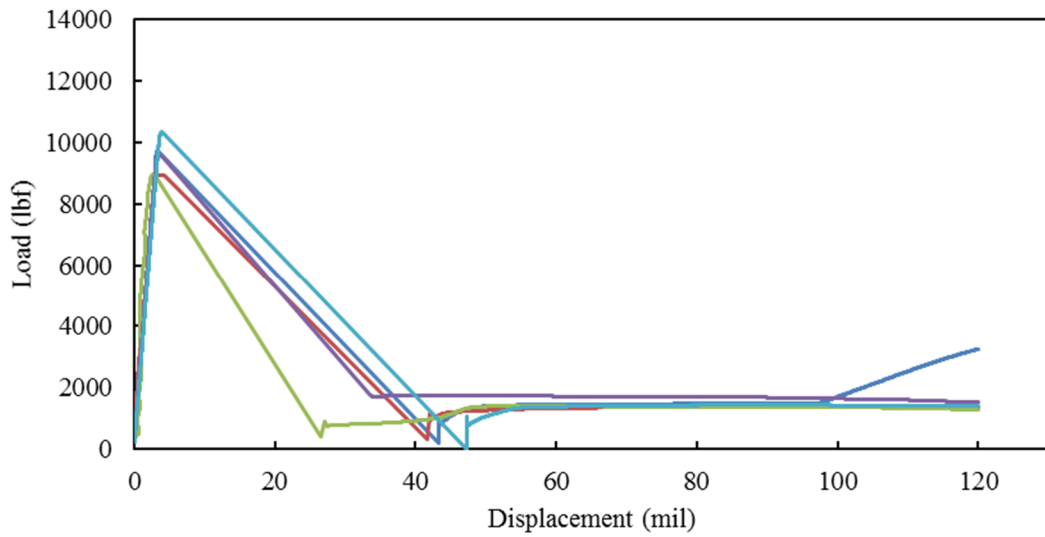


Figure D-13. Load versus displacement curves for H.S.T.5.25.

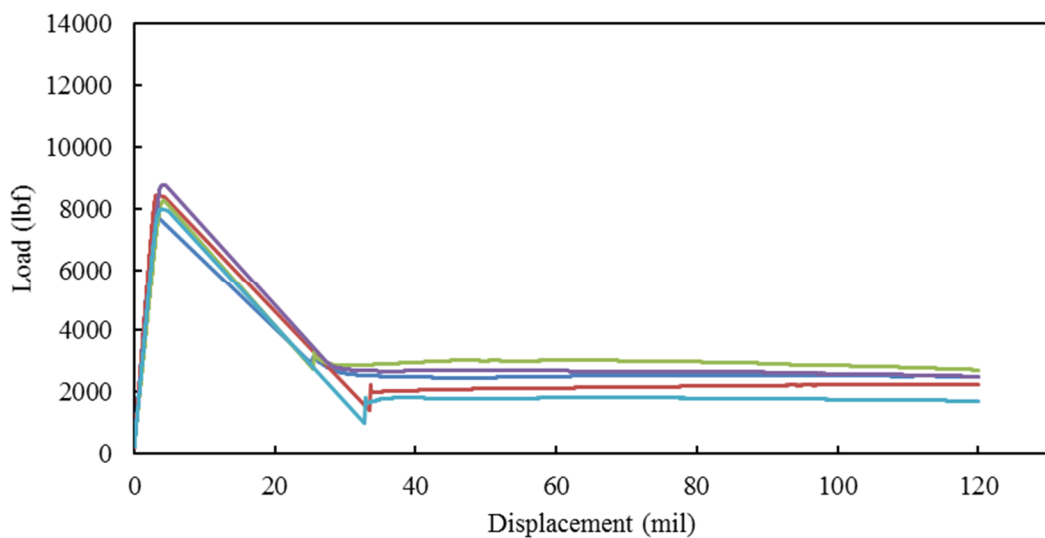


Figure D-14. Load versus displacement curves for H.S.T.5.5.

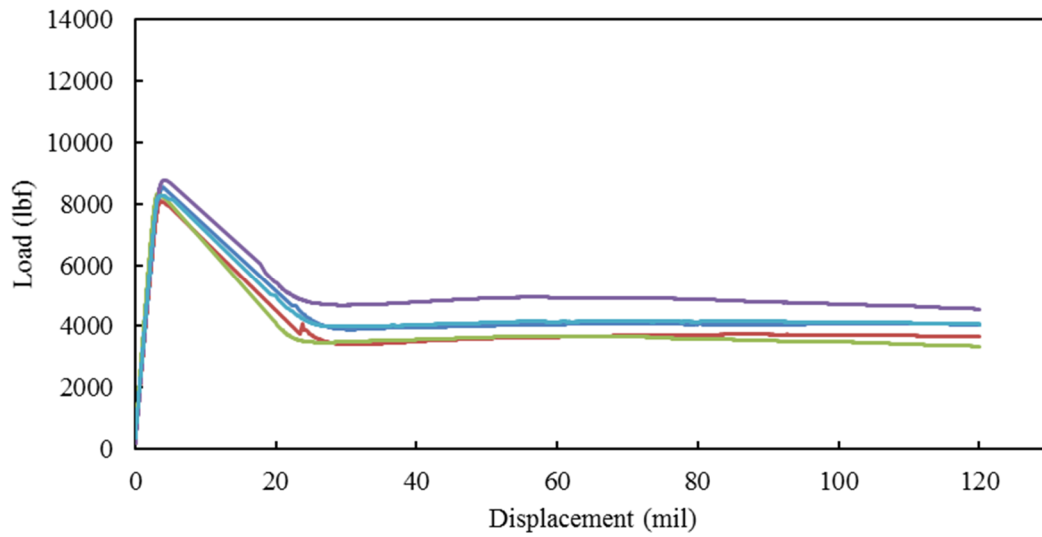


Figure D-15. Load versus displacement curves for H.S.T.5.75.

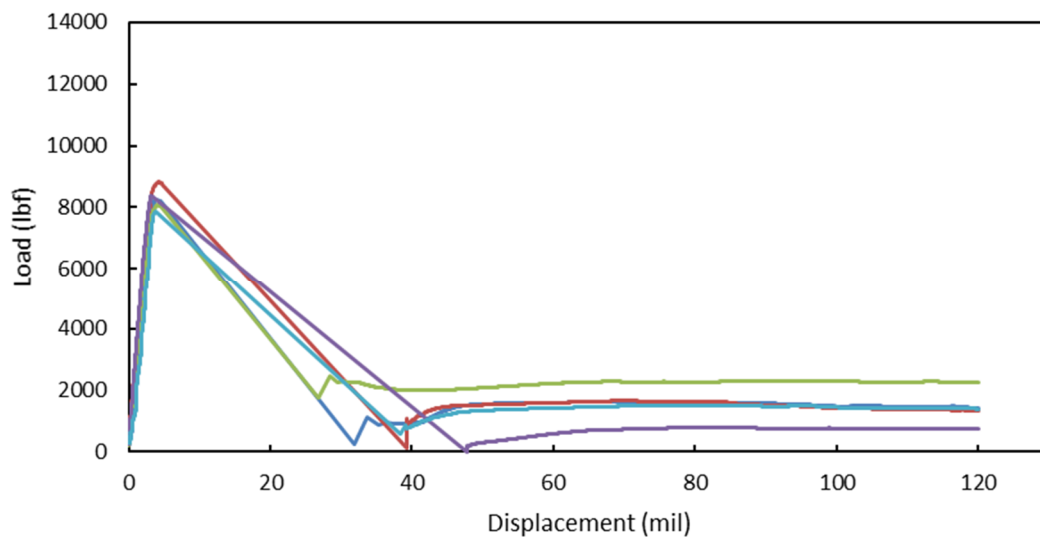


Figure D-16. Load versus displacement curves for H.S.C.6.25.

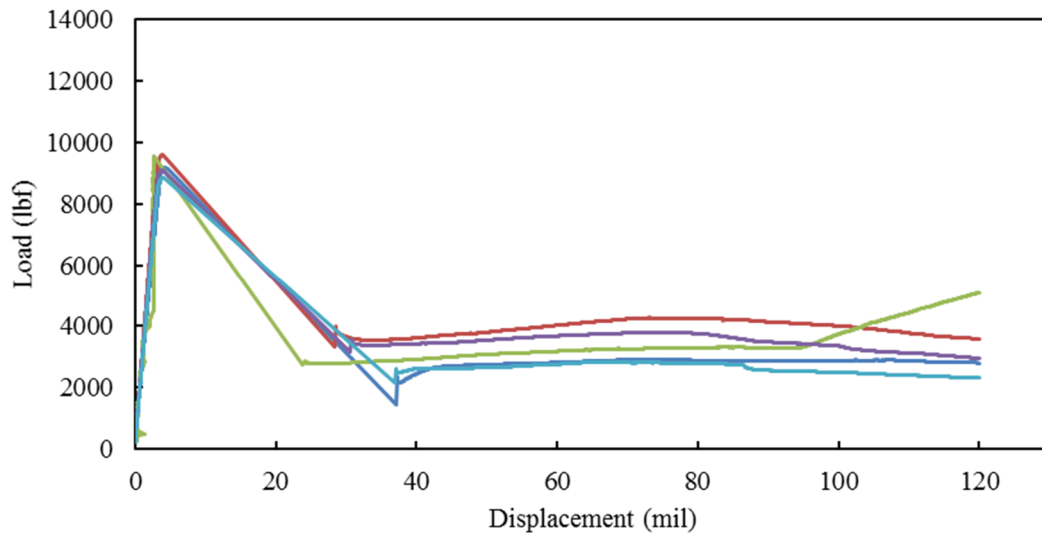


Figure D-17. Load versus displacement curves for H.S.C.6.5.

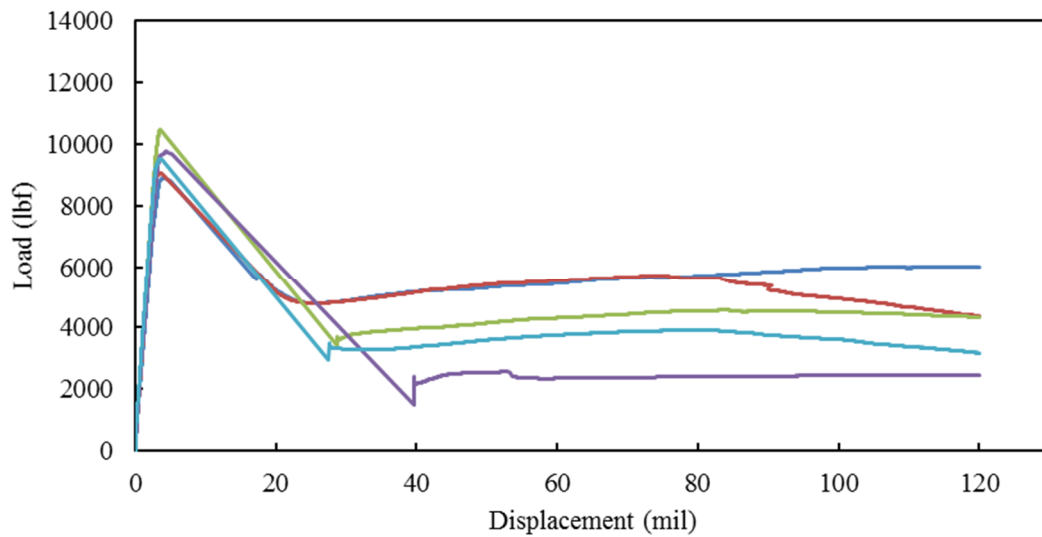


Figure D-18. Load versus displacement curves for H.S.C.6.75.

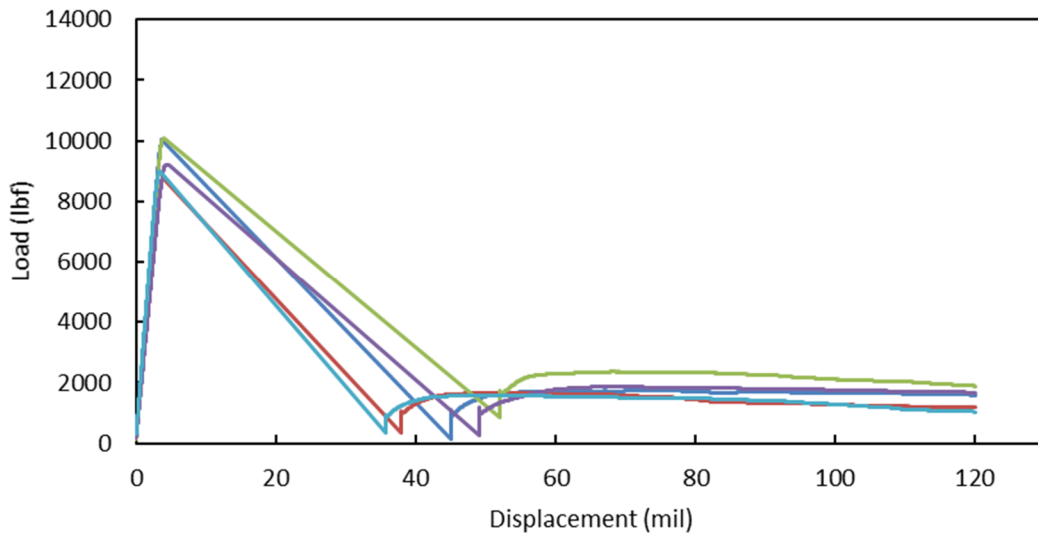


Figure D-19. Load versus displacement curves for H.S.E.7.25.

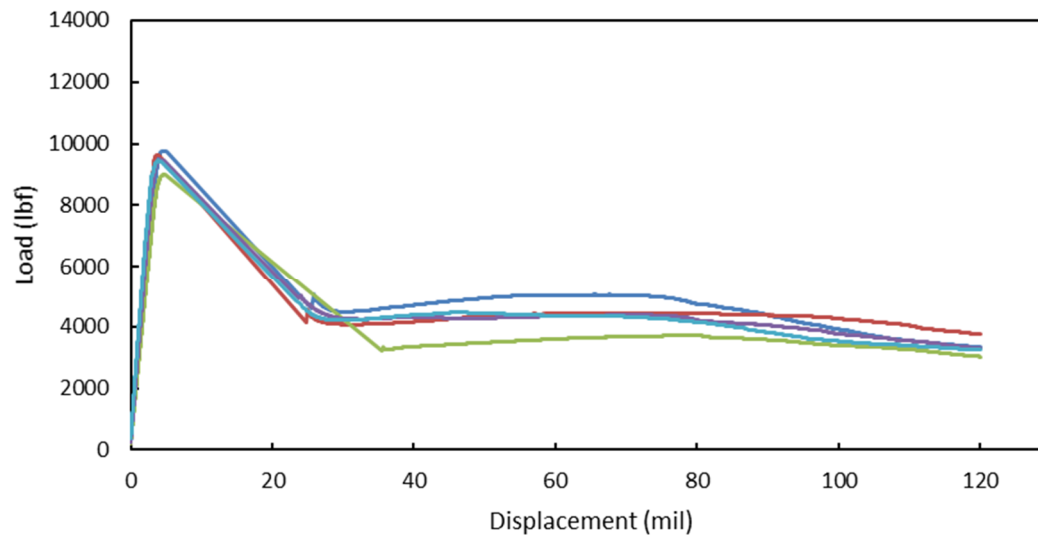


Figure D-20. Load versus displacement curves for H.S.E.7.5.

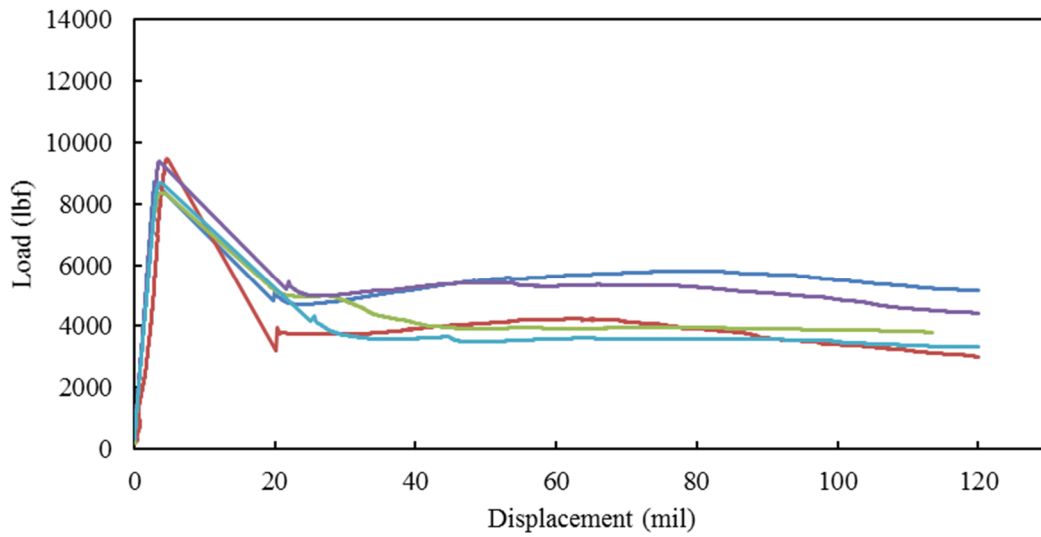


Figure D-21. Load versus displacement curves for H.S.E.7.75.

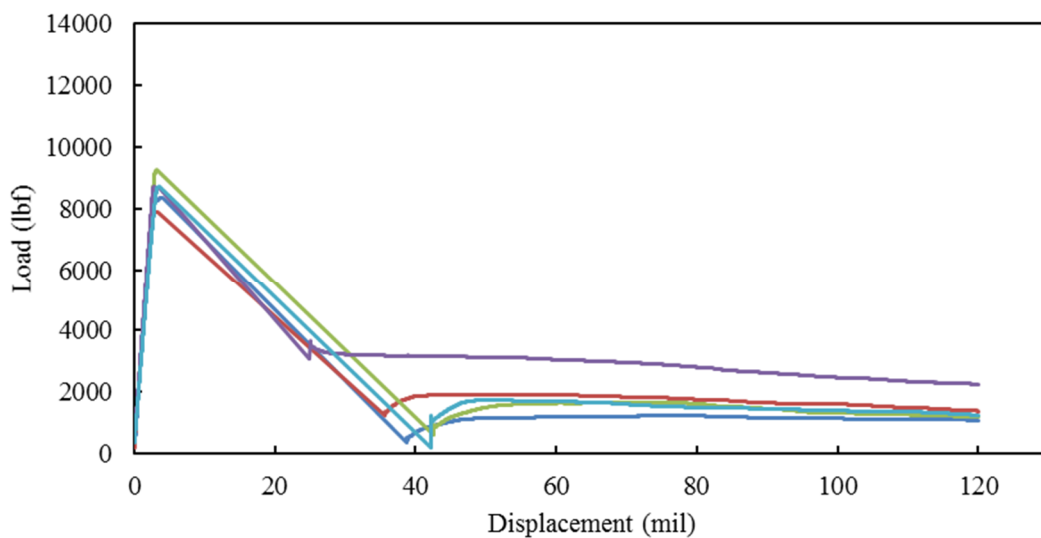


Figure D-22. Load versus displacement curves for H.S.E.8.25.

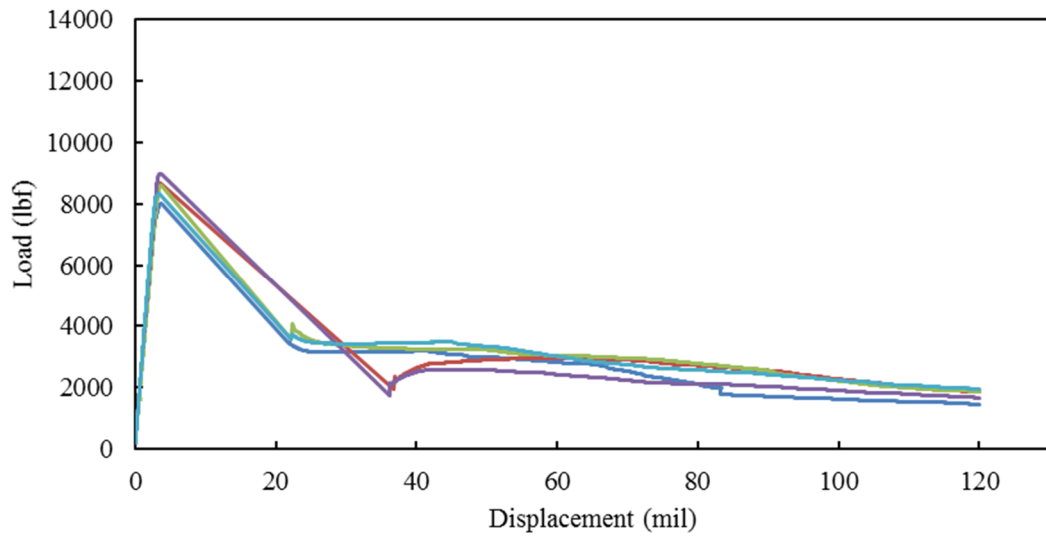


Figure D-23. Load versus displacement curves for H.S.E.8.5.

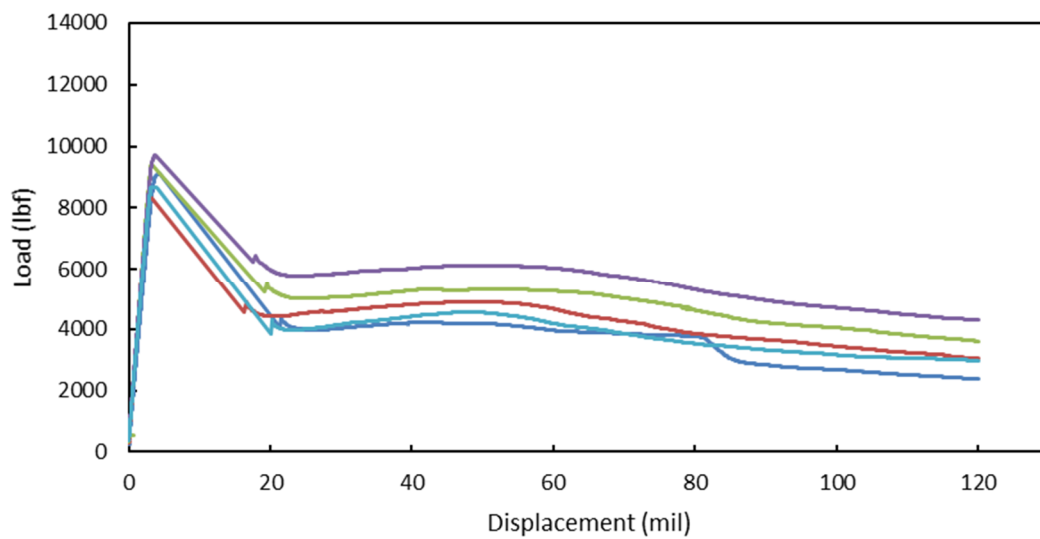


Figure D-24. Load versus displacement curves for H.S.E.8.75.

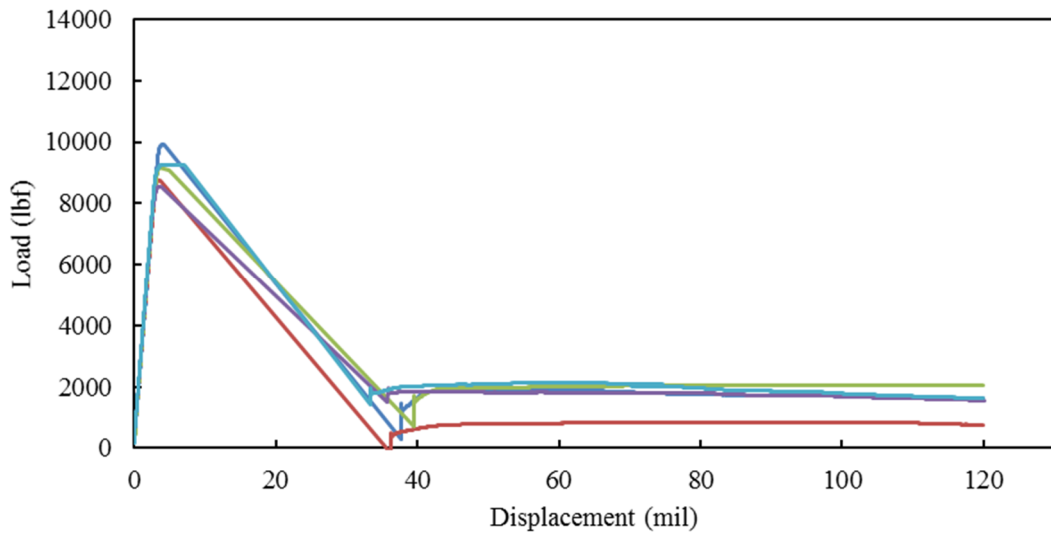


Figure D-25. Load versus displacement curves for H.S.E.9.25.

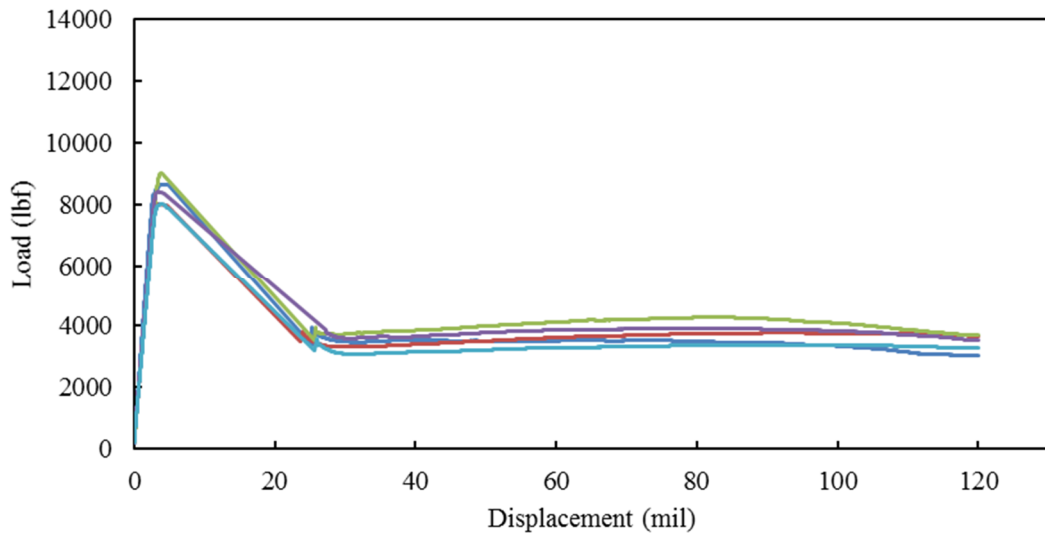


Figure D-26. Load versus displacement curves for H.S.E.9.5.

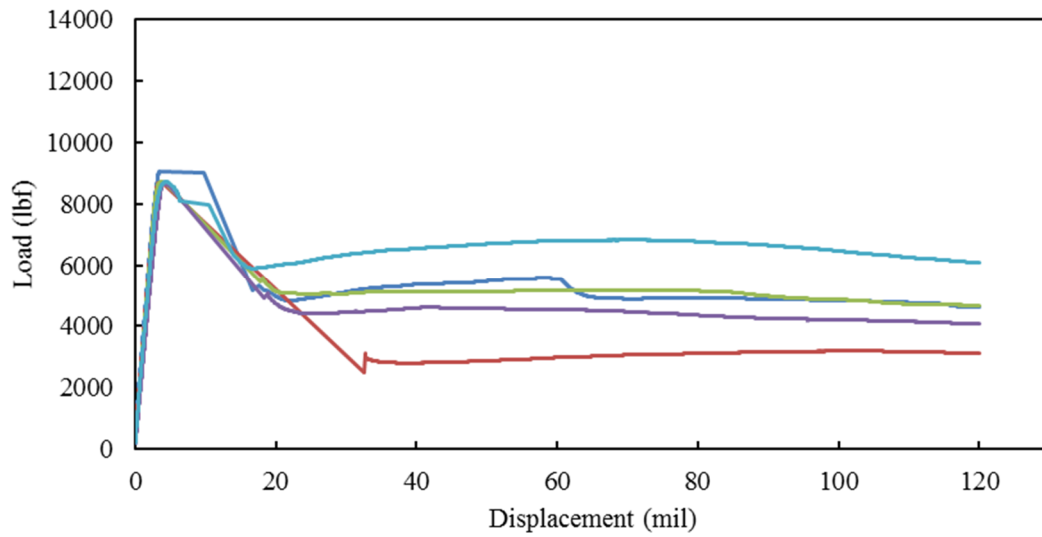


Figure D-27. Load versus displacement curves for H.S.E.9.75.

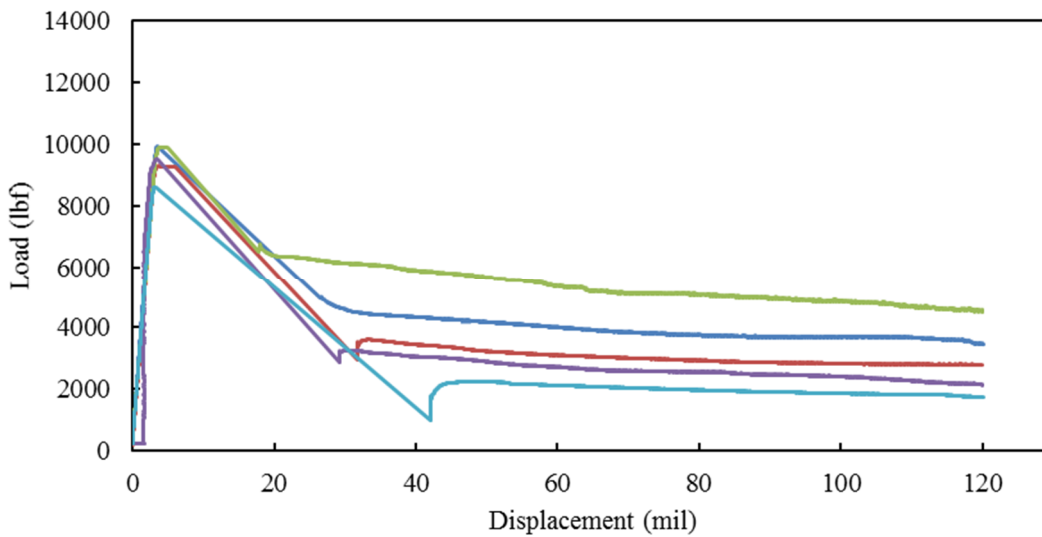


Figure D-28. Load versus displacement curves for H.L.EC.10.25.

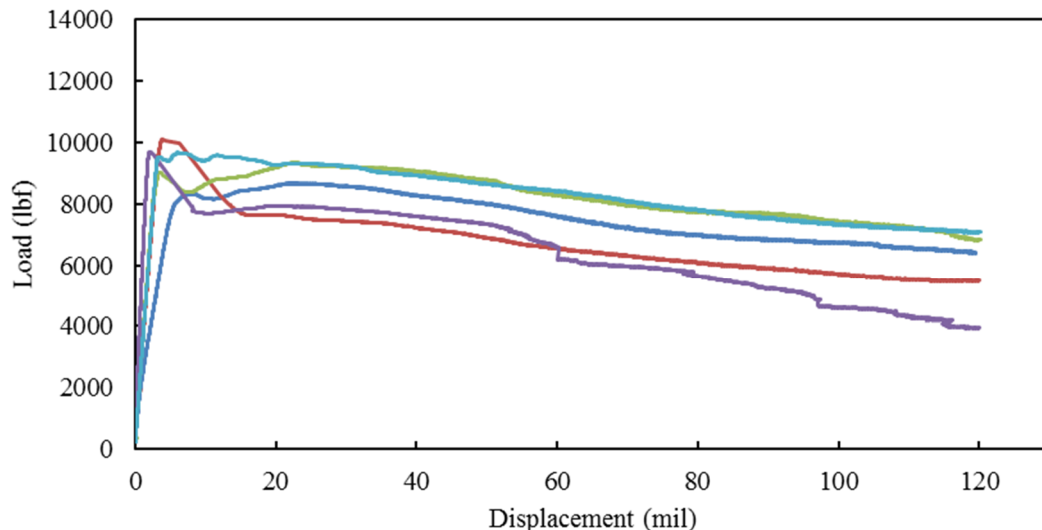


Figure D-29. Load versus displacement curves for H.L.EC.10.5.

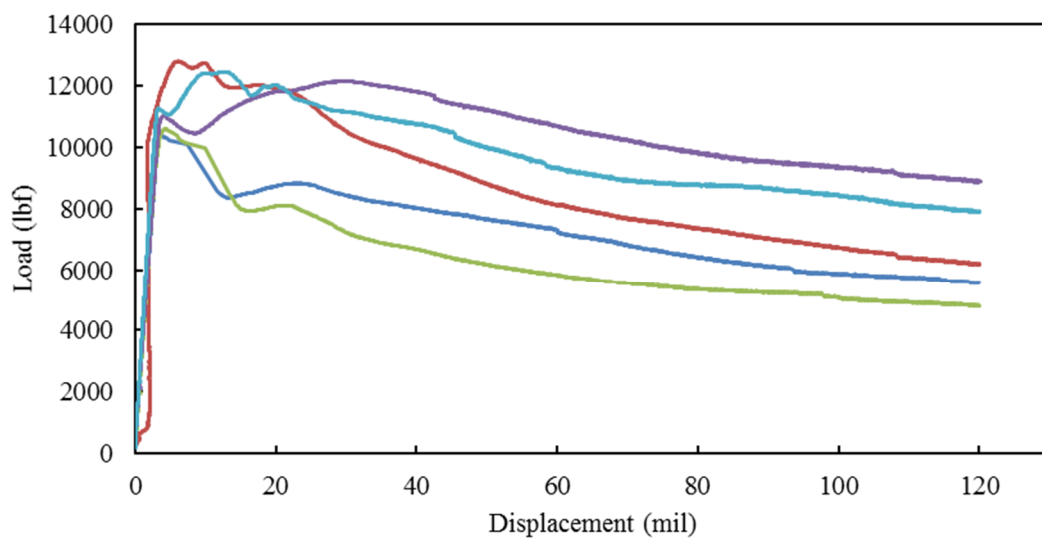


Figure D-30. Load versus displacement curves for H.L.EC.10.75.

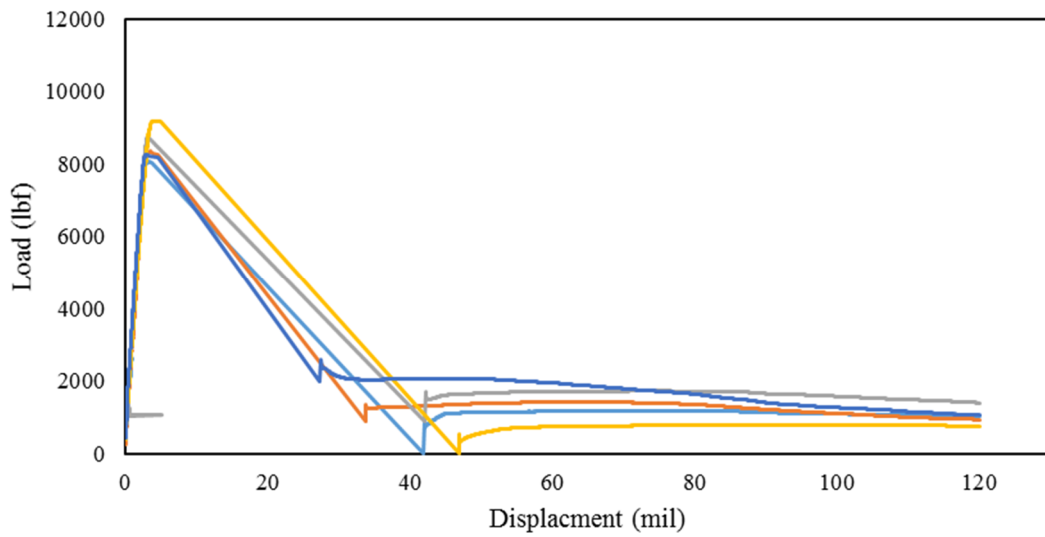


Figure D-31. Load versus displacement curves for H.S.T.11.25.

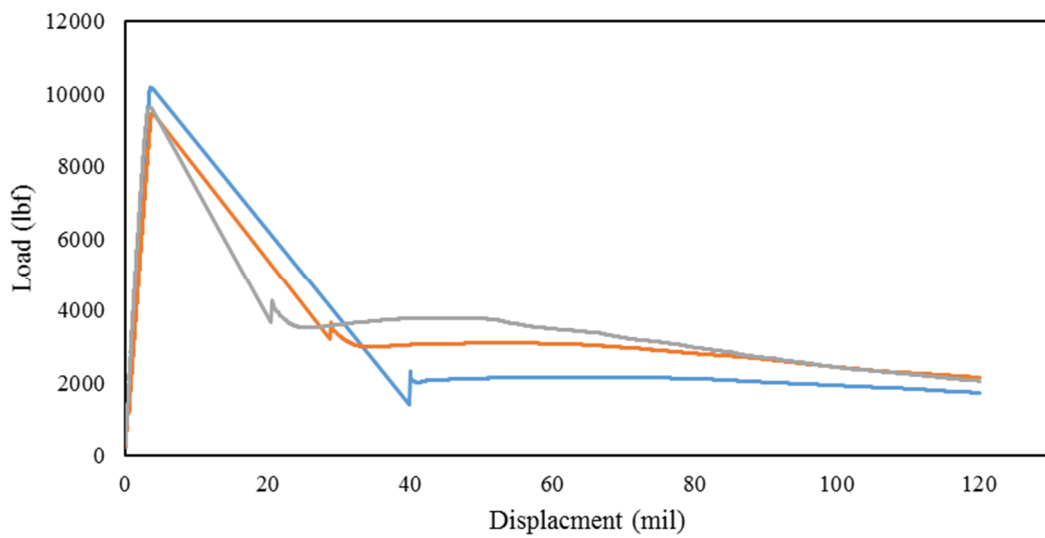


Figure D-32. Load versus displacement curves for H.S.T.11.5.

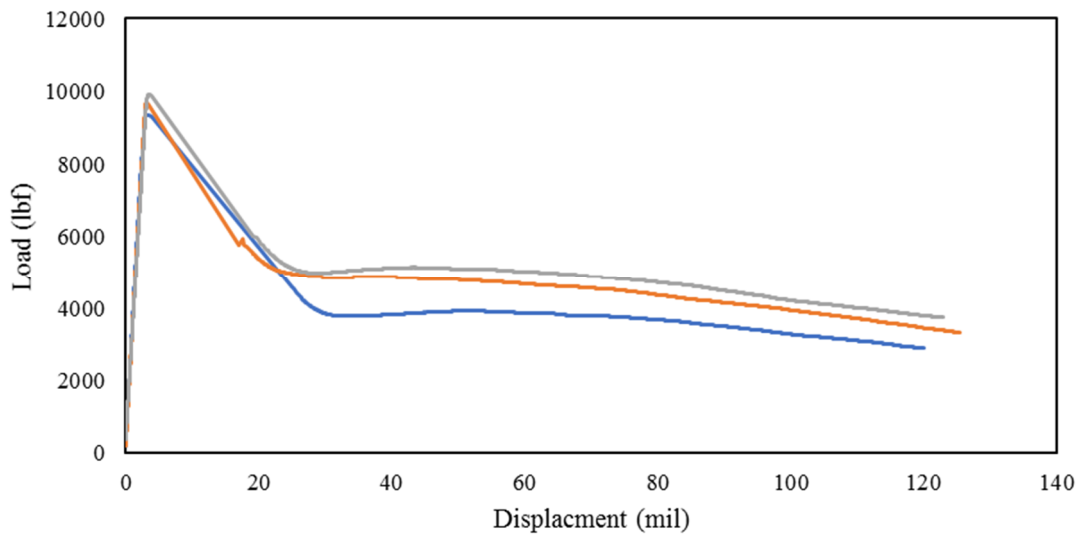


Figure D-33. Load versus displacement curves for H.S.T.11.75.

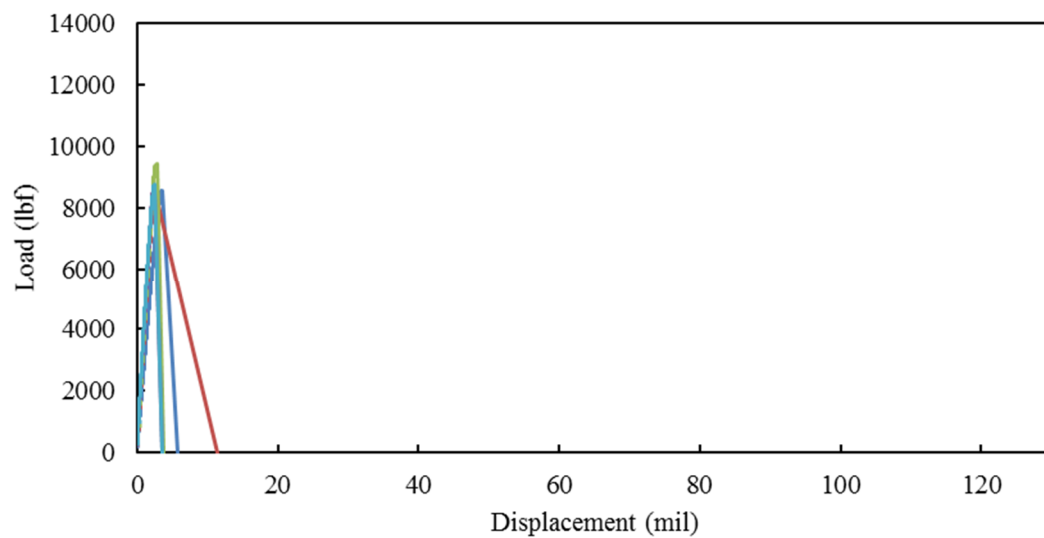


Figure D-34. Load versus displacement curves for a plain concrete mixture.

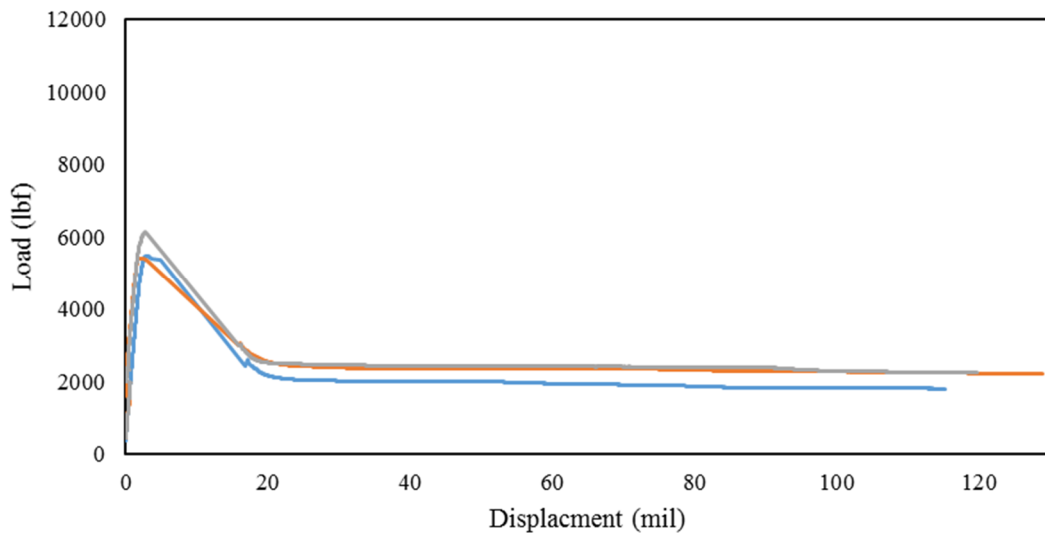


Figure D-35. Load versus displacement curves for L.S.S.4.5.

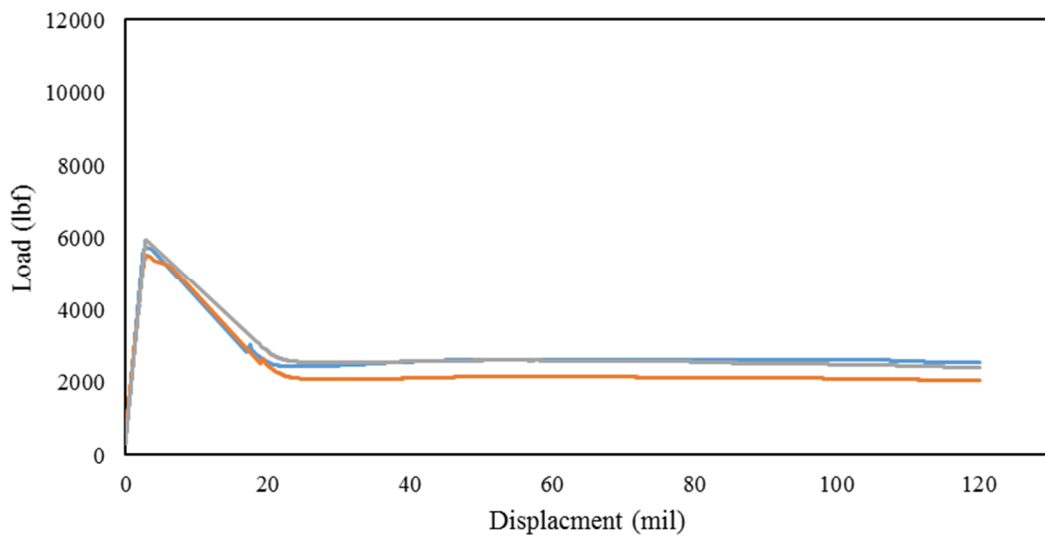


Figure D-36. Load versus displacement curves for L.S.T.5.5.

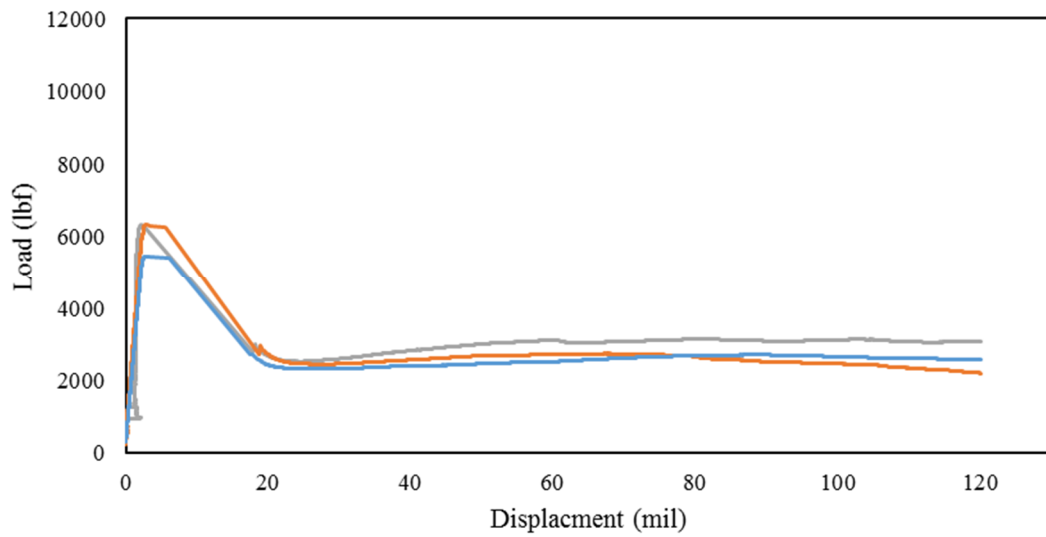


Figure D-37. Load versus displacement curves for L.S.C.6.5.

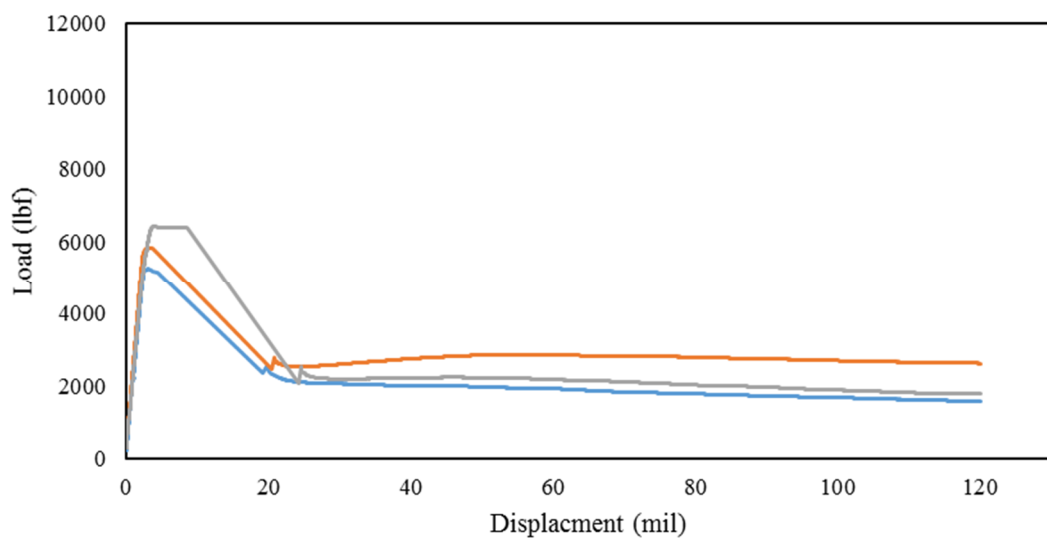


Figure D-38. Load versus displacement curves for L.S.E.9.5.

## **E APPENDIX: JOINT PERFORMANCE OF FRC**

### **1) Introduction**

Research being conducted adjacent to the flexural performance study considered the pavement joint performance of fiber reinforced concrete (FRC). In the body of this report, it was stated that FRC enhances durability, provides post crack strength, reduces plastic shrinkage, and increases impact strength; however, little was mentioned about the joint performance of FRC as it relates to concrete pavements. In many previous research studies (Barman, 2014; Raja and Snyder, 1995; Colley and Humphrey, 1967), the joint performance of concrete was determined by testing large size slabs. However, constructing large size slabs and testing them for joint performance is a very expensive task, especially when many variables are included in the test matrix. Barman and Vandenbossche (2014) briefly studied FRC joints and developed a method to rapidly evaluate the performance of FRC pavements.

### **2) Joint Performance Testing**

The joint performance contribution of the structural fibers will be studied using a small-scale test setup in the current study. In this test setup, 24-in x 6-in x 6-in dimension beams will be tested for determining the joint performance. The beams will be cracked at the mid-span of the beam 18 hours after casting and tested for joint performance at an average of 28 days. This test method is referred to as the Beam method. Figure E-1 shows a picture of the LTE test setup developed at the UMD. The principle of this test setup is similar to the one developed at the University of Pittsburgh by Barman and Vandenbossche (Barman, 2014). A larger detail on the test setup configuration and the test principle can be found in Dr. Barman's Ph.D. Dissertation (Barman, 2014).

This beam joint performance testing setup was designed to simulate the abrasive action that occurs in joints and cracks of in-service concrete pavements. In order to simulate the in-service pavement condition in the beam joint performance test setup, an actuator is used to apply vertical cyclic loading (both upward and downward) on one side of a pre-cracked concrete beam. The min and maximum load ( $\pm 1050$  lbf) is the equivalent to a wheel load from an equivalent single axle load (ESAL).

In Figure E-1, it can be seen that two layers of neoprene pads are provided both above and below the beam specimen. Adjacent to the neoprene pads are either a rigid frame or a rigid testing table. The stiffness of the neoprene pads simulates the stiffness of the layers under an in-service concrete overlay slab. The neoprene pads are compressed under the load both on the loaded side as well as the unloaded side. The magnitudes of the displacements in the loaded side and unloaded side are a function of the crack or joint stiffness. These displacements are measured by the LVDTs as shown in Figure E-1.



Figure E-1. Image of the joint performance test.

### 3) Joint Performance Properties: Load Transfer Efficiency (LTE)

The primary output from joint performance testing can be seen in Figure E-2 and includes load, loaded slab and unloaded slab displacements. The ratio of the displacement on the unloaded side ( $d_u$ ) and displacement on the loaded side ( $d_l$ ) multiplied by 100 is the LTE in percent (Equation 8). In the beam LTE method, since load is applied both in upward and downward directions, the LTE can be obtained in both directions. The average of the LTEs measured in two directions is considered as the LTE of the concrete specimen.

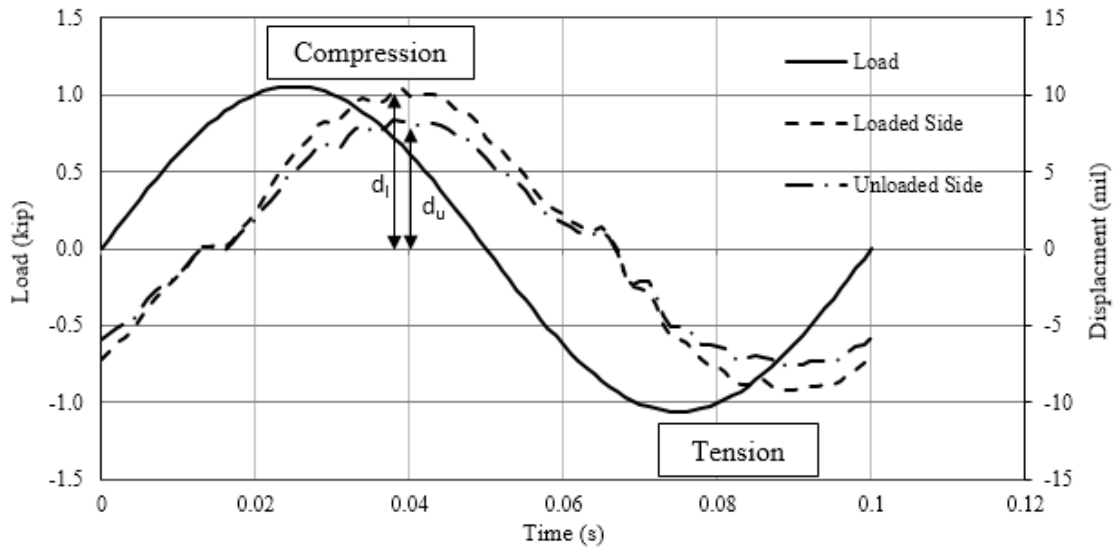


Figure E-2. General cyclical plot with description of variables.

Equation 8

$$LTE = \frac{d_u}{d_l} * 100\%$$

Where:

$d_l$  is the loaded slabs peak displacement

$d_u$  is the unloaded slabs peak displacement

#### 4) Joint Performance Properties: Differential Joint Energy Dissipation (DJD)

DJD represents the amount of energy released through the joint face in the joint performance test. Fundamentally, this property can be represented as the area inside the load versus differential joint displacement Hystereses (Figure E-3). This property is beneficial because it represents the performance of the slab for a varied applied load, unlike LTE which only measures the performance of the material at an ESAL.

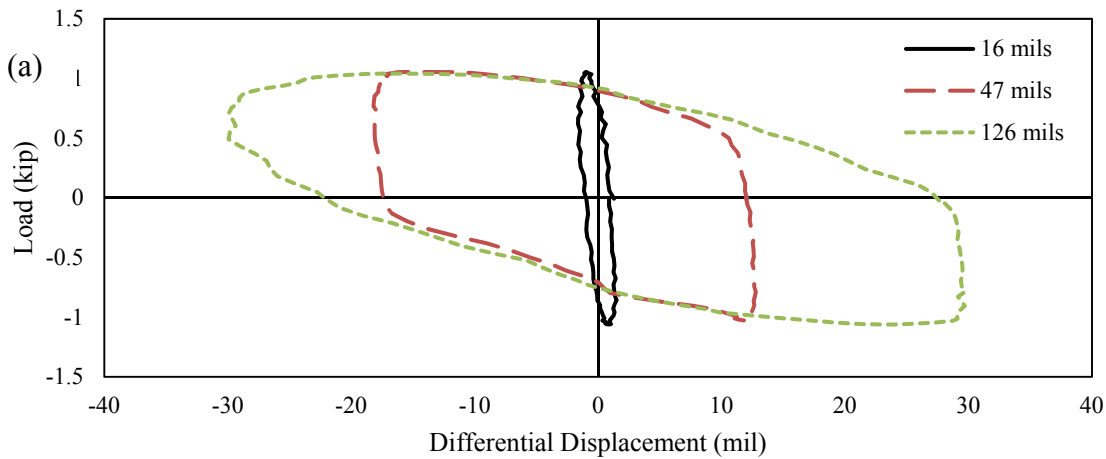


Figure E-3. Differential joint displacement as a function of load applied to the loaded slab.

#### 5) Testing Matrix and Plan

In this study, four fibers were examined at 0.50%  $V_f$ , 2 fibers were examined at 0.25%  $V_f$ , and a plain mixture was tested for the purpose of developing correlations and comparisons. The fibers in this work followed the nomenclature from the mixtures in the body of the thesis. The first four mixtures (0.5%  $V_f$ ) included S.S.4, S.T.5, S.C.6 and S.E.6, while the last two FRC mixtures (0.25%  $V_f$ ) included S.S.4 and S.E.9.

## **6) Plastic and Hardened Concrete Properties**

The fresh concrete properties and concrete compressive strength for all the mixtures reported in this work are in Table E-1. These results are presented as quality control measures and will not be part of the analysis in this report.

Table E-1. Plastic and hardened concrete properties for the mixtures in this work.

<b>Designation</b>	<b>Slump (in)</b>	<b>Air Content (%)</b>	<b>Compressive Strength (psi)</b>
Plain Concrete	2.5	8.5	6750
S.S.4.5	3	6.6	7190
S.T.5.5	2	6.9	7340
S.C.6.5	1	7.1	7490
S.E.9.5	2.5	8.5	6610
S.E.9.25	2	7.8	7470
S.S.4.25	2	8.5	6330

## **7) Joint Performance Results: Fiber Geometry**

Previous work found the effect that fiber properties had on the flexural performance was relatively significant; however, in this study little difference was seen between each fiber in terms of joint performance. Figure E-4, Figure E-5, and Figure E-6 show the LTE, DJD and loaded slab displacement trendlines as a function of crack width for an average of three specimens. There are few notable differences here; however, it is apparent that longer fibers consistently performed better than the shorter fibers at large crack widths, especially when exceeding 150 mils. When only considering Figure E-6, it is apparent though that the performance of the straight fiber was less than that of the other fibers.

While it may seem unexpected that these fibers would perform relatively the same, it generally makes sense. If bending stiffness is considered the driving force of a fibers ability to perform in a concrete pavement joint, the only factor to consider for

behavior is fiber dosage and fiber material. While bending stiffness of an individual fiber varies greatly due to various cross-sectional areas and material type (change in modulus of elasticity), the composite section will only vary in behavior due to fiber dosage and material type. This fact is because the area of fibers and the effective moment of inertia of a given FRC cross section will be generally the same assuming a typical fiber distribution at the crack face. Section 8) will discuss how fiber dosage effects joint performance.

It should be noted that the various fibers still may perform better than others by providing more macro crack propagation resistance. Providing more crack propagation resistance would reduce the crack width, subsequently increasing joint performance. It should also be noted that during this testing the specimen was in tension; therefore, the fibers were in tension, these results may vary as crack widths contract in warmer months and fibers become loose due to plastic elongation in cold months. Later work should seek to consider this.

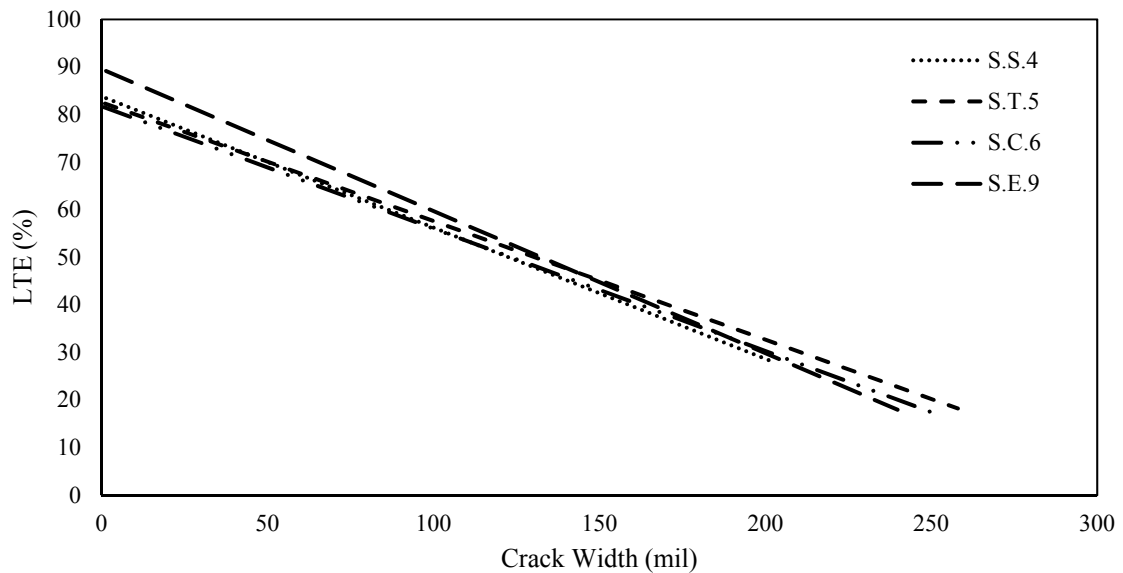


Figure E-4. LTE as a function of crack width for the fibers tested in this study for 0.5%  $V_f$ .

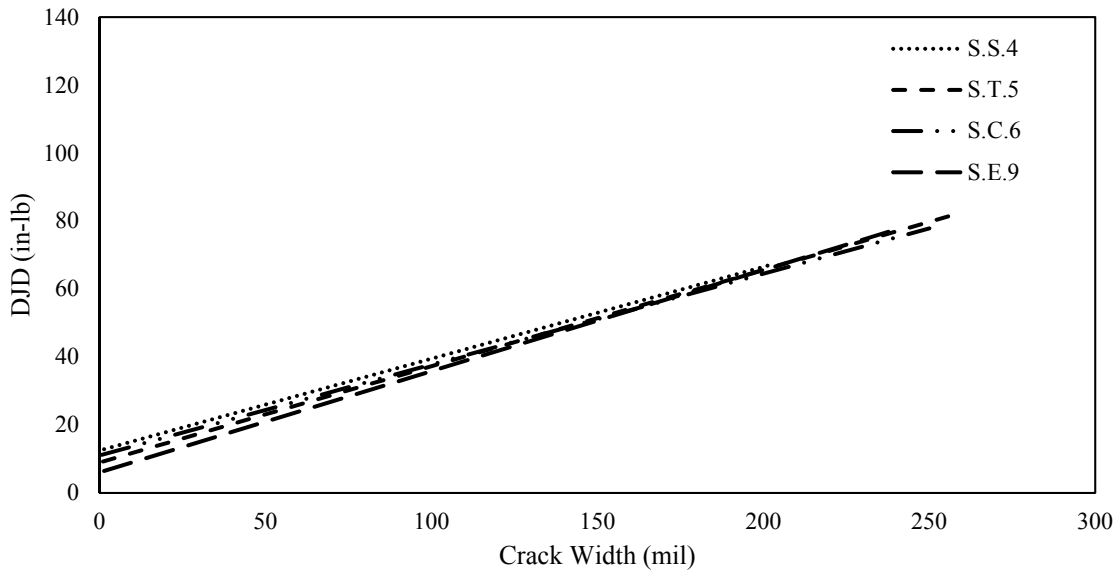


Figure E-5. DJD as a function of crack width for the fibers tested in this study at 0.5% Vf.

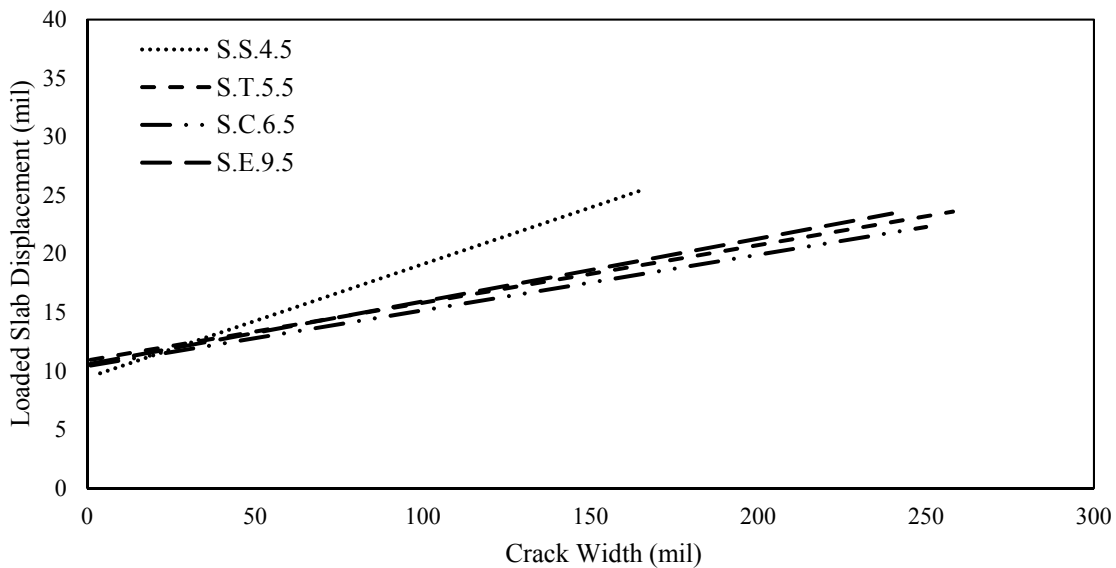


Figure E-6. Average loaded slab displacement as a function of crack width.

## 8) Joint Performance Results: Fiber Dosage

As previously stated, dosage may be the driving factor on achieving joint performance in concrete pavements. Figure E-7, Figure E-8, and Figure E-9 show average joint performance as a function of crack width for a plain concrete (no fibers) mixture and two fiber dosages. These plots are the average of all mixtures tested in the 1<sup>st</sup> and 4<sup>th</sup> phases

for their respective trendlines to show an average performance. These two plots show a significant increase in joint performance with fiber dosage.

To better understand this relationship, Figure E-10 and Figure E-11 depict joint performance as a function of fiber dosage for a range of crack widths. These plots were developed empirically from the trendlines and equations seen in Figure E-7 and Figure E-8. The equations used for these plots had very strong correlations and would likely grow stronger with an increase in data points.

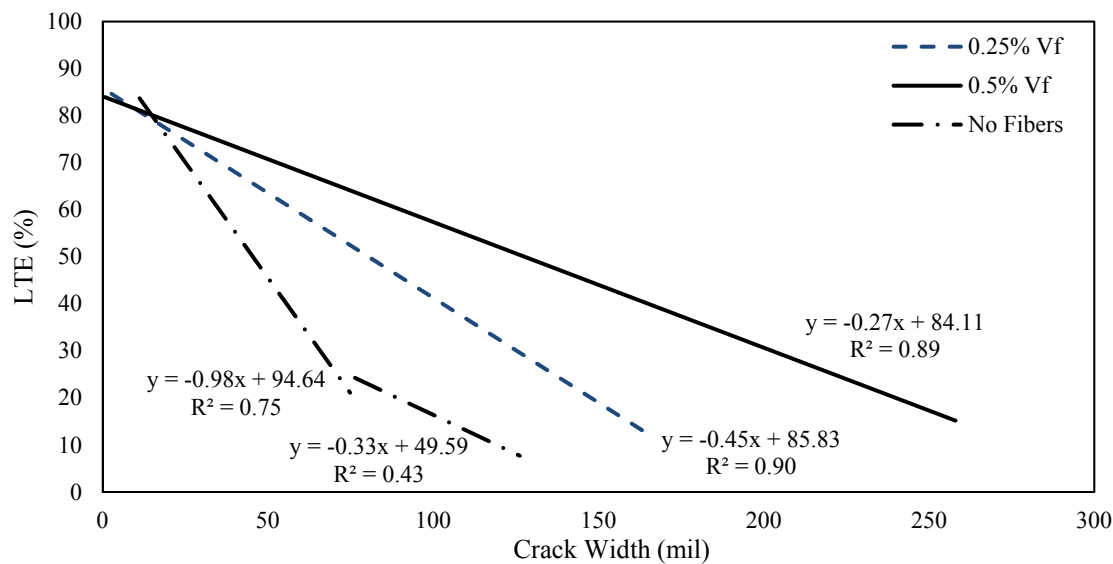


Figure E-7. LTE as a function of crack width to compare the effect of fiber dosage on joint performance.

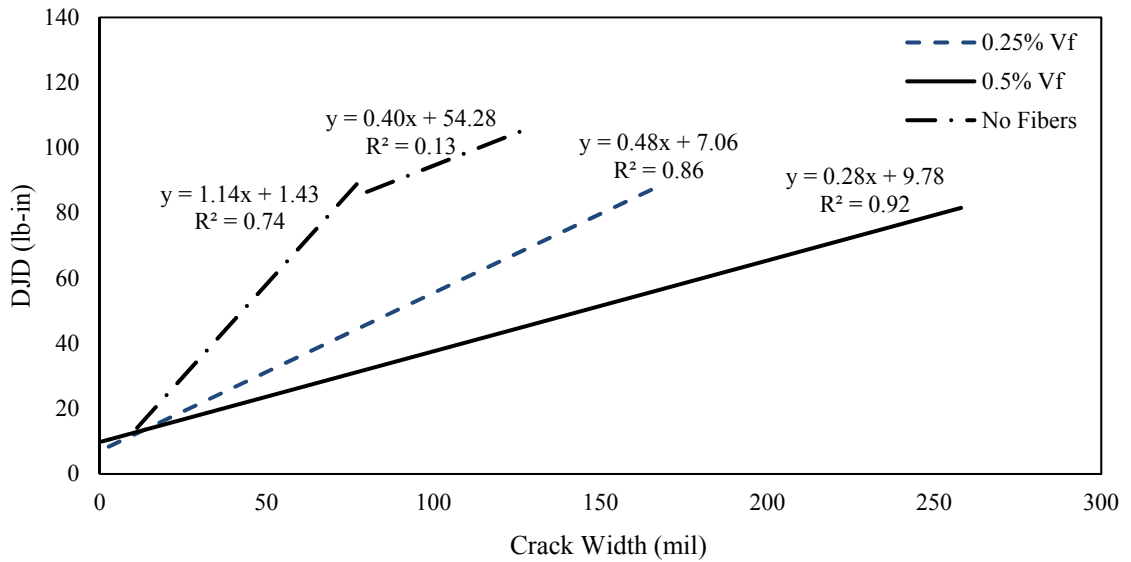


Figure E-8. Differential joint energy as a function of crack width to compare the effect of fiber dosage on joint performance.

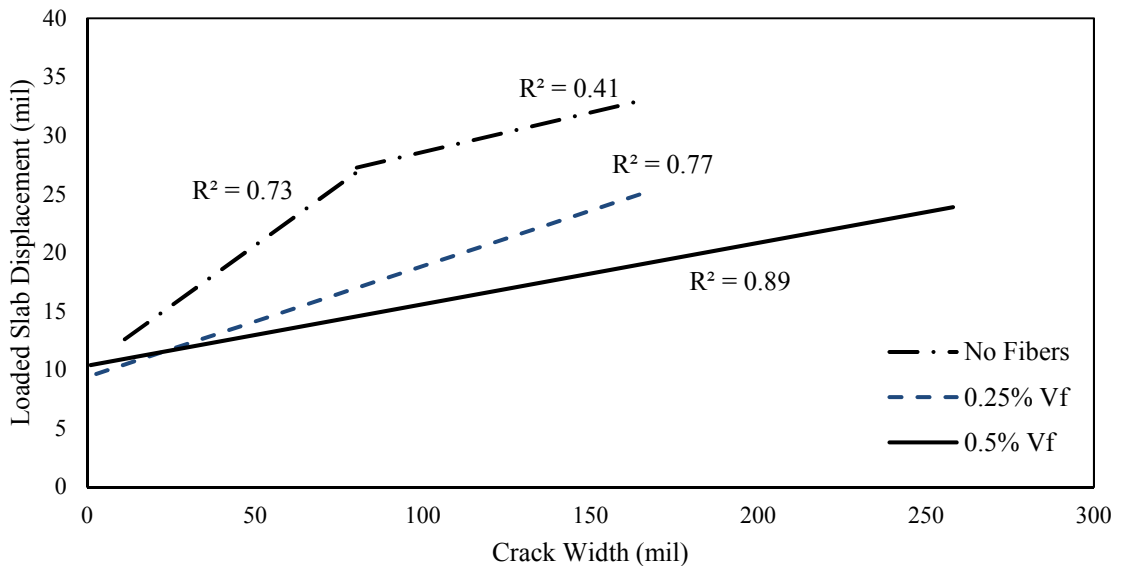


Figure E-9. Average loaded slab displacement as a function of crack width to compare the effect of fiber dosage on joint performance.

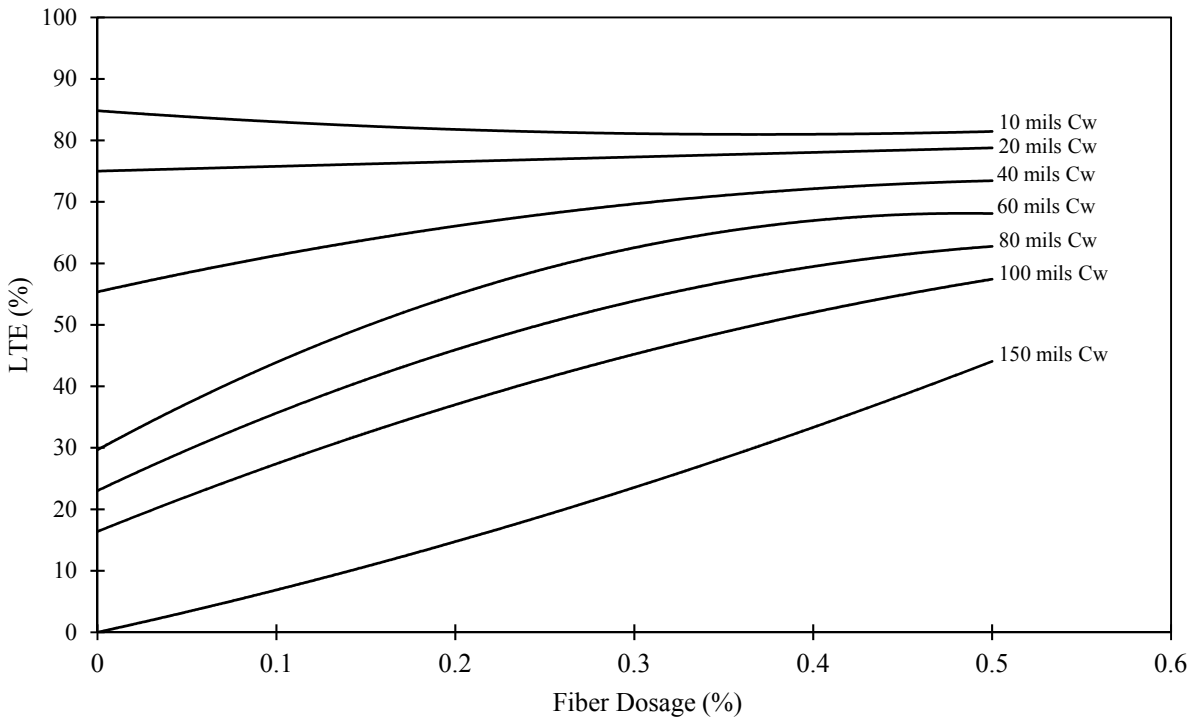


Figure E-10. LTE as a function of fiber dosage for a range of crack widths.

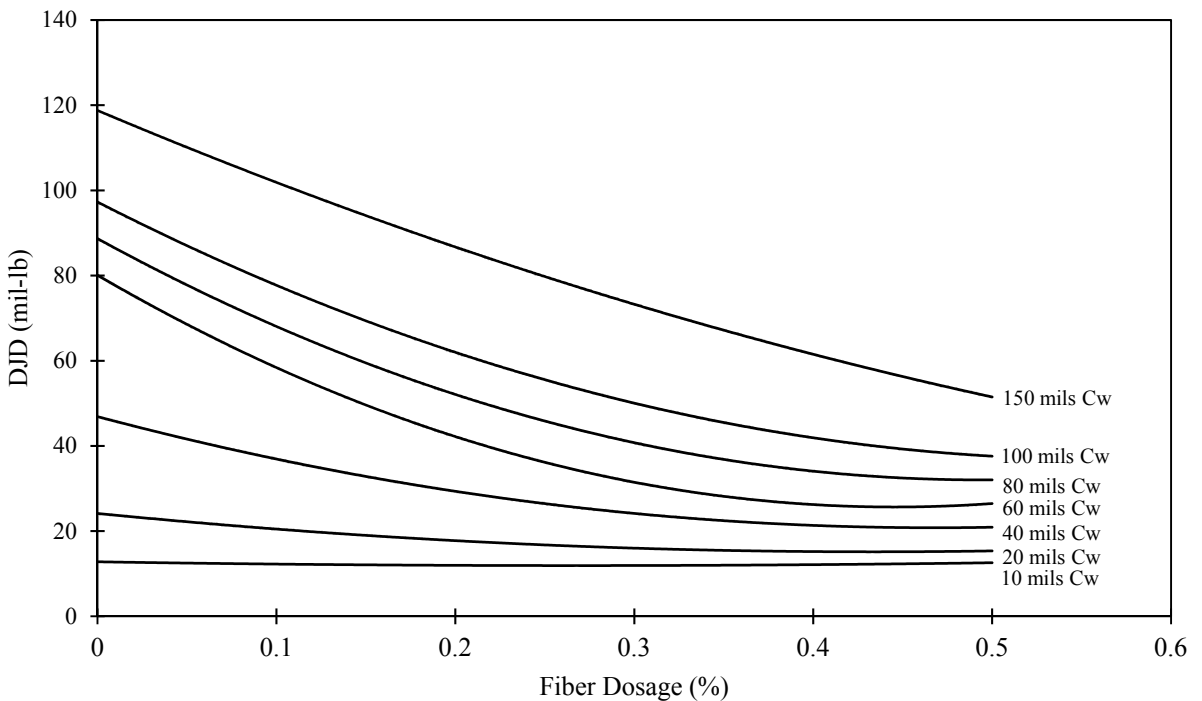


Figure E-11. DJD as a function of fiber dosage for a range of crack widths.

## 9) Joint Performance and Flexural Performance Correlation Charts

When seeking to implement these results into practice, it becomes important to be able correlate these results to common laboratory test procedures and practices. In this study, the strength of correlation between flexural and joint performance as a function of reinforcement index (RI) have been seen to be extremely strong; therefore, correlations can be drawn between joint performance and flexural performance. Using this correlation, a required residual strength in the ASTM C1609 test can be selected when knowing a maximum crack width and respective joint performance (LTE or DJD). RS was used for the flexural performance part of this correlation because it is the most generic of the flexural performance properties.

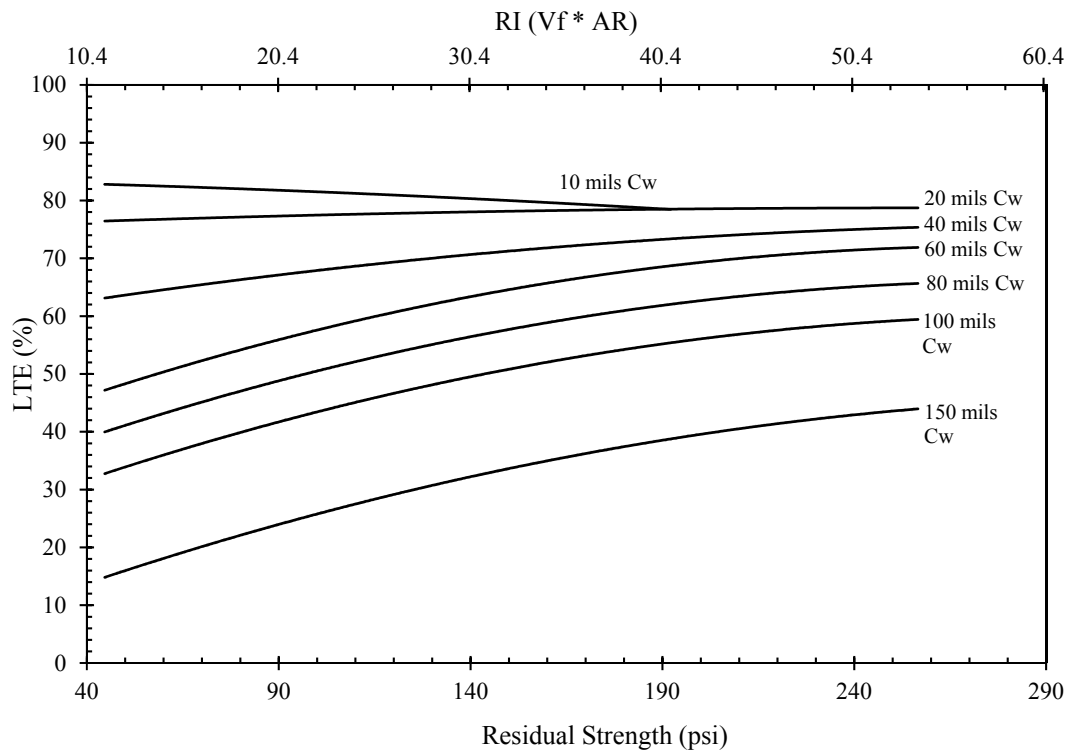


Figure E-12. Correlations between LTE, RS and suggesting an approximate RI.

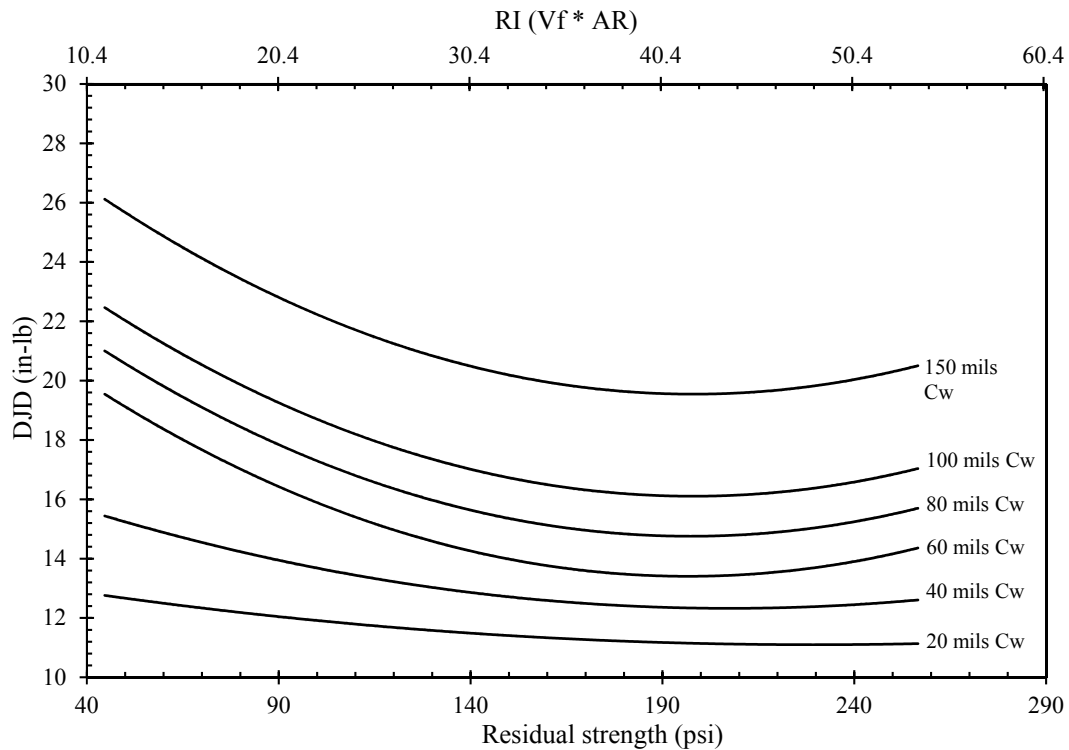


Figure E-13. Correlations between DJD, RS and suggesting an approximate RI.

## 10) Conclusion

Research conducted adjacent to the work in the body of this thesis considered the pavement joint performance of fiber reinforced concrete (FRC). In the body of this report it was stated and fibers added to the concrete enhances durability, provides post crack strength, reduces plastic shrinkage, and increases impact strength; however, little was mentioned about the joint performance of FRC as it relates to concrete pavements. This work showed the benefit of using FRC in concrete overlays and found the following:

- Fiber geometry generally has little effect on joint performance.
- Fiber dosage was found to be the largest variable in increasing joint performance.
- Macro crack propagation and resistance to plastic deformation, in the form of pulling from the concrete, may be the biggest difference between fibers.

- Fibers having a post crack performance (PCP) index of 6 would likely provide the best crack propagation resistance
- Correlations in this report can serve as a basis for estimating quality control measures and approximating RI.